

University of Cincinnati

Date: 8/16/2017

I, **Shenwen Huang**, hereby submit this original work as part of the requirements for the degree of Doctor of Philosophy in Biomedical Engineering.

It is entitled:

The effect of 120-kHz ultrasound on thrombolytic efficacy in porcine thromboembolism models

Student's name: **Shenwen Huang**

This work and its defense approved by:

Committee chair: Christy Holland, Ph.D.

Committee member: Todd Abruzzo, Ph.D.

Committee member: Kevin Haworth, Ph.D.

Committee member: Andrew Herr, Ph.D.

Committee member: Daria Narmoneva, Ph.D.



27979

The effect of low-frequency ultrasound on thrombolytic efficacy in porcine thromboembolism models

A dissertation submitted to
the Graduate School of the University of Cincinnati
in partial fulfillment of the requirements for the degree of

Doctor of Philosophy

in the Biomedical Engineering Program
Department of Biomedical, Chemical, and Environmental Engineering
College of Engineering and Applied Science

2017

Shenwen Huang

B.S. Massachusetts Institute of Technology, 2010

Dissertation Committee: Christy K. Holland, Ph.D. (Committee Chair)
Kevin Haworth, Ph.D.
Daria Narmoneva, Ph.D.
Andrew B. Herr, Ph.D.
Todd A. Abruzzo, M.D.

Abstract

Ischemic stroke affects nearly 700,000 patients in the United States each year and is the fifth most common cause of death. In less than 6% of ischemic stroke patients, lysis of the occlusive clot is attempted with recombinant tissue-plasminogen activator (rt-PA). The addition of Definity[®] microbubbles and 120-kHz ultrasound to rt-PA treatment has been shown to enhance lytic activity *in vitro* and *ex vivo*. However, preclinical trials must be completed in an animal model such as pigs prior to human clinical trials.

One porcine thrombosis model is the intracerebral hemorrhage model, in which an intracerebral hemorrhage is treated with a lytic and exposed to ultrasound. An assay for a biochemical marker of clot breakdown, D-dimer, was evaluated for quantification of thrombolysis in this model. A porcine D-dimer purification protocol was developed and the identity of the purified D-dimer was confirmed by immunoblotting and MALDI TOF-TOF analysis. We evaluated a commercially available D-dimer ELISA kit and 5 commercially available D-dimer antibodies for development of an in-house ELISA protocol. In porcine samples produced in an *in vitro* thrombolysis system, D-dimer concentration was shown to correlate with mass loss. However, no current assay is known to be able to quantitate D-dimer with adequate sensitivity (10 ng/mL).

To create an arterial thromboembolism model of ischemic stroke, porcine ascending pharyngeal arteries (APA) were occluded bilaterally. Most arteries were occluded with a single clot chosen to be about 1 mm larger than the inner diameter of the target artery. However, intraarterial treatment of the occluded arteries with rt-PA was ineffective and did not recanalize

any of the occluded arteries. A protocol for post-mortem APA excision from swine was also developed.

The lack of rt-PA efficacy in the porcine arterial thromboembolism model suggested that porcine clots were resistant to rt-PA thrombolysis. *In vitro* evaluation of the lytic response of porcine and human clots showed that the presence of human plasminogen either intercalated within the clot or in the surrounding plasma allows for more humanoid rt-PA thrombolytic efficacy. When perfused with human plasma, porcine clots and human clots showed equivalent fractional clot loss when treated with plasma alone, rt-PA, or rt-PA with Definity and adjuvant ultrasound exposure. Human whole blood clots perfused with porcine plasma exhibited less rt-PA lysis than human clots perfused with human plasma. However, adjuvant ultrasound exposure increased lysis to the same extent as in human clots perfused with human plasma.

Porcine clots doped with barium sulfate (BaSO_4) were evaluated for rt-PA thrombolytic efficacy. Non-doped and BaSO_4 -doped porcine clots demonstrated a similar degree of thrombolysis when treated with plasma alone, rt-PA, and rt-PA with adjuvant ultrasound exposure. However, the reduced susceptibility of porcine blood clots to rt-PA was evident. Porcine clots doped with human plasminogen showed increased rt-PA lysis compared to plasma alone, and US exposure adjuvant to rt-PA treatment showed US enhancement of rt-PA lysis. The resistance to rt-PA lysis in porcine clots suggest that biochemical alteration of porcine clots may be required to better mimic human hemostasis.

Acknowledgements

I am extremely thankful to my graduate advisor, Dr. Christy K. Holland, for her mentorship during my time in her lab. Her guidance has allowed me to hone my research abilities and her meticulous attention to detail has helped me develop significantly as a scientific writer. She is dedicated to her students and has often had more faith in my abilities than I have had. Her willingness to write grants in support of student-proposed projects has allowed me to expand my research abilities greatly.

I would also like to thank my committee members: Dr. Kevin Haworth, Dr. Daria Narmoneva, Dr. Andrew B. Herr, and Dr. Todd A. Abruzzo for taking the time to provide feedback on my work. I benefitted greatly from discussions with them on the course and progress of my research, and cannot overstate how much I have gleaned from their expertise in their respective fields. Dr. Todd Abruzzo has been instrumental in making sure our research remains clinically relevant. Dr. Andrew Herr has been a fantastic guide in the art of protein purification and characterization. Dr. Daria Narmoneva has provided keen insights on the biological impacts of my proposed work. Dr. Kevin Haworth has been a key resource for ultrasound characterization and signal processing.

I greatly appreciate the support of my colleagues, past and present, at the Image-Guided Ultrasound Therapeutics Laboratories. Kirthi Radhakrishnan (PhD) was my first mentor in the lab. Jonathan Sutton (PhD) laid the groundwork for much of the porcine experiments I was able to do. Himanshu Shekhar (PhD) introduced me to the *in vitro* time lapse microscopy system in which so many of the experiments presented in my dissertation were completed and has been a speedy, insightful editor for both manuscripts and dissertations. Kenneth Bader (PhD) provided

me with his extensive human clot width loss data as well as very insightful comments on my manuscript. Steve Perrin laid the groundwork on the project for quantification of porcine D-dimer. Guillaume Bouchoux (PhD) and Robert Kleven were instrumental in setting up the ultrasound insonation and detection system on two separate iterations of the *in vitro* static thrombolysis model (Chapter II.5). Jason Raymond (PhD), Matt Gruber (MS), and Karla Mercado (PhD) were wonderful colleagues in lab who were always willing to help in a time of need.

I would also like to thank the University of Cincinnati Medical Scientist Training Program (supported by the National Institute of General Medical Sciences - T32GM063483). Both program leadership and students have been supportive and were always willing to be a sounding board for ideas and thoughts.

Most of all, I would like to thank my family and friends, without whose support I could not have completed my graduate studies. My parents, Dr. Chunfa Huang and Zhenzhen Wu, have always instilled in me a drive for knowledge and supported my career choices. My brother Kevin Huang has motivated me to work harder to be a better role model. Lastly, Stefan Flessa has been a steady source of love and encouragement as I completed my graduate studies.

The work presented in this dissertation was supported by the National Institute of Neurological Diseases and Disorders (R01NS047603).

Specific chapters

Chapter II: Particular thanks go to Andrew Herr (PhD) and the members of his lab for all their help and resources in the purification and characterization of porcine D-dimer, and in teaching me all the basic biochemistry skills that are not readily available in an engineering

laboratory. In particular, thanks to Jeanette Miller for her expertise with immunoblotting and all things antibody, Alex Yarawsky for his help in learning the basics of circular dichroism spectroscopy, and KC Sullivan for her help in using the Akta L FPLC system. Additionally, thanks to Ken Greis (PhD) and Michael Wyder from the UC Proteomics & Mass Spectroscopy center for their assistance with the MALDI TOF-TOF analysis.

Thanks go as well to our collaborator Gail Pyne-Geithman (DPhil) for providing porcine D-dimer standard and Stephen Perrin for the groundwork on the project, including the production of a subset of the retracted clot *in vitro* thrombolysis samples. Thanks also to Paul Riley at Diagnostico Stago for our discussion about the Asserachrom D-dimer ELISA kit and Tania Hancock and Absolute Antibody for providing antibody 3b6 for the cost of shipping so that we could test the cross-reactivity.

Chapter III: I would like to thank our collaborator Todd Abruzzo (MD) for all of his expertise in both clinical practice and the porcine models of stroke. Nicole Hilvert is greatly appreciated for ensuring that pig experiments ran smoothly, and that we were prepared with all of the materials required for each day. Thanks go as well to Jasmine Hales and the rest of the veterinary technicians who helped us keep our pigs alive. Thank you to Brenda Wynn (DVM) for helping us investigate the cause of our premature pig deaths. Additionally, thanks to Yash Patil (MD) for his help with the post-mortem APA excision and Peter Pettigrew (PhD) for allowing us access to the Goodyear Microsurgery Lab for our dissections.

Chapter IV: I would like to thank the Cincinnati Children's Hospital Medical Center Anatomical Pathology Core for their help in producing and describing our histology and electron microscopy images, in particular Betsy A. DiPasquale, Kerri Nighting, and Dr. Kumar Shanmukhappa, DVM, PhD.

Publications

Original Articles

Huang S, Shekhar H, Holland CK. Comparative lytic efficacy of rt-PA and ultrasound in porcine versus human clots. *PLoS One*. 2017;12(5):e0177786.

Shekhar H, Bader KB, **Huang S**, Peng T, Huang S, McPherson DD, *et al*. In vitro thrombolytic efficacy of echogenic liposomes loaded with tissue plasminogen activator and octafluoropropane gas. *Physics in Medicine and Biology*. 2017;62(2):517–38.

Abstracts and Conference Presentations

Huang S, Shekhar H, Holland C. Comparative lytic efficacy of rt-PA and intermittent ultrasound in porcine versus human clots. In: *Journal of the Acoustical Society of America*. 2017 May 10;141(5):4012.

Shekhar H, **Huang S**, Peng T, Klegerman ME, Huang S-L, McPherson DD, *et al*. Thrombolytic efficacy of echogenic liposomes that co-encapsulate rt-PA and octafluoropropane gas. In: *Journal of the Acoustical Society of America*. 2016 Apr;139(4):2093.

Huang S, Shekhar H, Holland C. Lytic efficacy of tissue plasminogen activator and ultrasound in porcine clots doped with barium sulfate in vitro. In: *Journal of the Acoustical Society of America*. 2016 Apr;139(4):2030.

Table of Contents

Abstract	ii
Acknowledgements	v
Publications	viii
List of Figures	xii
List of Tables	xvii
Chapter I. Introduction	1
I.1 Background & Significance	1
I.2 Methods to assess thrombolytic efficacy.....	2
I.3 Sonothrombolysis.....	3
I.4 Animal models of thromboembolic stroke	4
I.5 Hypothesis and specific aims	5
I.6 Thesis Overview	7
Chapter II. Exploration of a biochemical metric for clot mass loss.....	9
II.1 Background.....	9
II.2 D-dimer Purification.....	11
II.2.1 Materials & Methods	11
II.2.2 Results.....	18
II.2.3 Discussion.....	23
II.3 Biochemical quantification of porcine D-dimer with the Asserachrom kit.....	25
II.3.1 Materials and Methods.....	26
II.3.2 Results.....	29
II.3.3 Discussion.....	32
II.4 Biochemical quantification of porcine D-dimer with commercially available primary antibodies	34
II.4.1 Materials and Methods.....	35
II.4.2 Results.....	42
II.4.3 Discussion.....	47
II.5 Preliminary quantification of porcine D-dimer in <i>in vitro</i> thrombolysis samples ..	49
II.5.1 Materials and Methods.....	49
II.5.2 Results.....	55
II.5.3 Discussion.....	60
II.6 Conclusions	65
Chapter III. Initial development of a porcine arterial thromboembolism model.....	66

III.1	Background	66
III.2	Materials and Methods	69
III.2.1	Porcine whole blood clot manufacturing	69
III.2.2	Animal experiment protocol	70
III.2.3	Thrombolytic efficacy	74
III.2.4	APA excision	74
III.3	Results	75
III.3.1	Establishment of arterial occlusion	75
III.3.2	Thrombolytic efficacy	76
III.3.3	APA excision	77
III.4	Discussion	78
III.5	Conclusions	82
Chapter IV.	Comparative lytic efficacy of rt-PA and ultrasound in porcine versus human clots	83
IV.1	Introduction	83
IV.2	Materials and Methods	86
IV.2.1	Preparation of plasma, rt-PA, and ultrasound contrast agents	86
IV.2.2	Preparation of human whole blood clots	87
IV.2.3	Preparation of porcine whole blood clots	88
IV.2.4	Comparison of rt-PA susceptibility in porcine and human clots using time-lapse microscopy <i>in vitro</i>	89
IV.2.5	Histology	94
IV.2.6	Electron Microscopy	94
IV.2.7	Statistical Analysis	95
IV.3	Results	95
IV.3.1	Comparison of rt-PA susceptibility in porcine and human clots	95
IV.3.2	Histological Examination of the clots	101
IV.3.3	SEM Examination of the clots	101
IV.4	Discussion	104
IV.5	Conclusions	113
Chapter V.	Lytic efficacy of tissue plasminogen activator and ultrasound in porcine clots doped with barium sulfate <i>in vitro</i>	115
V.1	Background	115
V.2	Materials and Methods	116
V.2.1	Preparation of porcine plasma, rt-PA, and Definity [®] microbubbles	116

V.2.2	Preparation of non-doped and BaSO ₄ -doped porcine whole-blood clots	117
V.2.3	Histology	118
V.2.4	<i>In vitro</i> static thrombosis experiments	118
V.2.5	<i>In vitro</i> thrombolysis experiments with flow and time-lapse microscopy	119
V.3	Results	120
V.3.1	<i>In vitro</i> static thrombosis experiments	120
V.3.2	<i>In vitro</i> thrombolysis with flow	121
V.3.3	Ultrasonic content of passively detected US emissions.....	122
V.3.4	Histological Examination of the clots.....	123
V.4	Discussion	124
V.5	Conclusions	128
Chapter VI.	Development of a "humanized" porcine thromboembolism model	129
VI.1	Background	129
VI.2	Materials and Methods	130
VI.2.1	Materials	130
VI.2.2	Preparation of human plasminogen-doped and aspirin-doped porcine whole blood clots	130
VI.2.3	<i>In vitro</i> thrombolysis experiments with flow and time-lapse microscopy.....	131
VI.2.4	Statistical Analysis.....	132
VI.3	Results	132
VI.3.1	Lytic efficacy	132
VI.3.2	Cavitation activity.....	133
VI.4	Discussion	134
VI.5	Conclusions	136
Chapter VII.	Conclusions and Future Work	137
VII.1	Summary	137
VII.2	Summary of Clot Models	139
VII.3	Future Directions	143
References	145	

List of Figures

Figure II.1. Summary of the approach to D-dimer purification using a combination of protein purification techniques.....	14
Figure II.2. (a) Representative chromatogram of a S200 gel filtration separation of fibrin degradation products with 50 mM sodium acetate buffer with 1 M NaBr and 5 mM CaCl ₂ , pH 5.3. (b) SDS-PAGE of purification steps, including fractions from the chromatograph: lane 1 – D-dimer lysate, 2 – Reconstituted 50% ammonium sulfate pellet, 3 – Fraction 14, 4 – Fraction 15, 5 – Fraction 16, 6 – Fraction 18, 7 – Fraction 19. The red arrow points out the porcine D-dimer and the green arrows point out the large-MW contaminant in the gel and the chromatogram.	19
Figure II.3. (a) A chromatogram of an anion exchange separation of fibrin degradation products. (The spike arose from a pause in the run.) (b) SDS-PAGE of the fractions from the chromatograph, with lane 1 – D-dimer lysate and 2 – 0.2- μ m filtered lysate, 3-20 – Fraction 26-43 respectively. The red arrow points out the porcine D-dimer and the yellow arrow points out the small-MW contaminant.....	20
Figure II.4. (a) Representative chromatogram of a S200 gel filtration separation of fibrin degradation products with 50 mM Tris buffer with 150 mM NaCl and 5 mM CaCl ₂ , pH 7.3. (b) SDS-PAGE of purification steps, including fractions from the chromatograph: 1 – Reconstituted 50% ammonium sulfate pellet, 2 – 0.2 μ m-filtered pellet, 3 – Fraction 16, 4 – Fraction 17, 5 – Fraction 18, 6 – Fraction 19, 7 – Fraction 20, 8 – Fraction 21, 9 – Fraction 22. The red arrow points out the porcine D-dimer and the yellow arrow points out the small-MW contaminant in the gel.....	21
Figure II.5. (a) SDS-PAGE and (b) Immunoblot (primary antibody: DD93, chemiluminescent signal overlaid on visible light images of the lanes) of D-dimer protein samples: lane 1 – D-dimer lysate, 2 – 50% ammonium sulfate pellet, 3 – Purified D-dimer, 4 – Purified D-dimer, previously frozen.	22
Figure II.6. CD spectra of pure D-dimer at a concentration of 0.1 mg/mL in 20 mM Tris buffer.	23
Figure II.7. (a) SDS-PAGE and (b) Immunoblot (primary antibody: DD93, chemiluminescent signal overlaid on visible light images of the lanes) of pure D-dimer protein samples from Dr. Gail Pyne-Geithman	27
Figure II.8. Absorbance (at 450 nm) plotted against porcine D-dimer concentration for (a) all samples from 2.5 ng/mL to 1280 ng/mL and (b) zoomed into samples below 100 ng/mL. (n=2 per point; no error bars shown if error bars are smaller than the height of the data symbol)	29
Figure II.9. Absorbance (at 450 nm) plotted against porcine D-dimer concentration for samples between 25 and 400 ng/mL (a) in the presence of 5 g/L and 50 g/L hemoglobin and (b) with	

5 g/L and 50 g/L hemoglobin with and without depletion with Hemoglobind. (n=2 per point; no error bars shown if error bars are smaller than the height of the data symbol) 30

Figure II.10. (a) Absorbance (at 450 nm) as a function of porcine D-dimer concentrations between 5 and 1000 ng/mL. Experiments from different dates in 2017 are plotted as different colors; "PF" indicates that the D-dimer sample was previously flash-frozen and stored at -80 °C. Historical data from 2014 is plotted in gray. (b) Absorbance (at 450 nm) as a function of pre-dilution concentration of human D-dimer standards as provided by the Asserachrom kit for experiment dates in 2017. (n=2 per point; no error bars shown if error bars are smaller than the height of the data symbol) 31

Figure II.11. Absorbance of samples from intermediate steps in the D-dimer purification process (Chapter II.2) in the Asserachrom kit (2017), plotted as an uncorrected absorbance value (black squares) and as absorbance corrected with the A280, a rough estimate of protein concentration. (n=2 per point; no error bars shown if error bars are smaller than the height of the data symbol)..... 32

Figure II.12. Immunoblot with the use of Anti-D-Peroxidase from the Asserachrom kit as a primary antibody (no secondary antibody was required for reporting) 37

Figure II.13. A SDS-PAGE (a) and immunoblots (b, c, d) with lanes as follows: 1 – plasma, 2 – defibrinated plasma, 3 – homogenized clot, 4 – D-dimer lysate, 5 – Purified D-dimer. Immunoblots use the antibodies abcam DD93 (b), Fitzgerald 10-1752 (c) and 10-1753 (d) and are overlaid with a visible light image to provide protein size references. A non-specific hemoglobin signal can be seen in Lane 3 at <20 kDa for each immunoblot, as hemoglobin is known have peroxidase activity (Kapralov et al. 2009)..... 46

Figure II.14. A photographic image of representative retracted (left) and unretracted (right) clots 50

Figure II.15. The experimental set-up used for the *in vitro* thrombolysis experiments without flow (*in vitro* static thrombolysis model). The clot is placed into a sample holder containing 30 mL of defibrinated plasma (and rt-PA and Definity® in relevant runs). Acoustical absorber is used to line the bottom and the wall of the tank to prevent reflections and constructive interference in the acoustic field. The focus of the PCD and the 120 kHz therapy transducer are orthogonally aligned with the clot in the sample holder. Each transducer is approximately 10 cm away from the sample holder..... 53

Figure II.16. (a) Bar graph showing mass loss for unretracted and retracted clots exposed to plasma only, rt-PA, or rt-PA with Definity® and US. For each treated group of unretracted clots, n = 8; for retracted clots, n = 17, 21, and 12 for the three treatment groups respectively. (b) A bar graph showing mass loss for a subset of retracted clot data for which there is D-dimer concentration information available (n = 15, 12, and 9) respectively. 56

Figure II.17. Bar graph showing a. D-dimer concentration and b. absolute D-dimer (corrected with homogenized clot and fluid volumes) in flash-frozen homogenized clot and surrounding fluid samples from retracted clots exposed to plasma alone, rt-PA, or rt-PA with Definity® and US. For clots treated with plasma alone, rt-PA, and rt-PA with Definity® and US, n = 15, 12, and 9 respectively. 58

Figure II.18. Box plots of the pH for undiluted, 1:2 diluted, and 1:21 diluted homogenized clot and surrounding fluid samples (n = 13 each).....	59
Figure II.19. Scatterplots of a. D-dimer concentration as a function of mass loss and b. absolute D-dimer (calculated with homogenized clot and fluid volumes) as a function of D-dimer. Data is shown for a subset of retracted clot experiments as previously included in Figure II.16 and Figure II.17 The dotted line indicates the linear regression line associated with the data and the error bars indicate the standard deviation from 2 absorbance measurements per point (no error bars shown if error bars are smaller than the height of the data symbol).....	60
Figure III.1. Representative CT digital subtraction angiography images of the common carotid artery and ascending pharyngeal artery (APA) (yellow arrow) a. pre-occlusion and b. following the occlusion of the APA with the exogenously formed clot.....	72
Figure III.2. Summary of artery outcomes for the 18 ascending pharyngeal arteries from the 9 pig experiments performed. Red indicates that the arteries were not recanalized at the end of 2 hrs and blue indicates that the arteries were recanalized at the end of 2 hrs. The number listed in each box refers to the number of arteries in that group.....	76
Figure III.3. (a) An overlay of a digital subtracted angiogram with corresponding unsubtracted CT image shows a mismatch between the radiopaque clot (ends denoted by the two yellow arrows) and the end of the contrast front (red arrow), (b) the original unsubtracted CT, (c) the original digital subtracted angiogram	79
Figure IV.1. The experimental set-up for the in vitro flow system. In a water tank held at 37 °C, the clot is mounted within a capillary tube through which plasma is drawn from an upstream plasma reservoir to a downstream syringe pump. Acoustic absorber was used to line the 4 vertical walls of the water tank (not shown) and the bottom of the tank (shown), with approximately 3 cm of the capillary tube visible through a window in the acoustic absorber. From: Huang <i>et al.</i> Comparative lytic efficacy of rt-PA and ultrasound in porcine versus human clots. <i>PLoS One</i> . 2017;12(5):e0177786.	90
Figure IV.2. Thrombolysis of human and porcine clots. a. Fractional clot loss (FCL) for porcine clots in porcine plasma (n=5, black), human clots in porcine plasma (n=12, light grey), and porcine clots in human plasma (n=12, dark grey) exposed to plasma alone, rt-PA (3.15 µg/mL), and rt-PA (3.15 µg/mL) with Definity [®] and intermittent 120 kHz ultrasound (US). Statistically significant differences in FCL (p<0.05) across treatments are denoted by (*). No difference (p>0.05) in FCL was observed for porcine clots in porcine plasma exposed to rt-PA without or with the use of Definity [®] and US as an adjuvant compared to plasma alone. b. Average lytic rate (ALR) for the same clots and treatments shown in 2(a). Statistically significant differences in ALR (p < 0.05) across treatments are denoted by (*). [†] Data with human clots in human plasma (n=12, white) was reproduced from (Bader et al. 2015b). From: Huang <i>et al.</i> Comparative lytic efficacy of rt-PA and ultrasound in porcine versus human clots. <i>PLoS One</i> . 2017;12(5):e0177786.	97
Figure IV.3. Measured ultraharmonic and broadband emissions for trials involving US exposure. Cavitation dose is shown for porcine clots in porcine plasma (black), human clots in porcine plasma (light grey), and porcine clots in human plasma (dark grey) when treated with rt-PA,	

Definity[®], and 120 kHz US. † Data with human clots in human plasma (dashed line) was reproduced from (Bader et al. 2015b). From: Huang *et al.* Comparative lytic efficacy of rt-PA and ultrasound in porcine versus human clots. *PLoS One*. 2017;12(5):e0177786. 100

Figure IV.4. Representative human (a) and porcine (b) clots with standard H&E staining. From: Huang *et al.* Comparative lytic efficacy of rt-PA and ultrasound in porcine versus human clots. *PLoS One*. 2017;12(5):e0177786. 101

Figure IV.5. Representative human (a, c, e) and porcine (b, d, f) SEM images of clot surfaces. Images are at 800x magnification (a, b; bar = 25 μm), 3500x magnification (c, d; bar = 5 μm), and 7000x magnification (e, f; bar = 2.5 μm) From: Huang *et al.* Comparative lytic efficacy of rt-PA and ultrasound in porcine versus human clots. *PLoS One*. 2017;12(5):e0177786. 103

Figure IV.6. Clot fibrin fiber diameter. Box plots showing the range, median, 25th quartile, and 75th quartile of measured fiber diameter for human (n = 130) and porcine (n = 140) clots as measured by blinded observers from SEM images. Outliers are represented by the symbol "+" and statistically significant differences are denoted with a "*". From: Huang *et al.* Comparative lytic efficacy of rt-PA and ultrasound in porcine versus human clots. *PLoS One*. 2017;12(5):e0177786. 104

Figure V.1. Mass loss as a function of rt-PA concentration in non-doped (blue, diamond) and BaSO₄-doped (red, square) porcine whole blood clots. (Plotted as mean \pm standard deviation) 121

Figure V.2. Fractional clot loss non-doped (blue) and BaSO₄-doped (red) clots treated with plasma alone, rt-PA, and rt-PA with Definity and US plotted as mean \pm standard deviation. 122

Figure V.3. Box plot of the total measured ultraharmonic or broadband dose over the 30 minute treatment period for non-doped (blue) and BaSO₄-doped (red) clots treated with rt-PA, Definity, and 120 kHz intermittent US. 123

Figure V.4. Histological images (4x magnification) of a. non-doped and b. BaSO₄-doped porcine clots on sutures. The suture is noted with a blue arrow on each clot. The BaSO₄ is pointed out with yellow arrows. The non-doped porcine clot image (a) is from: Huang *et al.* Comparative lytic efficacy of rt-PA and ultrasound in porcine versus human clots. *PLoS One*. 2017;12(5):e0177786. 124

Figure VI.1. Fractional clot loss for aspirin-doped (blue) and plasminogen-doped (red) clots in response to plasma only (n = 5), rt-PA (n = 5), and rt-PA with US and Definity[®] (n = 5 for aspirin-doped, n = 4 for plasminogen-doped). For convenience, previously published data in non-doped porcine clots (black), human clots (white), and human clots perfused with porcine plasma (grey) is also plotted (Bader et al. 2015b; Huang et al. 2017). 133

Figure VI.2. Measured ultraharmonic and broadband emissions for aspirin-doped (blue) and plasminogen-doped (red) clots. For convenience, previously published data in non-doped porcine clots (black), human clots (light grey), and human clots perfused with porcine plasma (dark grey) is also plotted (Bader et al. 2015b; Huang et al. 2017). 134

List of Tables

Table II.1. Absorbance over time for D-dimer lysate and a porcine clot sample (P101.11C), with noted Asserachrom kit lot and length of TMB development.....	32
Table II.2. An outline of the sandwich ELISA protocol followed. Experiments using Asserachrom Anti-D-Peroxidase skipped steps 11-14 (italicized) as the antibody is already conjugated.....	40
Table II.3. A summation of the sandwich ELISA with each pair of antibodies evaluated.....	44
Table III.1. A summary of the 9 pig experiments performed.	73
Table IV.1. Tukey p-values for cross-species thrombolysis experiments within each combination of clot/plasma.....	98
Table IV.2. Tukey p-values for cross-species thrombolysis experiments within each treatment protocol.....	99
Table IV.3. Human and porcine blood composition and coagulation characteristics.	111
Table VII.1. A summary of clot models and thrombolysis systems used in this dissertation	140

Chapter I. Introduction

I.1 Background & Significance

Ischemic stroke affects nearly 700,000 patients in the United States each year and is the fifth most common cause of death (Benjamin et al. 2017). Currently, two main treatment modalities are used in the management of acute ischemic stroke: intravenous (IV) administration of recombinant tissue-type plasminogen activator (rt-PA), or removal of the thrombi via mechanical thrombectomy. However, rt-PA must be administered within 4.5 hours of symptom onset and there are contraindications such as recent history of central nervous system surgery and known bleeding diatheses (Benjamin et al. 2017). As a result, less than 6% of acute ischemic stroke patients are actually treated with rt-PA (Benjamin et al. 2017). Mechanical thrombectomy may be performed up to 8 hours after symptom onset, but can only be performed when clots are located in larger cranial vessels, such as the distal intracranial carotid artery, the proximal 2 (of 4) segments of the middle cerebral artery, or the proximal 2 (of 3) segments of the anterior cerebral artery (Berkhemer et al. 2015; Zaidat et al. 2013a). As a result, eligibility for mechanical thrombectomy is limited to 4-14% of the acute stroke patients, and not all hospitals employ neurointerventionalists able to perform this procedure (Zaidat et al. 2013a). The limited use of current treatment modalities motivates alternative and adjuvant therapies for treating acute ischemic stroke.

I.2 Methods to assess thrombolytic efficacy

Various quantitative methods to measure thrombolytic efficacy exist for *in vitro* applications, including direct measurement of mass loss (Datta et al. 2006; Datta et al. 2008; Hitchcock et al. 2011; Sutton et al. 2013b) and optical measurement of clot width over time (Bader et al. 2015a; Bader et al. 2015b; Gruber et al. 2014; Meunier et al. 2009). For *in vivo* thrombolysis studies in the vasculature, thrombolytic efficacy is measured by the degree of recanalization, the reopening of the occluded artery. Expert evaluation of images produces a categorical score to indicate the degree of blood flow past the occluded artery and perfusion distal to the occlusion. For example, the Thrombolysis in Cerebral Ischemia (TICI) scale uses MRI or CT to rate occlusions from 0 (no perfusion) to 3 (complete perfusion) (Higashida et al. 2003). A porcine intracerebral hemorrhage model has been developed (Morgan et al. 2008; Wagner et al. 1996; Wagner et al. 1999; Wagner 2007), but evaluation of thrombolytic efficacy is limited to measurement of mechanically aspirated clot volume. In this model, a biochemical assay to measure clot breakdown may be useful for quantification of thrombolytic efficacy *in situ*.

D-dimer is used clinically as a metric for thrombosis and thrombolysis, particularly as a test for excluding conditions such as venous thromboembolism, deep vein thrombosis, and disseminated intravascular coagulation (Adam et al. 2009). D-dimer is the product of three separate enzymes in the thrombogenic and thrombolytic pathways: thrombin, Factor XIIIa, and plasmin. Thrombin cleaves fibrinogen to form fibrin strands, which polymerize into a fibrin mesh. Isopeptide bonds are then formed between the glutamate and lysine residues of adjacent D-domains in the fibrin mesh by Factor XIIIa, separately activated by thrombin. Lastly, plasmin degrades the cross-linked fibrin mesh, forming D-dimer as well as other smaller fibrin degradation products (FDPs) (Adam et al. 2009). The complex pathway required for formation

allows the detection of D-dimer to be very specific to thrombosis breakdown, rather than the degradation of fibrinogen that has not been cross-linked. No commercially available kit for measuring porcine D-dimer currently exists, despite the wide use of pigs in studies of thrombosis and thrombolysis, both for *in vitro* and *ex vivo* studies (Datta et al. 2006; Flight et al. 2006; Hitchcock et al. 2011; Holland et al. 2008; Sutton et al. 2013b) as well as *in vivo* studies (Culp et al. 2004; Gao et al. 2014; Nederhoed et al. 2014).

I.3 Sonothrombolysis

Sonothrombolysis is the use of ultrasound to promote clot lysis, which may be used either as an adjuvant to thrombolytic therapy such as rt-PA, or alone (Bader et al. 2016; Hitchcock and Holland 2010). This approach has shown promise *in vitro* (Bader et al. 2015a; Bader et al. 2015b; Petit et al. 2012; Petit et al. 2015), and has been implemented in several clinical trials (Alexandrov et al. 2004; Tsivgoulis et al. 2010). However, one trial utilizing low-frequency (300-kHz) ultrasound was halted early due to the increased occurrence of intracerebral hemorrhage (ICH) in the ultrasound treatment arm (Daffertshofer et al. 2005). Retrospective analysis suggested that the increased ICH incidence was due to an acoustic standing wave causing damage to intracranial vessels. Such adverse reactions must be prevented with a more thorough preclinical investigation into the mechanisms and biosafety of sonothrombolysis (Alexandrov and Barlinn 2012; Baron et al. 2009; Tsivgoulis et al. 2010). More recent studies using low-frequency (120-500 kHz) ultrasound have found no propensity for negative bioeffects (Bouchoux et al. 2014a; Shimizu et al. 2012). Our lab has shown that sustained microbubble activity, or stable cavitation, nucleated by an ultrasound contrast agent (UCA) can enhance thrombolysis (Bader et al. 2015b; Hitchcock et al. 2011; Sutton et al. 2013a). Stable cavitation is

theorized to increase the penetration of drug into clots (Bader et al. 2015b; Datta et al. 2006; Hitchcock et al. 2011) and induce acoustic radiation force to "shake" the clots (Bader et al. 2015b), thereby aiding the diffusion of the lytic.

I.4 Animal models of thromboembolic stroke

Pre-clinical studies to evaluate the safety and efficacy of sonothrombolysis require an appropriate animal model. Large animal models such as pigs or sheep are best suited for sonothrombolysis to allow use of ultrasound equipment designed for humans in animal experiments due to the similarity of anatomical scales. Porcine blood is commonly used as an alternative to human blood for thrombolysis research (Datta et al. 2006; Flight et al. 2006; Hitchcock et al. 2011; Holland et al. 2008; Sutton et al. 2013b) due to its availability and price, and is biochemically similar to human blood (Lewis 1996). However, the presence of a *rete mirabile* capillary network between the extracranial circulation and intracranial circulation in swine (Daniel et al. 1953) makes intracranial, intraarterial clot placement difficult or impossible.

Previous porcine thromboembolism models have instead occluded the extracranial ascending pharyngeal artery (APA) to evaluate both thrombectomy devices (Gralla et al. 2006; Jahan 2010) and sonothrombolysis (Culp et al. 2004; Gao et al. 2014). Studies assessing mechanical thrombectomy devices for clinical use the additional innovative technique of doping clots with barium sulfate (BaSO₄) (Gralla et al. 2006; Jahan 2010). This contrast agent allows visualization of clot fragmentation and evaluation of the likelihood of downstream emboli from device use (Gralla et al. 2006; Jahan 2010). This evaluation of biosafety would be valuable when evaluating sonothrombolysis as well. However, it is unknown how BaSO₄ doping affects clot thrombolysis. Additionally, pigs appear to be resistant to rt-PA thrombolysis due to decreased

porcine plasminogen activity (Flight et al. 2006). The degree to which thrombolysis differs between humans and pigs should be investigated to evaluate the appropriateness of pigs as a model of human hemostasis. Modification of porcine clotting may be required for a porcine animal model of ischemic stroke to mimic human hemostasis more accurately.

I.5 Hypothesis and specific aims

The goal of the studies described in this dissertation was to lay a foundation for evaluating the combination of rt-PA, ultrasound contrast agents, and 120 kHz ultrasound in an *in vivo* porcine model of ischemic stroke as a precursor to clinical trials. **The central hypothesis of this dissertation is that the application of 120 kHz ultrasound enhances the efficacy of rt-PA via stable cavitation.** This hypothesis has been evaluated in *in vitro* and *in vivo* porcine thrombolysis models and thrombolytic efficacy was quantified using physical and biochemical metrics. The following specific aims were designed to investigate the use of a porcine model as a human thrombotic stroke model:

Hypothesis 1: Porcine D-dimer concentration correlates with mass loss in porcine clots *in vitro*.

Specific Aim 1 (Chapter II): Investigate the correlation between D-dimer concentration and thrombolytic efficacy as measured by mass loss in porcine blood clots.

Aim 1a. Based on previously established protocols for purification of human D-dimer, produce and purify porcine D-dimer.

Aim 1b. Evaluate the use of a commercially available Asserachrom D-dimer ELISA kit and several anti-D-dimer antibodies for measurement of porcine D-dimer.

Aim 1c . Measure porcine D-dimer concentration in *in vitro* thrombolysis samples and correlate D-dimer concentration with mass loss.

Hypothesis 2: The addition of a barium sulfate radiopaque dopant to porcine whole blood clots does not affect rt-PA susceptibility.

Specific Aim 2: Establish an *in vivo* protocol to occlude the porcine ascending pharyngeal arteries bilaterally and investigate the effect of doping porcine whole blood clot with the radiocontrast agent barium sulfate (BaSO₄).

Aim 2a (Chapter III). Perform a pilot study occluding the porcine APAs bilaterally with radiopaque and non-radiopaque clots and evaluate the thrombolytic efficacy of intraarterial rt-PA in this animal model.

Aim 2b (Chapter V). Determine the thrombolytic efficacy of rt-PA with and without 120 kHz intermittent ultrasound and Definity[®] microbubbles on BaSO₄-doped and non-doped clots *in vitro*.

Hypothesis 3: The presence of human plasminogen affects rt-PA thrombolytic efficacy in porcine clots *in vitro*.

Specific Aim 3: Evaluate the effect of introducing human plasminogen into an *in vitro* porcine model of thrombolysis.

Aim 3a (Chapter IV). Evaluate rt-PA thrombolysis with and without 120 kHz intermittent ultrasound and Definity[®] microbubbles in porcine clots perfused with porcine plasma, porcine clots perfused with human plasma, and human clots perfused with porcine plasma to investigate the role of human plasminogen in rt-PA lysis.

Aim 3b (Chapter VI). Perform a pilot study to evaluate rt-PA thrombolysis in porcine whole blood clots doped with human plasminogen and aspirin.

I.6 Thesis Overview

The focus of this dissertation is the use of swine as a model for human thrombolysis, especially stroke. Two *in vitro* systems were used to evaluate the lytic response of porcine blood clots treated with rt-PA, with and without the addition of Definity[®] microbubbles and exposure to 120 kHz ultrasound. Additionally, a pilot *in vivo* study was done to produce a protocol for occlusion of the porcine ascending pharyngeal arteries as an arterial thromboembolism model. Please note that a vertical line in the left margin denotes text reprinted from a published paper (Huang et al. 2017).

In Chapter II, porcine D-dimer was evaluated as a metric for thrombolytic efficacy. Prior to this study, a protocol for purification of porcine D-dimer had not been published. The work described in Chapter II establishes a protocol for production and purification of porcine D-dimer. Additionally, we evaluated the use of a commercially available Asserachrom D-dimer ELISA kit and several commercially available D-dimer antibodies for use in an in-house ELISA kit to measure porcine D-dimer. Lastly, preliminary data was gathered for use of a D-dimer assay to measure thrombolytic efficacy *in vitro* thrombolysis samples.

In Chapter III, we present a pilot study in which the porcine APAs were bilaterally occluded with radiopaque and non-radiopaque clots. Recanalization was evaluated in clots treated with intraarterial rt-PA and saline. Additionally, a protocol was established for post-mortem excision of the ascending pharyngeal arteries.

An *in vitro* time lapse microscopy system was used to evaluate rt-PA thrombolysis in multiple permutations of porcine clots in Chapter IV - Chapter VI. In Chapter IV, cross-species thrombolysis experiments were completed to evaluate the effect of human plasminogen (found physiologically in human plasma) on rt-PA lytic susceptibility in porcine clots. Though the differential activity of human and porcine plasminogen was previously investigated (Flight et al. 2006), no studies have demonstrated the effects of this differential activity on thrombolysis in whole blood clots. This work has been published in Plos ONE (Huang et al. 2017).

In Chapter V, an *in vitro* thrombolysis system without flow (*in vitro* static thrombolysis system) and the *in vitro* time-lapse microscopy system were used to evaluate the effect of using BaSO₄ as a radiopaque dopant on rt-PA susceptibility of porcine whole blood clots. The possible effect of BaSO₄ on thrombolysis has not been investigated previously and represents a gap in knowledge.

In Chapter VI, pilot data is presented investigating the effects of human plasminogen and aspirin as two separate dopants to modify porcine thrombosis and thrombolysis activity. Modification of porcine clots is a step in developing a thrombotic stroke model in swine that mimic human hemostasis. The increased activity of human plasminogen compared to porcine plasminogen has been hypothesized to be a key factor for the resistance to rt-PA lysis shown by porcine clots (Flight et al. 2006; Huang et al. 2017). Aspirin has been shown to modify the structure of fibrin clots, increasing fibrin diameter, clot permeability, and rate of fibrinolysis (He et al. 2006; Williams et al. 1998).

In Chapter VII, the findings presented in this dissertation will be summarized and directions for future work will be discussed.

Chapter II. Exploration of a biochemical metric for clot mass loss

II.1 Background

The development of new therapies for ischemic stroke, such as sonothrombolysis, necessitates preclinical animal trials as a bridge between *in vitro* experiments and clinical trials. Historically, clinical metrics of recanalization and perfusion have been used in preclinical trials. For example, clinicians use the Thrombolysis in Brain Ischemia (TIBI) scale with transcranial Doppler to rate occlusions from 0, which indicates absent flow, to Grade 5, indicating normal flow (Demchuk et al. 2001), or the Thrombolysis in Cerebral Ischemia (TICI) scale with MRI or CT to grade occlusions from Grade 0, which indicates no perfusion, to Grade 3, indicating complete perfusion (Higashida et al. 2003). Though categorical recanalization is the clinical gold standard, the use of a continuous variable to detect differences between different treatment modalities may allow more sensitive detection of differences between treatment modalities, particularly in pre-clinical trials. Additionally, not all *in vivo* thrombolysis can be evaluated by metrics such as mass loss or recanalization. The porcine intracerebral hemorrhage (ICH) model is an example of a static *in vivo* thrombolysis model (Morgan et al. 2008; Wagner et al. 1996; Wagner et al. 1999; Wagner 2007) in which a biochemical assay to measure clot breakdown may be used to quantify thrombolytic efficacy.

D-dimer is a protein produced by the breakdown of fibrin by plasmin and is used as a metric clinically for diagnosis of certain thrombotic and thrombolytic diseases, particularly diseases involving venous thromboembolism (Adam et al. 2009). Previous *in vitro* studies have

employed commercial human D-dimer enzyme-linked immunosorbant assay (ELISA) kits to show that D-dimer concentration correlates with clot mass loss (Kimura et al. 1994; Pfaffenberger et al. 2003) or clot width loss (Petit et al. 2015). However, the evaluation of porcine D-dimer using human assays has shown varying success, with Munster *et al.* finding that D-dimer is not detectable using the Chromogenix Dimertest Gold EIA (Münster et al. 2002) and Velik-Salchner *et al.* finding that D-dimer was measurable using the D-Dimer Plus immunoassay from the (now defunct) Dade Behring (Velik-Salchner et al. 2006). More recent studies which have used human D-dimer assays to evaluate porcine D-dimer note that a lower D-dimer measurement is expected than the kit shows due to the species mismatch (Kjærgaard et al. 2012; Martini et al. 2014). No studies have established that a D-dimer ELISA kit for porcine samples is currently commercially available.

The objective of this chapter was to establish a protocol for measurement of porcine D-dimer concentration as an alternative metric for thrombolytic efficacy. In section II.2, we will present a protocol for the purification of porcine D-dimer for use as an assay standard. In section II.3, we will present data evaluating a commercially available human D-dimer assay for porcine use. In section II.4, we will present preliminary data evaluating commercially available anti-D-dimer antibodies for use in an in-house ELISA protocol. In section II.5, we will present preliminary data evaluating the hypothesis that porcine D-dimer concentration correlates with mass loss in porcine clots *in vitro*.

II.2 D-dimer Purification

II.2.1 Materials & Methods

Fibrin clots were produced using porcine plasma, then minced and lysed with the aid of rt-PA and human plasminogen. This lysate was sequentially purified using an ammonium sulfate precipitation and a gel filtration column. Known human and porcine fibrinogen sequences were aligned to produce a predicted porcine D-dimer sequence in order to calculate the expected molar mass, N-glycosylation, and the extinction coefficient to estimate protein concentration. D-dimer purity was evaluated on an SDS-PAGE and the protein identity was confirmed with immunoblotting and MALDI TOF-TOF analysis.

II.2.1.1 Materials

Frozen pooled porcine plasma anticoagulated with sodium citrate was purchased from Lampire Biological Laboratories (Lampire Biological Laboratories, Inc. Pipersville, PA, USA). Bovine thrombin was purchased from BioPharm Laboratories (BioPharm Laboratories, LLC, Bluffdale, UT, USA). Human plasminogen was purchased from Athens Research (Athens Research & Technology, Athens, GA, USA). Recombinant tissue-type plasminogen activator (rt-PA) was obtained from Genentech (Activase, Genentech, San Francisco, CA, USA), reconstituted with sterile water according to manufacturer instructions to a concentration of 1 mg/mL, and aliquotted and stored at -80 °C until use, which has been shown to have stable activity for at least 7 years (Shaw et al. 2009b). Chemical reagents (acetic acid, ammonium sulfate, calcium chloride, citric acid, Coomassie Brilliant Blue R-250, cysteine, EDTA, glycine, methanol, sodium acetate, sodium bromide, sodium chloride, sodium dodecyl sulfate, Tris-base) were obtained from ThermoFisher Scientific (Waltham, MA, USA).

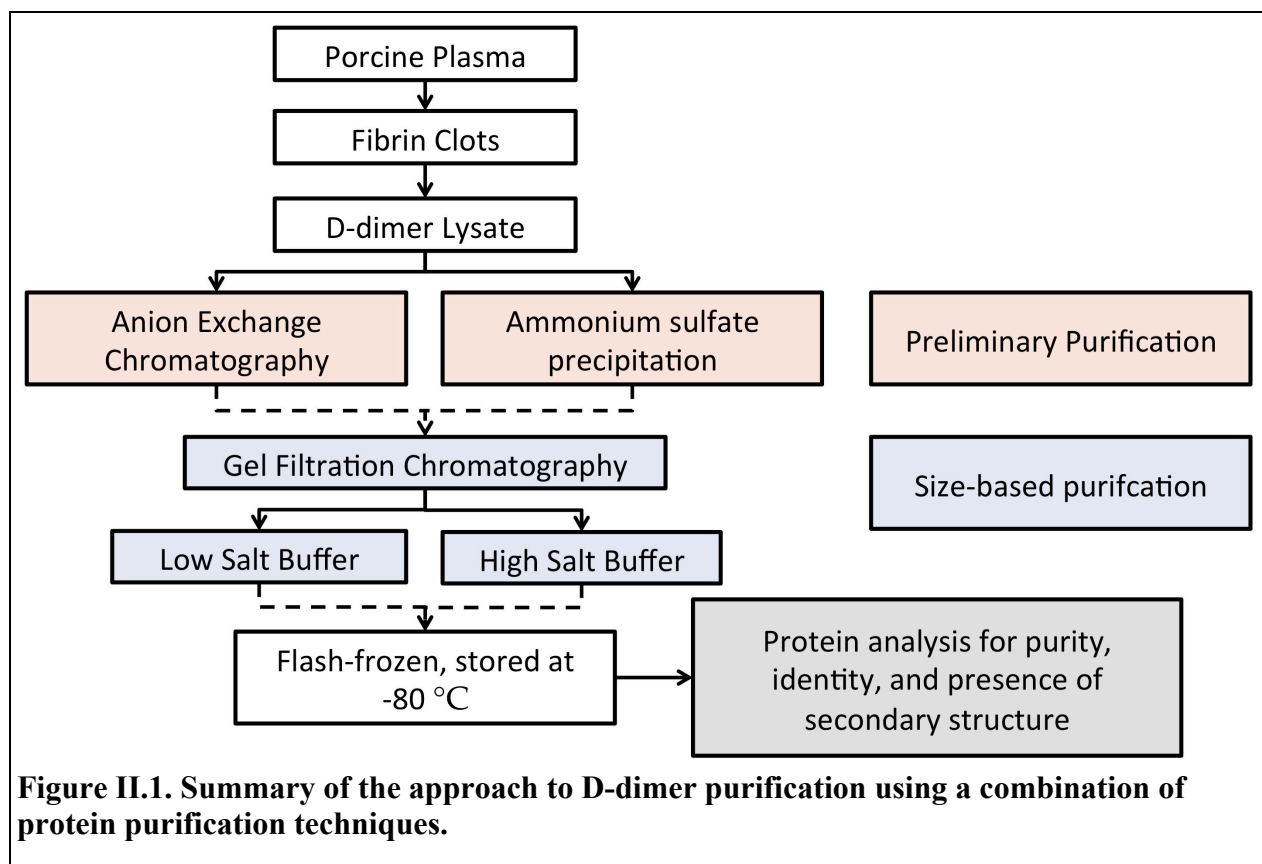
II.2.1.2 Production of porcine D-dimer

A protocol for producing purified porcine D-dimer was adapted from previously published studies purifying human D-dimer (Masci et al. 1985; Olman et al. 1998; Spraggon et al. 1997). Frozen porcine plasma was thawed and filtered through 4x4 gauze pads (Fisher Healthcare, Pittsburgh, PA, USA) to remove fibrin clots that had formed in transit. Porcine plasma was centrifuged at 2000xg for 15 minutes in a refrigerated centrifuge. In 15 mL centrifuge tubes (Globe Scientific, Paramus, NJ, USA), platelet-poor supernatant was combined with calcium chloride (40 mM final concentration), cysteine (6 mM final concentration), and bovine thrombin (5 U/mL final concentration), and vortexed to mix thoroughly. Fibrin clots were allowed to form over 2 hours at room temperature and then were pressed between low-lint tissue (Kimberly-Clark Professional, Roswell, GA, USA) under a heavy tray for 10 minutes. Clots were washed for 1 hour at 4 °C in 0.67 mM citric acid, 150 mM sodium chloride, and 40 mM EDTA buffer, at pH 7.4. The clots were rinsed with a 150 mM sodium chloride solution three times, and washed for at least 16 hrs in 150 mM sodium chloride at 4 °C. Clots were blotted again between pieces of low-lint tissue paper for 10 minutes. The blotted clots were weighed and minced using a razor. Minced clots were added to a lysis buffer with 50 mM Tris, 150 mM NaCl, 5 mM CaCl₂, 0.5 U/mL human plasminogen, and 240 µg/mL rt-PA and placed at 37 °C for 3 hours. Lysis was allowed to continue at 4 °C overnight and the lysate was centrifuged for 30 minutes at 4800g to remove insoluble fibrin fragments. The resultant lysate can be seen in lane 1 of Figure II.2b.

II.2.1.3 Purification of porcine D-dimer

D-dimer purification was approached using a combination of protein separation techniques based on protein charge, solubility, and size, which are summarized in Figure II.1. In

anion exchange chromatography, proteins are bound to a positively charged resin based on electrostatic interactions and the negative ions in a buffer with a progressively increasing salt concentration releases proteins from the resin by competing for binding sites. Anion exchange can be of limited use when the protein of interest and contaminants are similar in sequence and charge, as proteins may elute off the column in overlapping peaks. Protein separation based on solubility was attempted by adding ammonium sulfate stepwise, gradually increasing hydrophobic interactions between proteins and decreasing protein solubility, until the protein of interest has been precipitated. Ammonium sulfate precipitations also have the effect of concentrating the protein of interest, which can help preserve protein yield. Lastly, gel filtration chromatography relies on protein size and shape to separate proteins, with large proteins passing through a gel filtration column more quickly than small proteins. Each gel filtration column has an approximate size cut-off, above which size proteins cannot be reliably separated, and size-based separation can also depend on the selection of an appropriate buffer to prevent aggregation and co-migration of discrete protein species.



In brief, anion exchange chromatography and ammonium sulfate precipitation were investigated as a preliminary purification step prior to the use of gel filtration chromatography. We expected that in the D-dimer lysate, gel filtration would be necessary as many of the proteins would be derived from fibrin and fibrinogen and have similar charge and solubility. On SDS-PAGE analysis of the D-dimer lysate, we see our D-dimer band between 150 and 250 kDa, as well as many contaminants. There is a large-molecular weight (MW) contaminant (>250 kDa) that is most likely fibrinogen (340 kDa). D-monomer can be seen at approximately 100 kDa and there are many smaller peptides that are likely other fibrin degradation products (Ferguson et al. 1975).

An AktaPure L fast protein chromatography (FPLC) system (GE Healthcare Life Sciences, Pittsburgh, PA, USA) was used for column chromatography, with 4 mL fractions collected through each run. Anion exchange chromatography was performed with 5 mL HiTrap

Q HP Column (GE Healthcare Life Sciences). D-dimer lysate was dialyzed into a starting buffer of 20 mM Tris buffer with 50 mM NaCl and 5 mM CaCl₂, pH 7.4. Protein was loaded into the column and subsequently eluted with a linear gradient from the starting buffer to 40% 20 mM Tris buffer with 1 M NaCl and 5 mM CaCl₂, pH 7.4.

Gel filtration chromatography was also evaluated with a HiLoad 16/600 Superdex 200 (S200) prep grade column (GE Healthcare Life Sciences). Prior to the gel filtration column, D-dimer was partly purified using an ammonium sulfate precipitation step. Saturated ammonium sulfate solution was added to the lysate to an ammonium sulfate saturation of 35% and placed on ice for 10 minutes. The lysate was centrifuged (10 min, 16000g) and the supernatant retained. Saturated ammonium sulfate was further added to the lysate to an ammonium sulfate saturation of 50%, placed on ice for 10 min, and centrifuged at 16000g for 10 min. Two gel filtration buffers were evaluated, and the ammonium sulfate pellet was directly reconstituted with the gel filtration buffer in use. First, a standard low salt gel filtration buffer of 20 mM Tris with 150 mM NaCl and 5 mM CaCl₂, pH 7.3 was used. Second, a high salt buffer of 50 mM sodium acetate buffer with 1 M NaBr and 5 mM CaCl₂, pH 5.3 was used, based on a published protocol for purification of human d-dimer (Spraggon et al. 1997). Prior to the SDS-PAGE analysis, fractions with 1 M NaBr were dialyzed into a lower-salt buffer (20 mM Tris buffer with 150 mM NaCl, 5 mM CaCl₂, pH 7.4).

II.2.1.4 Evaluation of porcine D-dimer concentration & storage

The amino acid sequences for human fibrinogen (accession numbers AAC97143, AAA18024, and AAB59531 for the α , β , and γ chains respectively) and predicted porcine fibrinogen (accession numbers XP_003129178, XP_013834277, and XP_003361238 for the α , β , and γ chains, respectively) were aligned using the T-COFFEE online Multiple Sequence

Alignment server (Centre for Genomic Regulation, Barcelona, Spain) (Di Tommaso et al. 2011; Notredame et al. 2000). The sequence for human D-dimer (Protein Data Bank 1FZB) was used to determine the most likely cleavage sites on porcine fibrinogen to produce a predicted porcine D-dimer sequence. The ProtParam tool (Swiss Institute of Bioinformatics, <http://web.expasy.org/protparam/>) was used to calculate the non-glycosylated MW (168269.4 g/mol) and extinction coefficient (343320 to 345320 M⁻¹ cm⁻¹, depending on reduction of cysteine residues) based on the predicted porcine D-dimer sequence. The NetNGlyc 1.0 Server (Gupta et al.) (Center for Biological Sequence Analysis, <http://www.cbs.dtu.dk/services/NetNGlyc/>) was used for N-glycosylation site prediction. It was assumed that each glycosylation site had a complex biantennary core N-glycan (MW of 1623.5 g/mol each, adjusted D-dimer MW of 171516.3 g/mol). The purified protein concentration was measured as the absorbance at 280 nm (A₂₈₀) using a NanoDrop 2000 UV-Vis Spectrophotometer (ThermoScientific, Wilmington, DE, USA) and converted to g/mL using the extinction coefficient and molecular weight. The protein concentration was adjusted to 1 mg/mL and the protein was aliquotted, flash-frozen, and stored at -80 °C to prevent degradation.

II.2.1.5 SDS-PAGE and Coomassie Staining

SDS-PAGE was conducted using 4-20% Mini-PROTEAN® TGX™ Precast Protein Gels (Bio-Rad Laboratories, Inc., Hercules, CA, USA) at 175 V for 40 min at 25 °C with a 25 mM Tris, 250 mM glycine, and 0.1% SDS (TGS) running buffer (pH 10). Samples were combined with Laemmli sample buffer (Bio-Rad Laboratories, Inc.) under non-reducing conditions and heated at 95 °C for 5 min before loading. Precision Plus Protein Dual Color Standards were used for protein size identification (Bio-Rad Laboratories, Inc.). Gels were stained with Coomassie

R250 (0.1% Coomassie R250, 50% methanol, 10% acetic acid, and 40% ddH₂O) to visualize all proteins or transferred to a nitrocellulose membrane for immunoblotting.

II.2.1.6 Immunoblotting

The SDS-PAGE gel produced for the immunoblotting used a target D-dimer protein loading of 3-4 µg per lane. An Invitrogen Novex Semi-Dry Blotter (ThermoFisher Scientific, Waltham, MA, USA) was used to transfer proteins from protein gel to 0.45 µm nitrocellulose paper (GE Healthcare Lifesciences, Pittsburgh, PA, USA) at 10-12 V for 75 min at 25 °C with a 25 mM Tris, 190 mM glycine, 20% methanol transfer buffer. Nonspecific binding sites on the membrane were blocked in 5% powdered milk (Meijer, Grand Rapids, MI, USA) for 30 min, and blotted with mouse anti-human-D-dimer primary antibody (DD93, abcam, Cambridge, MA, USA) at 5 µg/mL and a sheep anti-mouse-HRP secondary antibody (NXA931, GE Healthcare Life Sciences) at 1:5000 dilution. DD93 had previously been discovered in our lab to cross-react with porcine D-dimer. The membrane was developed with chemiluminescent substrate (ThermoFisher Scientific) for 5 min prior to imaging.

II.2.1.7 Circular Dichroism (CD) Spectroscopy

CD spectroscopy was performed to confirm presence of secondary structure and evaluate any prospective adverse effects from freeze/thaw cycles. Far-UV spectra were evaluated at 25 °C using a AVIV Circular Dichroism Spectrometer (Model 315, AVIV Biomedical, Inc., Lakewood, NJ, USA). CD spectra were calculated from the average of 3 wavelength scans for each protein sample. Protein samples were dialyzed into 10 mM Tris buffer with 50 mM NaF, pH 7.4 and diluted to 0.1 mg/mL for measurement in a 0.50-mm quartz cuvette (Hellma Analytics, Müllheim, Germany). Mean residue ellipticity ($[\theta]$, MRE) was calculated from machine units in millidegrees (θ) using the following equation:

$$[\theta] = \frac{\theta \times MRW}{10 \times c \times l} \quad (\text{II.1})$$

where MRW is the mean residue weight (MW/# of residues), c is the protein concentration in mg/mL, and l is the path length in cm.

II.2.1.8 Matrix Assists in Laser Desorption/Ionization-Time of Flight Tandem Mass

Spectroscopy (MALDI TOF-TOF)

The protein band of interest was excised from a Coomassie-stained SDS-PAGE gel, reduced with dithiothreitol, alkylated with iodoacetamide, and digested with trypsin. The peptides were extracted, dried, and resuspended in 0.1% formic acid, then mixed with alpha cyano 4-hydroxy cinnamic acid (HCCA) matrix and spotted for MALDI TOF-TOF analysis. The resultant sequences were compared to the Mascot database.

II.2.2 Results

II.2.2.1 Purification of D-dimer

The protocol that produced the purest porcine D-dimer employed a high-salt (1 M NaBr) buffer over the S200 gel filtration column (Figure II.2). The leading peak was largely D-dimer, but exhibited a shoulder on the front end that contained a large-molecular weight (MW) contaminant (Figure II.2, fraction 14; see green arrow). Leading peak fractions (fraction 15-16) that did not contain this large-MW contaminant were pooled to form the D-dimer standard. A small-MW contaminant can also be seen in the leading peak around 75-100 kDa in size.

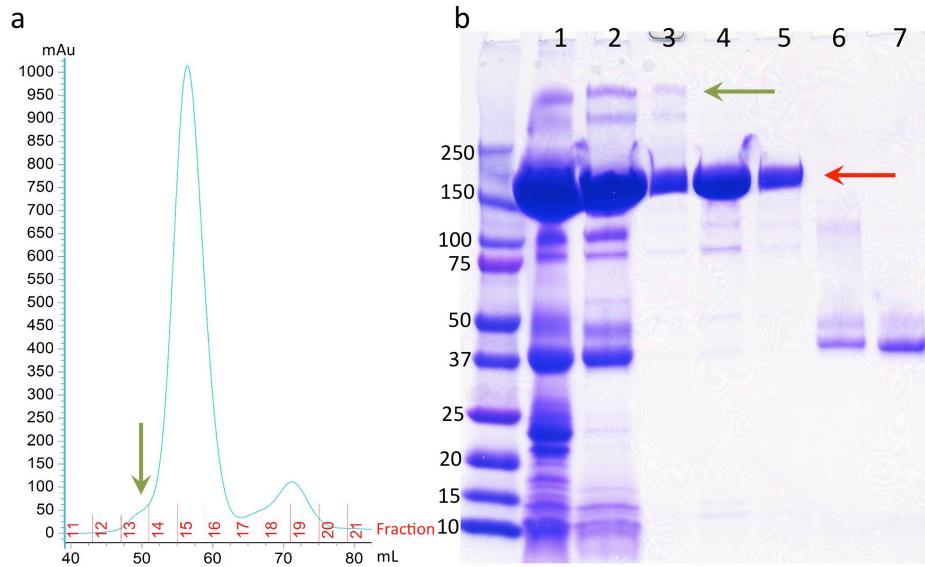


Figure II.2. (a) Representative chromatogram of a S200 gel filtration separation of fibrin degradation products with 50 mM sodium acetate buffer with 1 M NaBr and 5 mM CaCl₂, pH 5.3. **(b)** SDS-PAGE of purification steps, including fractions from the chromatograph: lane 1 – D-dimer lysate, 2 – Reconstituted 50% ammonium sulfate pellet, 3 – Fraction 14, 4 – Fraction 15, 5 – Fraction 16, 6 – Fraction 18, 7 – Fraction 19. The red arrow points out the porcine D-dimer and the green arrows point out the large-MW contaminant in the gel and the chromatogram.

The anion exchange protocol and gel filtration using a standard low-salt buffer both yielded some separation of D-dimer from other protein species (Figure II.3 & Figure II.4 respectively). However, in both cases, a small-MW species (approximately 37 kDa) migrated through the column with the D-dimer and could not be separated.

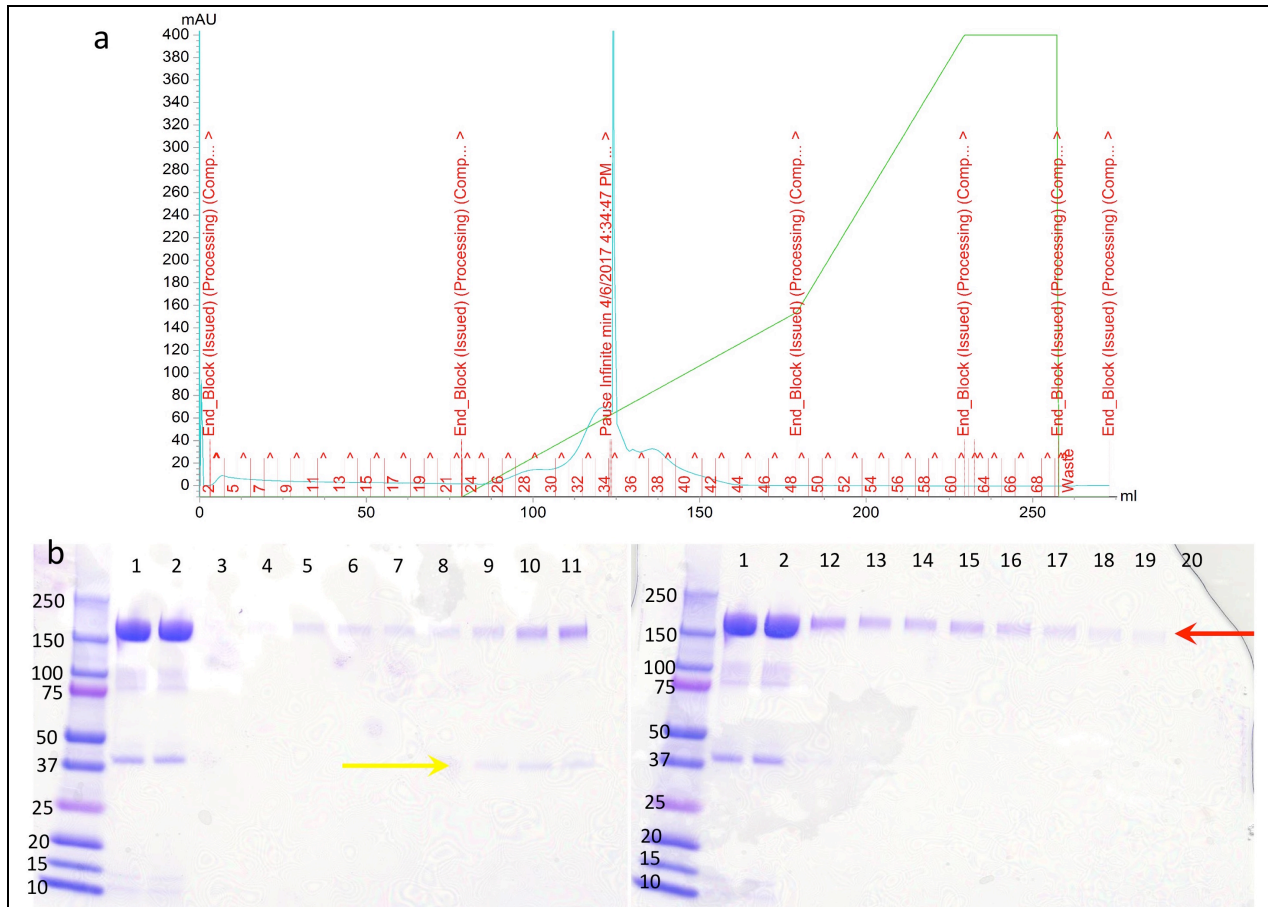
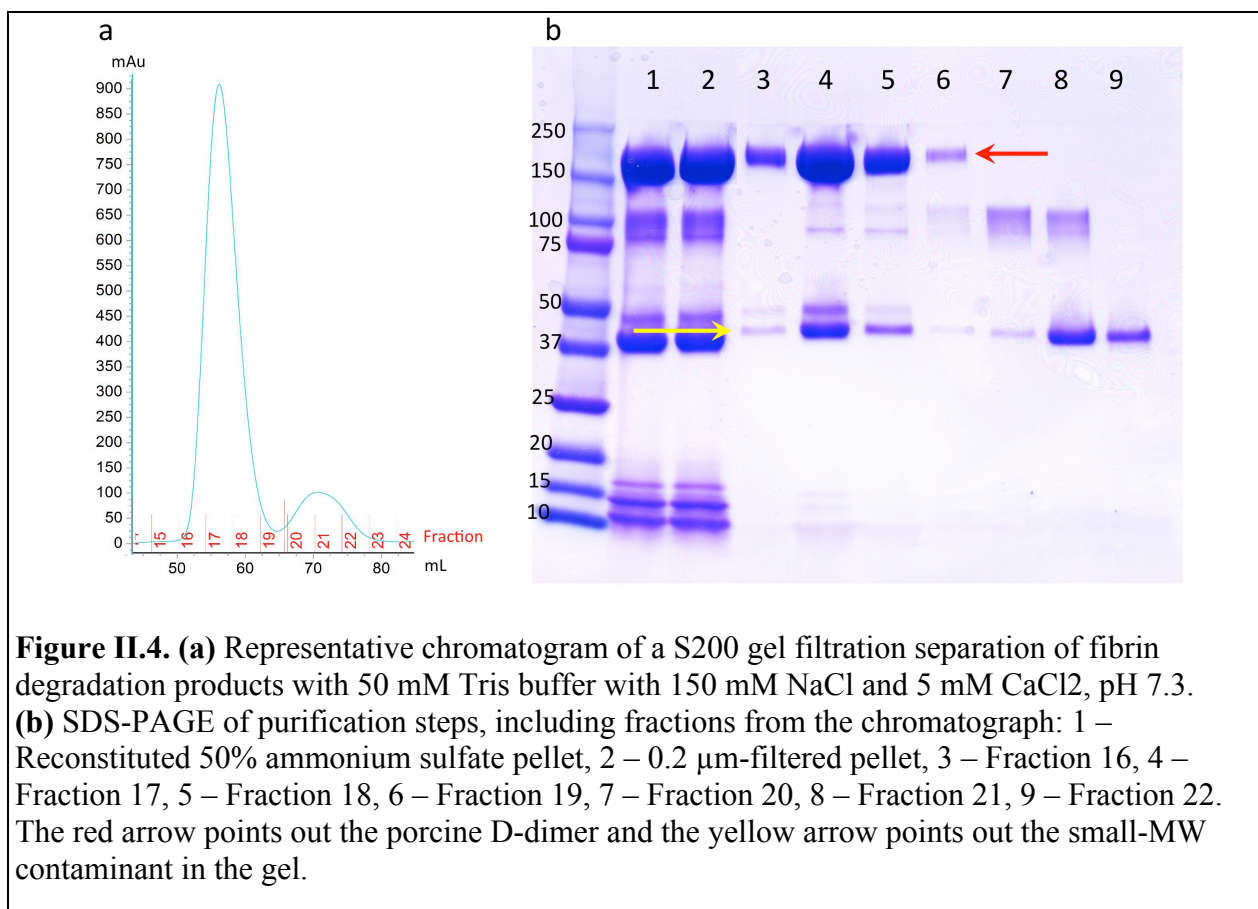


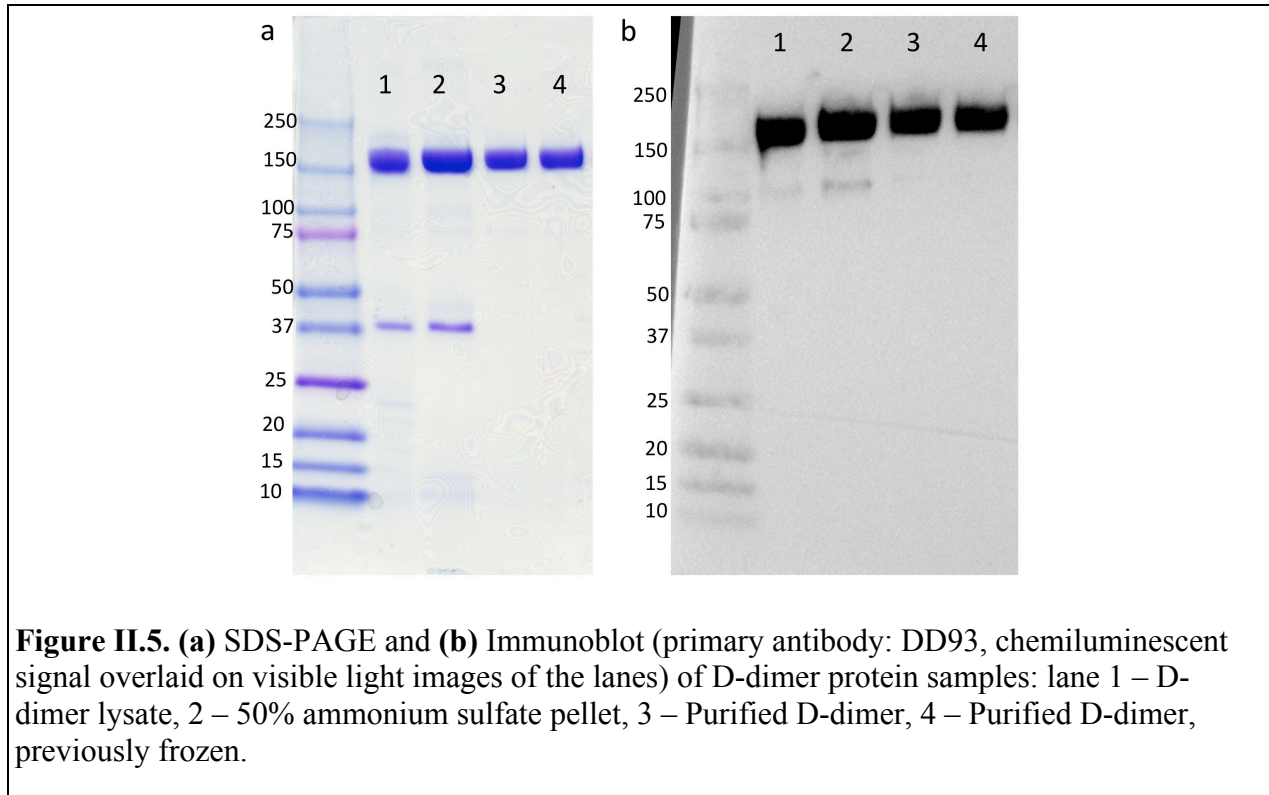
Figure II.3. (a) A chromatogram of an anion exchange separation of fibrin degradation products. (The spike arose from a pause in the run.) **(b)** SDS-PAGE of the fractions from the chromatograph, with lane 1 – D-dimer lysate and 2 – 0.2-µm filtered lysate, 3-20 – Fraction 26-43 respectively. The red arrow points out the porcine D-dimer and the yellow arrow points out the small-MW contaminant.



II.2.2.2 Confirmation of D-dimer identity and secondary structure

Immunoblotting was performed on purified and non-purified D-dimer samples (Figure II.5) and confirmed the presence of a D-dimer species that matches the SDS-PAGE band of our expected protein. Far-UV CD spectra (Figure II.6) of the purified D-dimer samples showed a strong negative mean residue ellipticity (MRE) between 210 and 230 nm, with a minimum around 220 nm. The spectrum is indicative of a folded protein containing a mixture of β -sheet and α -helical secondary structures, which show characteristic minima near 217 nm (β -sheet) or at 208 and 222 nm (α -helix) (Chen et al. 1972). These data are consistent with published crystal structures of human fibrin D-dimer, which shows both alpha helical (27% of total residues) and beta sheet (20% of total residues) secondary structure (Spraggon et al. 1997). The flash-frozen D-dimer sample exhibited a spectrum that was slightly less negative near the minimum

compared to the never-frozen sample, but the two spectra otherwise overlapped, showing minimal effect from the freeze/thaw cycle, with the previously frozen spectra showing roughly 95% of signal of the never-frozen spectra.



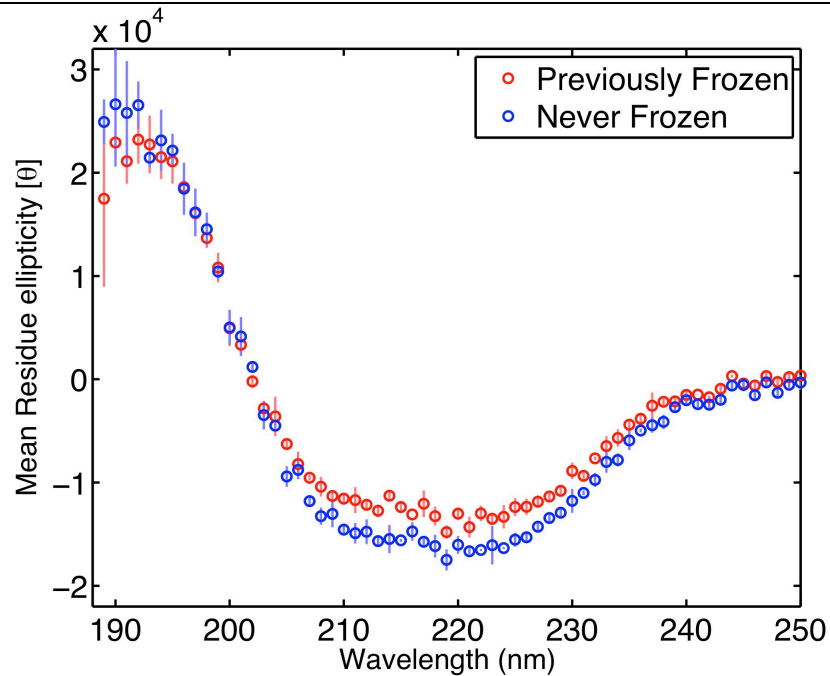


Figure II.6. CD spectra of pure D-dimer at a concentration of 0.1 mg/mL in 20 mM Tris **buffer**.

MALDI TOF-TOF analysis of the D-dimer band showed sequence matches with the alpha- and beta-chains of porcine fibrinogen. Four unique peptide sequences were detected that matched the porcine fibrinogen-beta (27% coverage compared to the predicted porcine D-dimer beta chain), and 2 unique peptide sequences were detected that matched porcine fibrinogen-alpha (24% coverage compared to predicted porcine D-dimer alpha chain). Peptide sequences that matched porcine fibrinogen- γ were not detected. The overall coverage of the predicted porcine D-dimer sequence was 17%.

II.2.3 Discussion

The purification of porcine D-dimer, a fibrin degradation product (FDP), presented several challenges. No papers have been published detailing the purification of porcine D-dimer. Though comparison of human and porcine fibrinogen showed 90, 99, and 99 sequence

conservation for the α , β , and γ chains respectively, it was non-trivial to find sufficiently cross-reactive antibodies and adapt previously published human D-dimer purification protocols (Masci et al. 1985; Olman et al. 1998; Spraggon et al. 1997) for use with porcine proteins. For instance, Spraggon *et al.* added ammonium sulfate to 25% saturation to precipitate out human D-dimer (Spraggon et al. 1997), and we found that porcine D-dimer precipitated between 35 and 50% ammonium sulfate saturation, indicating a marked difference in solubility. At ammonium sulfate saturations of 10, 20, and 30%, minimal D-dimer was precipitated.

The other challenge was that the D-dimer lysate contained fibrin, D-dimer, and many other FDPs that were difficult to distinguish from D-dimer biochemically. We observed this in the anion exchange chromatography, in which we observed a protein species at approximately 37 kDa elute with our protein of interest (Fig 2). Given the size difference, it may have been feasible to combine anion exchange with size exclusion chromatography following a concentration step. However, we elected to combine ammonium sulfate precipitation with size exclusion chromatography instead to preserve protein yield. A standard low-salt, neutral-pH gel filtration buffer also produced fractions with D-dimer and a low-MW contaminant at approximately 37 kDa. The high-salt, low-pH gel filtration buffer, previously used by Spraggon *et al.* (Spraggon et al. 1997), allowed sufficient separation between D-dimer and the low-MW contaminant. This is likely due to either aggregation of either multiple low-MW contaminant proteins or the low-MW contaminant with D-dimer in the low-salt buffer that was interrupted by either the high salt or a change in protein charge due to a lower pH.

The identity of our purified D-dimer was confirmed using immunoblotting and MALDI-TOF/TOF sequencing. DD93 is noted to cross-react with a cross-linked region of D-dimer on the gamma chain and exhibit limited non-specific binding (e.g., to D-monomer). MALDI TOF-TOF

analysis showed that our protein sample matched sequences from the alpha and beta chains of fibrinogen at approximately 25% coverage, though no sequence matches from the gamma chain were seen. The lack of sequence matches from the gamma chain is most likely due to the presence of cross-linking in the D-dimer gamma chain (specifically between Gln398 and Lys406 (Spraggon et al. 1997)), which is not always reflected in protein sequence databases.

CD spectroscopy was also used to evaluate the presence of secondary structure. It is known that alpha helical secondary structure contributes to a strong negative signal between 205 nm and 230 nm, with global minima around 208 and 220 nm (Chen et al. 1972). Alpha helices also cause a positive global maximum around 190-195 nm (Chen et al. 1972). Our CD spectra show evidence of strong alpha helical structure. However, there is a stronger negative signal around 210 nm than would be derived from alpha helices alone. Beta sheet secondary structure produces a small negative signal in the CD spectra around 217 nm (Chen et al. 1972), likely contributing to the "smoothing out" of our CD spectra between 210 and 230 nm. Any residues in an unordered secondary structure confirmation would depress the alpha helical signal at lower wavelengths (205 nm and lower). While no CD spectra of either human or porcine D-dimer have been previously published, our data is consistent with published X-ray crystallography data for human D-dimer, which shows that D-dimer has both alpha helical (27% of total residues) and beta sheet (20% of total residues) secondary structure (Spraggon et al. 1997). The rest of the protein (53%) is in an unordered confirmation (Spraggon et al. 1997).

II.3 Biochemical quantification of porcine D-dimer with the Asserachrom kit

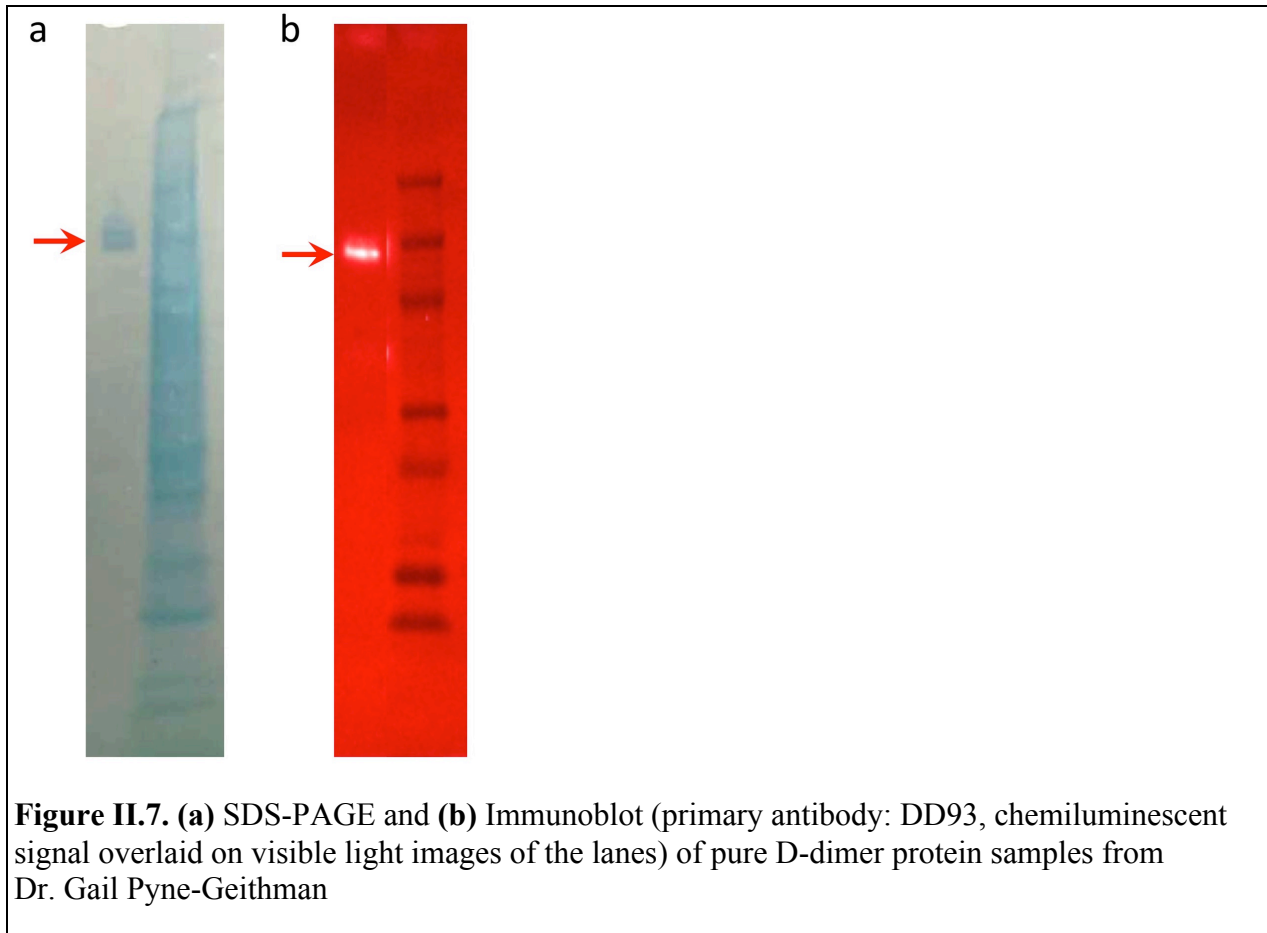
As noted in previously published literature, the homology between human and porcine D-dimer has allowed use of human D-dimer quantification assays to quantify porcine D-dimer

(Münster et al. 2002; Petit et al. 2015; Velik-Salchner et al. 2006). However, as noted in Chapter II.2.3, even two proteins with 90-99% conserved amino acid sequence may have significantly different surface properties, affecting solubility as well as the binding of antibodies to surface epitopes. As a result, there is no guarantee that any one anti-human D-dimer immunoassay would also detect porcine D-dimer. The Asserachrom D-dimer ELISA kit has previously been used in multiple clinical trials for thrombotic disease (Adam et al. 2009; Indik and Alpert 2000). This type of microplate ELISA features a high sensitivity to human D-dimer but does not require the use of proprietary equipment (Adam et al. 2009). The objective of this study was to evaluate the cross-reactivity of the Asserachrom assay with porcine protein. Additionally, the experiments presented in this section were completed in 2 3-month spans 3 years apart, and each experiment and the associated results will accordingly be labeled as occurring in 2014 or 2017.

II.3.1 Materials and Methods

II.3.1.1 Materials

An Asserachrom D-dimer ELISA kit (Diagnostico Stago, Asnieres sur Seine, France) was purchased from Diagnostico Stago. Two sources of porcine D-dimer were used over the course of the experiments presented in this section. The porcine D-dimer used for evaluation of the Asserachrom ELISA kit in 2014 experiments was acquired from Dr. Gail Pyne-Geithman in frozen aliquots at a concentration of 1 mg/mL prior to the development of our D-dimer purification protocol (Chapter II.2). The identity of this porcine D-dimer was verified using SDS-PAGE and immunoblotting using the primary anti-D-dimer antibody DD93 as detailed in Chapter II.2.1 (Figure II.7). Porcine D-dimer used for evaluation of the Asserachrom kit in 2017 was produced as detailed in Chapter II.2. Additionally, separate lots of the Asserachrom kit were used for the 2014 and 2017 experiments as each kit expires roughly 1 year after purchase.



II.3.1.2 Evaluation of the sensitivity of the Asserachrom ELISA kit to porcine D-dimer (2014)

Each purchased ELISA kit included 96-well sized test strips (pre-incubated with capture antibody), anti-D-peroxidase, 3,3',5,5'-tetramethylbenzidine (TMB) solution, dilution buffer, wash buffer, and human D-dimer calibrator. Porcine D-dimer standard was serially diluted using the kit dilution buffer to in-well concentrations from 2.5 to 1280 ng/mL to evaluate the sensitivity of the kit to a known porcine standard. The kit protocol was otherwise followed as written. Briefly, the samples or standards were incubated within the wells of the test strips for 1 hr and washed with kit wash buffer. Anti-D-peroxidase was added and allowed to incubate for 1 hour. After a second wash with kit wash buffer, TMB solution was plated into wells and

allowed to develop for 5 min, after which sulfuric acid is used to stop conversion of colorless TMB into tetramethylbenzidine diimine. For simplicity, the concentration of porcine D-dimer standards will be discussed in terms of in-well concentration. Each standard or sample was evaluated in duplicate. The sensitivity of the kit was chosen to be the lowest concentration at which the blank-subtracted mean absorbance minus 2 times the standard deviation was greater than 0.

II.3.1.3 Evaluation of porcine D-dimer detection with the Asserachrom ELISA kit with and without hemoglobin (2014)

Porcine D-dimer standards were combined with 2 concentrations of porcine hemoglobin (5 g/L and 50 g/L in-well) to evaluate the effect of hemoglobin on the sensitivity of the Asserachrom kit. Additionally, Hemoglobind (Biotech Support Group) was used to deplete hemoglobin from contaminated samples according to manufacturer's instructions to evaluate the effect of removing hemoglobin on D-dimer concentration. Briefly, equal parts Hemoglobind and sample were combined, vortexed for 30 seconds, and mixed by inversion for 15 min. Samples were centrifuged for 2 minutes at 9000 rpm and the supernatant was retained for testing.

II.3.1.4 Evaluation of the sensitivity of the Asserachrom ELISA kit to porcine D-dimer over time (2017)

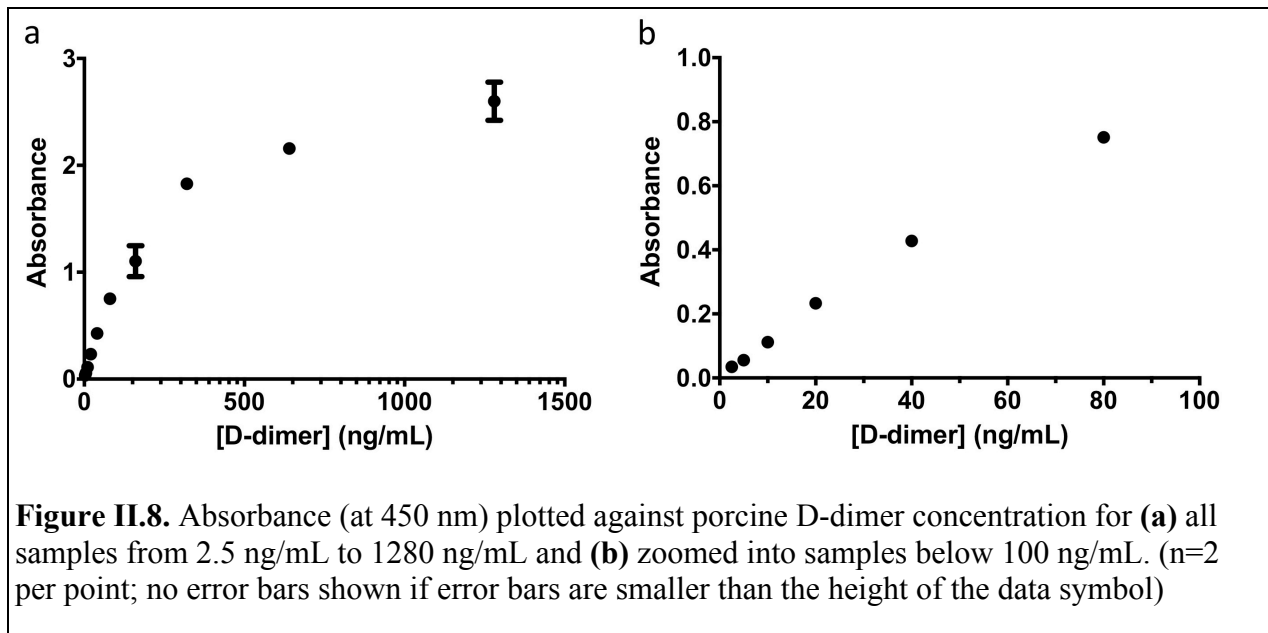
As mentioned, the previously described preliminary assessments of Asserachrom kit sensitivity to D-dimer were completed in 2017. More recently, the Asserachrom kit has been reevaluated using porcine D-dimer standard prepared as detailed in Chapter II.2 and newly purchased . Porcine D-dimer was diluted in kit dilution buffer to in-well concentrations between 5 ng/mL and 1000 ng/mL and the kit protocol was followed as described previously, with the exception that the TMB was allowed to develop for longer than 5 min. Samples were taken after

each step in the porcine D-dimer purification process and evaluated using the Asserachrom kit for cross-reactivity. Additionally, an aliquot of a previously analyzed porcine clot sample (analyzed in the Asserachrom kit, 2014) (see Chapter II.5.1 for the generation of clot samples) was re-analyzed with the current set of Asserachrom kits (2017). The aliquot was stored at -80 °C in the intervening 3 years.

II.3.2 Results

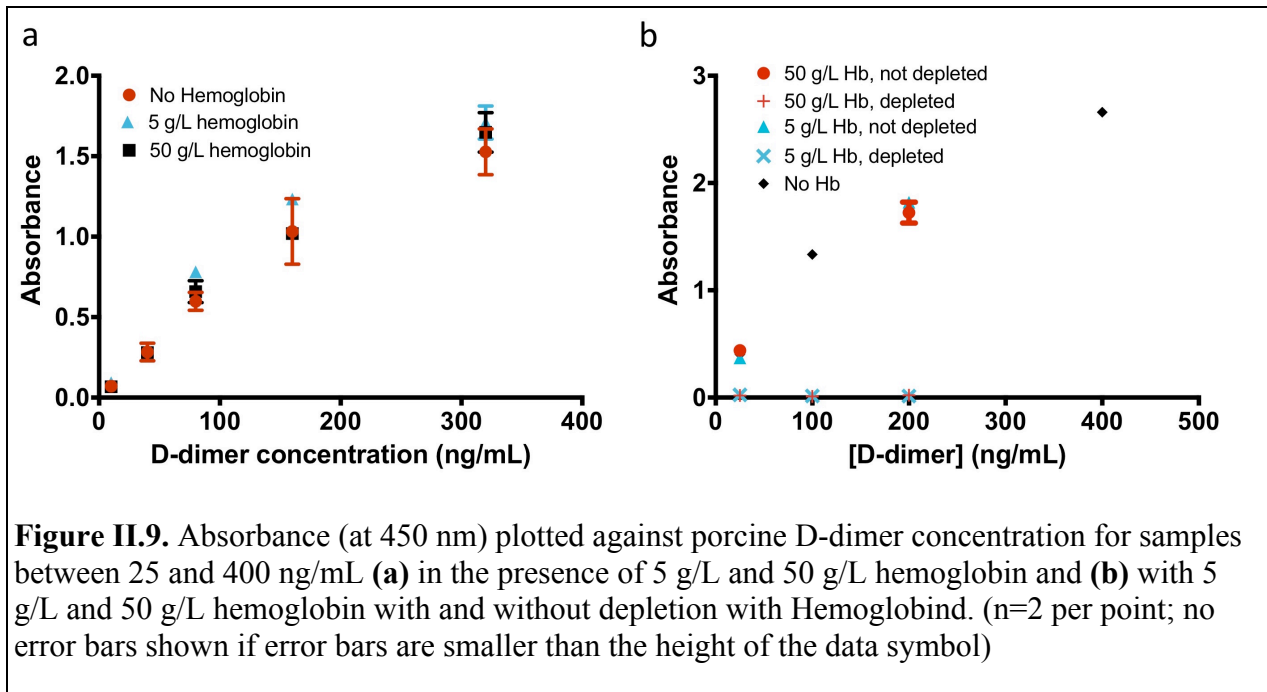
II.3.2.1 Evaluation of the sensitivity of the Asserachrom ELISA kit to porcine D-dimer (2014)

Porcine D-dimer was recognized by the Asserachrom kit at concentrations between 2.5 and 1280 ng/mL (Figure II.8). At concentrations of 320 ng/mL and above, the slope of the absorbance vs. D-dimer concentration approaches zero. The sensitivity limit of the Asserachrom kit was an in-well porcine D-dimer concentration of 5 ng/mL.



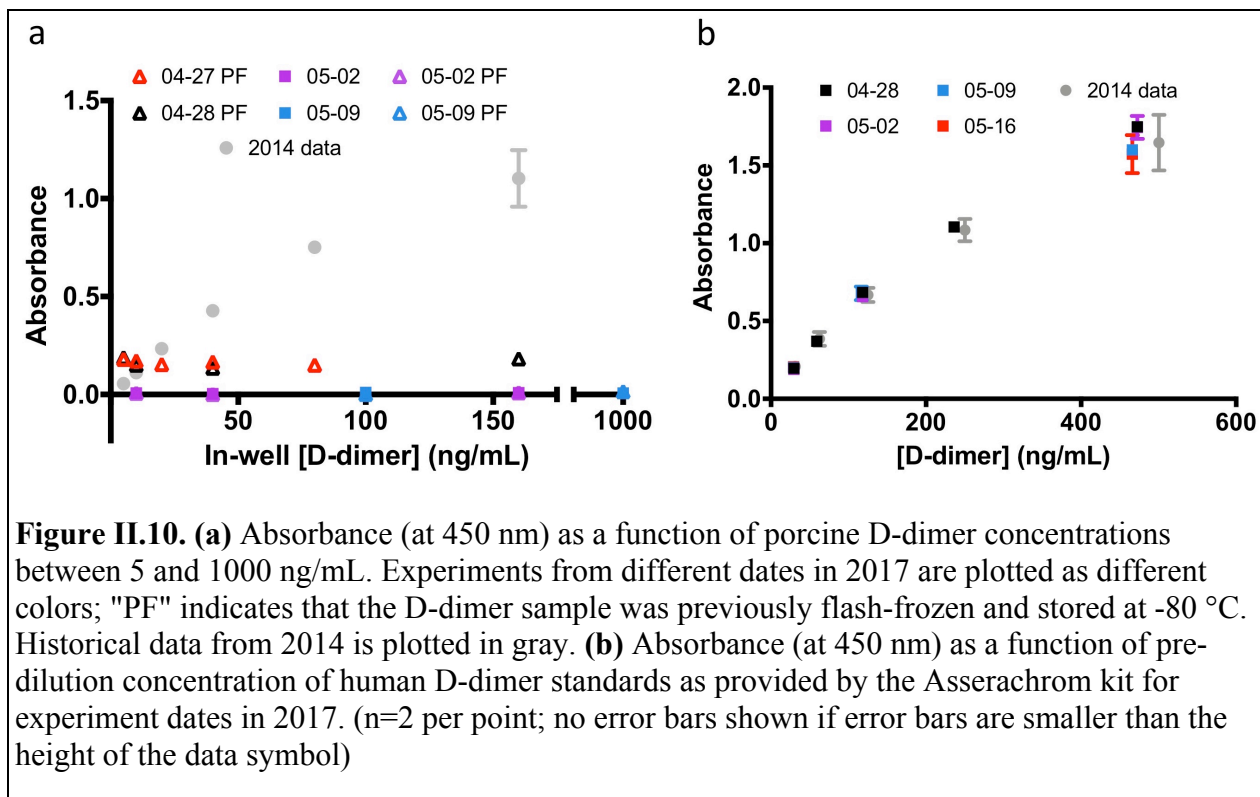
II.3.2.2 Evaluation of porcine D-dimer detection with the Asserachrom ELISA kit with and without hemoglobin (2014)

The addition of up to 50 g/L hemoglobin did not significantly change the detection of D-dimer by the Asserachrom kit (Figure II.9a). However, the use of Hemoglobind to deplete hemoglobin-containing D-dimer samples reduced the signal from the Asserachrom kit to an undetectable level (Figure II.9b).



II.3.2.3 Evaluation of the sensitivity of the Asserachrom ELISA kit to porcine D-dimer over time (2017)

Recent use of the Asserachrom kit (2017) has shown that the kit no longer exhibits sufficient reactivity to porcine samples even at in-well concentrations of up to 1000 ng/mL (Figure II.10a). Simultaneous use of the kit with the human kit standard exhibited the expected increased absorbance with increased D-dimer concentration (Figure II.10b).



To evaluate whether our new D-dimer purification process had affected D-dimer structure or stability, we incubated samples following each step of D-dimer purification in the Asserachrom kit (Figure II.11). However, these samples also showed low absolute absorbance values (0.5 and lower) at each step. The absorbance divided by A₂₈₀ (correcting the raw absorbance with an approximate estimate of total protein concentration [see Chapter II.2.1.4]) is similar between the different steps of the purification protocol. Additionally, reanalysis of a historically evaluated sample shows that Asserachrom kits in 2017 exhibits lower absorbance with a longer TMB incubation compared to the kits used in 2014 (Table II.1).

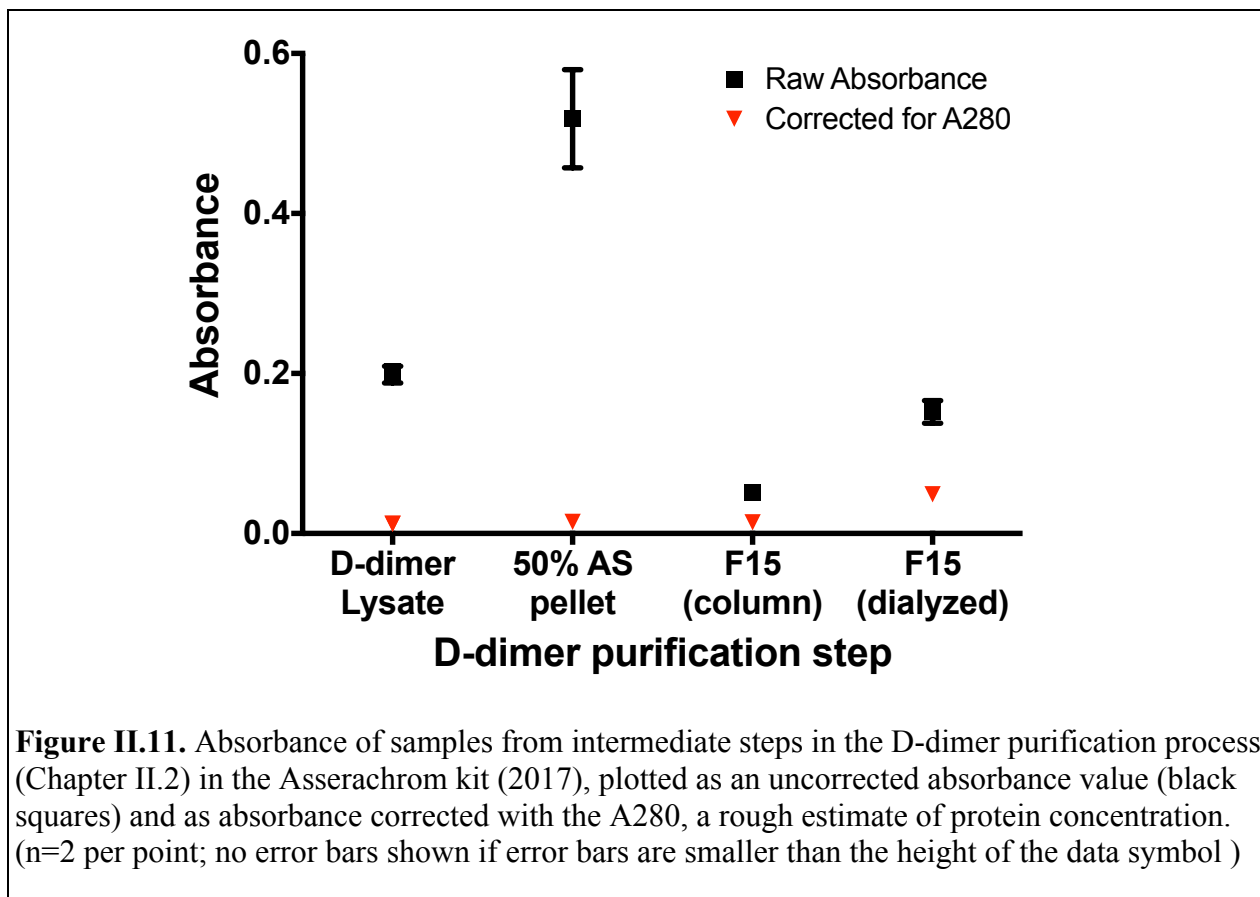


Table II.1. Absorbance over time for D-dimer lysate and a porcine clot sample (P101.11C), with noted Asserachrom kit lot and length of TMB development.

Sample	Date	Asserachrom Lot	TMB Incubation (min)	Absorbance
P101.11C	Apr-15-14	109367	5	0.3628
	May-16-17	250066	11	0.09

II.3.3 Discussion

The initially successful use of the Asserachrom ELISA kit to quantitate porcine D-dimer highlights the homology that exists between human and porcine proteins. However, the Asserachrom kit was less sensitive to porcine protein than to human protein. The sensitivity of the kit for porcine protein was approximately 5 ng/mL in-well, but the kit is sensitive to human protein down to approximately 0.5 ng/mL in-well, or 10 ng/mL undiluted. At a porcine sample

dilution of 1:2 rather than the dilution of 1:21 suggested by the kit, porcine D-dimer would be measurable down to 10 ng/mL as well.

The addition of hemoglobin as a contaminant did not affect the reading of porcine D-dimer significantly, but the removal of hemoglobin from the sample with Hemoglobind appears to have also removed the D-dimer from the sample. This is not a concern for this particular protocol, as the protocol includes several wash steps to remove nonspecific proteins such as hemoglobin. However, this would present a challenge for any peroxidase-based assay in which hemoglobin is not completely removed, as hemoglobin is also able to act as a peroxidase (Kapralov et al. 2009).

Use of the Asserachrom kit in 2017 showed that it could no longer be used to quantitate porcine D-dimer. Since the porcine D-dimer standards used in 2014 and 2017 were produced by different protocols, we confirmed the identity of the 2017 D-dimer using immunoblotting and MALDI TOF/TOF analysis (Chapter II.2). Additionally, we detected the presence of secondary structure consistent with D-dimer using CD spectroscopy (Chapter II.2.2.2), suggesting that D-dimer was not being denatured during manufacturing process. This is consistent with Asserachrom analysis of samples taken after each step in the D-dimer purification process. When the absolute absorbance is corrected for protein concentration, the absorbances measured were very similar and there was no noticeable drop in absorbance after any individual step in the process.

Lastly, separate aliquots of the same clot sample were analyzed in 2014 and 2017. In 2017, the TMB solution was allowed to incubate for longer, which would lead to a higher absorbance, all things being equal. Conversely, the absorbance in 2017 was lower than that measured in 2014, despite the longer TMB incubation. Literature has shown that D-dimer stored

at temperatures <-60 °C is stable for at least 3 years (Böhm-Weigert et al. 2009; Lewis et al. 2001), so we would not expect that any protein degradation occurred in the intervening time.

Literature from Diagnostico Stago discussing D-dimer immunoassays describes the production of monoclonal anti-D-dimer antibodies using hybridoma technology (Amiral et al. 1986; Vieilledent et al. 1987). Briefly, Balb C mice were immunized with human D-dimer, followed by extraction of the spleen. Immunocytes are extracted from the spleen and fused with a myeloma cell line in order to produce a variety of hybridomas, cell lines that produce monoclonal antibodies. The hybridomas which produce the most specific antibodies with the highest binding affinity were chosen for the capture antibody (pre-plated in the test strips). Polyclonal antibodies were also raised from D-dimer immunization of Balb C mice and conjugated with HRP to make the Anti-D-Peroxidase, the detection antibody (Amiral et al. 1986; Vieilledent et al. 1987). It is possible that the hybridoma cell lines may have mutated over the years, giving rise to a monoclonal capture antibody that no longer cross-reacts with porcine D-dimer. Correspondence with a Diagnostico Stago representative did not yield any conclusive reason for the decline in kit sensitivity to porcine D-dimer.

II.4 Biochemical quantification of porcine D-dimer with commercially available primary antibodies

The variability over time of the sensitivity of the Asserachrom D-dimer ELISA kit precluded the use of this assay for porcine D-dimer quantification. We investigated the possibility of creating an in-house ELISA protocol using commercially available anti-D-dimer antibodies. A variety of anti-D-dimer antibodies with listed reactivity to human protein are commercially available on the market, but it is difficult to know which ones are the most likely

to cross-react with porcine D-dimer. As noted in Chapter II.2, though human and porcine D-dimer share a 90-99% conserved amino acid sequence, the two proteins had significantly different surface properties as measured by solubility. Antibodies bind to the epitopes on the surface of proteins, thus any one specific anti-human D-dimer antibody does not necessarily also bind to porcine D-dimer. Additionally, for a sandwich ELISA similar to the Asserachrom kit, two antibodies that do not bind to the same (or adjacent) D-dimer epitope are required. This section presents a few preliminary studies in which anti-D-dimer antibodies were evaluated for their cross-reactivity with porcine protein and as part of an antibody pair for sandwich ELISAs. Our target sensitivity for an ELISA kit is 5 ng/mL or less in-well porcine D-dimer concentration. Additionally, we expect to use this quantitative assay on samples that would be contaminated with blood and plasma components, we will perform a matrix interference experiment to evaluate the sensitivity in the presence of contaminants.

II.4.1 Materials and Methods

II.4.1.1 Materials

Anti-D-dimer primary antibodies were acquired from Abcam (DD93, Abcam, Cambridge, MA, USA), Fitzgerald (10-1752, 10-1753, 61-1009, Fitzgerald Industries International, Acton, MA, USA), and Absolute Antibody (3b6, Absolute Antibody, Oxford, United Kingdom). The Fitzgerald antibodies were noted to have cross-reactivity with canine protein as well as human, suggesting that they bound to evolutionarily preserved epitopes that were likely to also be present in porcine protein. Additionally, Fitzgerald 10-1752 and 10-1753 were noted to bind to separate epitopes from Fitzgerald 61-1009 and each was sold with 61-1009 as a matched antibody pair. Anti-D-Peroxidase from the Asserachrom D-dimer kit (Diagnostico Stago, Asnieres sur Seine, France) was also used as a horseradish peroxidase (HRP)-conjugated

primary antibody separate from the rest of the kit components. Diagnostico Stago Asserachrom Anti-D-Peroxidase is provided as a lyophilized cake with instructions to rehydrate with 8 mL kit dilution buffer. When used separately from the kit, a portion of the Diagnostico Stago Asserachrom Anti-D-Peroxidase cake was weighed according to the desired post-reconstitution volume (if the cake was 40 mg total, 5 mg cake was weighed out for each desired mL of Anti-D-Peroxidase) and reconstituted with 0.5% BSA-PBST. Sheep anti-mouse-HRP secondary antibody was acquired from GE Life Sciences (NXA931, GE Healthcare Life Sciences, Pittsburgh, PA, USA) for use with abcam DD93, Fitzgerald 10-1752 and 10-1753, and Absolute Antibody 3b6. Neutralite Avidin-HRP was acquired from Southern Biotech (7200-05, Southern Biotech, Birmingham, AL, USA) for use with Fitzgerald 61-1009. The porcine D-dimer used as a standard was produced according the protocol outlined in Chapter II.2.

II.4.1.2 Direct-bind ELISA

The monoclonal antibodies Absolute Antibody 3b6 and Fitzgerald 10-1752, 10-1753, and 61-1009 were evaluated for cross-reactivity with porcine D-dimer samples using a standard direct-bind ELISA. Abcam DD93 and Asserachrom Anti-D-Peroxidase were not evaluated with direct-bind ELISA as they were already known to cross-react with porcine D-dimer. Abcam DD93 was previously shown in our lab to have cross-reactivity with porcine D-dimer (see Figure II.5). Asserachrom Anti-D-Peroxidase is a polyclonal antibody and has been shown to react to porcine D-dimer and other D-dimer lysate components through immunoblotting (Figure II.12, Experiment date: 2017-02; Asserachrom Lot 114305X1, Expiration date 2017-06).

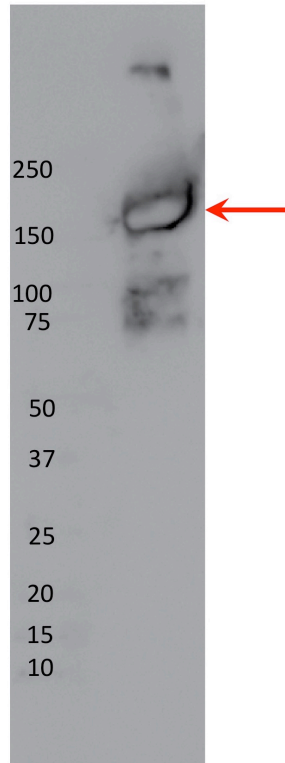


Figure II.12. Immunoblot with the use of Anti-D-Peroxidase from the Asserachrom kit as a primary antibody (no secondary antibody was required for reporting)

Pure porcine D-dimer was serially diluted in phosphate buffered saline (PBS) to concentrations between 10 and 1000 ng/mL and incubated in high-binding 96-well ELISA microplates (MICROLON[®] 600, Greiner Bio-One International GmbH, Kremsmünster, Austria) for 1 hr. For a positive control, human D-dimer was also incubated in the wells at concentrations between 10 and 1000 ng/mL. Wells were washed with phosphate-buffered saline with 0.5% Tween-20 (PBST) after each incubation. Nonspecific binding was blocked with 5% bovine serum albumin in PBST (5% BSA-PBST) for 30 min. Primary antibody was diluted in 0.5% BSA-PBST to concentrations from 0.5-5 µg/mL (based on recommended manufacturer concentrations) and incubated for 1 hr, followed by a second 30 min block with 5% BSA-PBST. The secondary antibody was diluted 1:5000 (recommended manufacturer dilution 1:4000-

1:8000) in 0.5% BSA-PBST and incubated for 1 hr in the wells. 3,3',5,5'-tetramethylbenzidine (TMB) solution (ThermoFisher Scientific) is added to each well and allowed to develop for 5-20 min until wells appear turquoise. Sulfuric acid (2N) was added to each well to stop the reaction and the absorbance at 450 nm was measured for each well.

For each antibody, we determined 1. whether the antibody cross-reacted with porcine protein, 2. whether there was a positive signal from simultaneously tested human samples, and 3. whether the antibody concentration affected the colorimetric signal from the porcine D-dimer.

II.4.1.3 Sandwich ELISA

Primary antibodies that showed cross-reactivity with porcine D-dimer were evaluated as prospective capture and detection antibodies in a standard sandwich ELISA. Specifically, abcam DD93 and Fitzgerald 10-1752 and 10-1753 were used as capture antibodies and Fitzgerald 61-1009 and Asserachrom Anti-D-Peroxidase were used as detection antibodies. Asserachrom Anti-D-Peroxidase cannot be used as a capture antibody with our current colorimetric reporting technique, as it has peroxidase activity. Fitzgerald 61-1009 is specifically recommended by the manufacturer to be a detection antibody. Abcam DD93 and Fitzgerald 10-1752 and 10-1753 could not be used as detection antibodies as there was not a suitable non-mouse antibody candidate for capture. Absolute Antibody 3b6 did not react to porcine D-dimer. Capture antibodies are diluted in PBS to concentrations of 0.5 to 10 $\mu\text{g/mL}$ based on manufacturer's recommendations. A 5% BSA-PBST solution was prepared to block nonspecific binding. Porcine D-dimer was diluted to 10-500 ng/mL in PBS. Antibody 61-1009 was diluted in 0.5% BSA-PBST to concentrations from 1 $\mu\text{g/mL}$ to 5 $\mu\text{g/mL}$. Anti-D-Peroxidase was reconstituted in 0.5% BSA-PBST according to kit reconstitution proportions. No other Anti-D-Peroxidase concentrations were evaluated.

A standard sandwich ELISA protocol was used as outlined in Table II.2, with some protocol refinement as familiarity with the protocol increased. The protocol is very similar to the direct-bind ELISA protocol outlined in Chapter II.4.1.2. High-binding ELISA plates were incubated in succession with capture primary antibody, D-dimer antigen, detection primary antibody, and secondary antibody for reporting (as needed). Between incubation steps, the wells are washed with PBST and non-specific binding was blocked with 5% BSA-PBST. Wells were washed 2 times after antigen and antibody incubations. Most frequently, anti-D-Peroxidase was used as the detection antibody and did not require further blocking and incubation. Fitzgerald antibody 61-1009 was also used as a detection antibody and required the secondary antibody avidin-HRP (diluted 1:5000 in 0.5% BSA-PBST). The assay was developed with TMB solution for 5-25 min, then stopped with 2 N sulfuric acid, and the absorbance was read at 450 nm.

Based on the previous achieved sensitivity with the Asserachrom assay and preliminary data on the expected D-dimer concentration in experimental samples (see Chapter II.5.2.2), the target sensitivity for a sandwich ELISA was 5-10 ng/mL. During our sandwich ELISA screening experiments, samples were run singly to preserve antibody stock. For a given combination of antibodies, a minimum detectable D-dimer concentration was reported as the lowest D-dimer concentration providing an absolute blank-subtracted absorbance value of at least 0.05. Antibody pairs with a minimal detectable D-dimer concentration ≤ 50 ng/mL were evaluated for matrix interference.

Table II.2. An outline of the sandwich ELISA protocol followed. Experiments using Asserachrom Anti-D-Peroxidase skipped steps 11-14 (italicized) as the antibody is already conjugated

Step	Action	Time
1	Incubate primary antibody for capture (Abcam DD93, Fitzgerald 10-1752 and 10-1753, 1 – 10 µg/mL)	1 hr
2	Wash with PBST, 2-3x	
3	Block non-specific binding	30 min
4	Wash with PBST, 1x	
5	Incubate antigen (D-dimer, 10-500 ng/mL)	1 hr
6	Wash with PBST, 2-3x	
7	Block non-specific binding	30 min
8	Wash with PBST, 1x	
9	Incubate primary antibody for detection (Fitzgerald 10-6009, 1-5 µg/mL – follow all italicized directions [Steps 11-14], and Asserachrom Anti-D-peroxidase, reconstituted according to kit instructions – skip to step 15)	1 hr
10	Wash with PBST, 2-3x	
<i>11</i>	<i>Block non-specific binding</i>	<i>30 min</i>
<i>12</i>	<i>Wash with PBST, 1x</i>	
<i>13</i>	<i>Incubate secondary antibody</i> <i>(Southern Biotech Avidin-HRP, 1:5000)</i>	<i>1 hr</i>
<i>14</i>	<i>Wash with PBST, 2-3x</i>	
15	Incubate with TMB for color development	5-25 min
16	Add sulfuric acid and measure absorbance at 450 nm	

II.4.1.4 Matrix Interference

Defibrinated plasma and homogenized clot were prepared as diluents to evaluate the effect of contaminants on the immunoassay. The process to produce defibrinated plasma is described in greater detail in Chapter II.5.1.3. Briefly, bovine thrombin was added to pooled porcine fresh frozen plasma (Lampire Biological Laboratories, Pipersville, PA, USA) to a concentration of 5 U/mL and allowed to clot for 1 hour at room temperature. Fibrin clots were removed and glass wool was added to the plasma, which was placed at 4 °C overnight to allowed

continued clotting. Plasma was filtered through 4x4 gauze pads (Fisher Scientific), aliquotted, and frozen at -80 °C until use.

Homogenization of clots is described in greater detail in Chapter II.5.1.4. Briefly, porcine blood was drawn less than 10 minutes before incubation, following a protocol approved by the UC Institutional Animal Care and Use Committee. Blood was pipetted in 1.5 mL aliquots into 16 mm glass tubes (366441, BD, Franklin Lakes, NJ, USA) and placed at 37 °C for 3 hours, followed by at least 72 hours at 4 °C. Clots were removed from the culture tubes and placed into a tissue grinder (7725-13, Corning Pyrex, Corning, NY, USA). 100 µL PBS was added to the tissue grinder and the clot was homogenized until no noticeable clot debris remained. Homogenized clot samples were flash frozen and stored at -80 °C until use.

To evaluate the effect of matrix interference on a given combination of antibodies on an assay, D-dimer standards were diluted into defibrinated plasma and homogenized clot. A standard sandwich ELISA protocol was otherwise followed as outlined in Chapter II.4.1.3. The antibody pairs evaluated for matrix interference were 10-1752 with Anti-D-Peroxidase and 10-1753 with Anti-D-Peroxidase as they showed a minimum detectable porcine D-dimer concentration of ≤ 50 ng/mL with uncontaminated porcine D-dimer standards. Again, a minimum detectable D-dimer concentration is reported as the lowest D-dimer concentration providing an absolute blank-subtracted absorbance value of at least 0.05, where the blank absorbance is measured from a sample of the matrix (plasma or homogenized clot) with 0 ng/mL D-dimer. In the sandwich ELISA with 10-1752 and Anti-D-Peroxidase, a small protocol refinement of an additional PBST wash after each antigen or antibody incubation was added to attempt to reduce non-specific binding.

II.4.1.5 SDS-PAGE and Immunoblotting

Immunoblotting was performed to evaluate the cross-reactivity of primary antibodies 10-1752, 10-1753, and DD93 with non-D-dimer species in porcine plasma, defibrinated plasma, homogenized clot, and D-dimer lysate similarly to the protocol outlined previously in Chapter II.2.1.5 and II.2.1.6. Briefly, samples with a target D-dimer loading of approximately 5 µg per lane were combined with Laemmli sample buffer under non-reducing conditions and heated at 95 °C for 5 min. Samples run in quadruplicate on 4-20% Mini-PROTEAN® TGX™ Precast Protein Gels (Bio-Rad Laboratories) at 175 V for 40 min at 25 °C in TGS running buffer. One set of samples were stained with Coomassie R250 to visualize all proteins, while an Invitrogen Novex Semi-Dry Blotter (ThermoFisher Scientific) was used to transfer proteins from SDS-PAGE gel to 0.45 µm nitrocellulose paper (GE Healthcare Lifesciences, Pittsburgh, PA, USA) at 10-12 V for 75 min at 25 °C. Nonspecific binding sites on the membrane were blocked in 5% powdered milk (Meijer) for 30 min. Each membrane was blotted with one of the three primary antibodies at 5 µg/mL, followed by a sheep anti-mouse-HRP secondary antibody (NXA931, GE Healthcare Life Sciences) at 1:5000 dilution. The membrane was developed with chemiluminescent substrate (ThermoFisher Scientific) for 5 min prior to imaging.

II.4.2 Results

II.4.2.1 Direct-bind ELISA

Antibody 3b6 did not cross-react with porcine D-dimer at concentrations of porcine D-dimer from 10 to 1000 ng/mL and antibody concentrations from 0.5 to 5 µg/mL. The human positive control showed strong absorbance at 250 ng/mL D-dimer and a change in antibody concentration did not significantly affect the signal for the human protein.

Fitzgerald antibodies 10-1752 and 10-1753 both cross-reacted with porcine D-dimer (concentrations of 50-1000 ng/mL). The human positive control also showed a strong signal and the absorbance values associated with equivalent concentrations of human D-dimer were higher than the values for porcine D-dimer. Changing the antibody concentration of either Fitzgerald 10-1752 or 10-1753 did not affect the colorimetric signal measured.

Fitzgerald antibody 61-1009 also cross-reacted with porcine D-dimer at all concentrations tested (50-1000 ng/mL). The human positive control showed a strong signal and again the absorbance values higher for human protein than for porcine protein at equivalent concentrations. For porcine D-dimer, increasing the concentration of the antibody increased the absorbances values measured at a single concentration (by approximately 20-25% from 1 to 5 $\mu\text{g/mL}$). This effect was not observed with the human D-dimer.

II.4.2.2 Sandwich ELISA

The sandwich ELISA results are summarized in Table II.3. Briefly, three antibody pairs did not have sufficient a minimum detectable porcine D-dimer concentration less than 100 ng/mL and were removed from consideration. The Fitzgerald 10-1752/61-1009 antibody pair did not produce any signal for porcine D-dimer, up to a tested D-dimer concentration of 1000 ng/mL. The Fitzgerald 10-1752/Asserachrom Anti-D-Peroxidase and Fitzgerald 10-1753/Asserachrom Anti-D-Peroxidase antibody pairs showed the best sensitivity, detecting porcine D-dimer in the 20-50 ng/ml range.

Table II.3. A summation of the sandwich ELISA with each pair of antibodies evaluated.

Capture Antibody (concentration)	Detection antibody (concentration)	Minimum Detectable porcine D-dimer Concentration
DD93 (5 µg/mL)	Anti-D-peroxidase	100 ng/mL
10-1752 (5 µg/mL)	61-1009 (5 µg/mL)	n/a
10-1753 (5 µg/mL)	61-1009 (5 µg/mL)	100 ng/mL
10-1752 (2-5 µg/mL)	Anti-D-peroxidase	<50 ng/mL
10-1753 (5 µg/mL)	Anti-D-peroxidase	<20 ng/mL

II.4.2.3 Matrix Interference

The antibody pairs Fitzgerald 10-1752/Asserachrom Anti-D-Peroxidase and Fitzgerald 10-1753/Asserachrom Anti-D-Peroxidase were evaluated for matrix interference. Neither antibody pair allowed detection of D-dimer above a matrix-only blank value in defibrinated plasma (tested up to 500 ng/mL). The Fitzgerald 10-1753/Anti-D-Peroxidase pair had a minimum detectable D-dimer concentration of 180 ng/mL in homogenized clot (20-180 ng/mL tested). The Fitzgerald 10-1752/Anti-D-Peroxidase pair had a minimum detectable D-dimer concentration of <50 ng/mL in homogenized clot (50-500 ng/mL tested).

II.4.2.4 SDS-PAGE and Immunoblotting

Figure II.13a shows the SDS-PAGE with porcine plasma, defibrinated porcine plasma, homogenized porcine clot, porcine D-dimer lysate, and purified porcine D-dimer. D-dimer can be seen between the 150 and 250 kDa size markers. The SDS-PAGE shows a D-dimer sized protein in each lane. However, the immunoblots (Figure II.13b-d) show that more specific anti-D-dimer antibodies (abcam DD93 in b, and Fitzgerald 10-1753 in d) do not cross-react with the D-dimer sized protein in lanes 1-3, suggesting that the protein is the same size as D-dimer but is not D-dimer. Abcam DD93 (b) and the Fitzgerald 10-1753 (d) are similar in specificity, though

Fitzgerald 10-1753 recognizes a few larger-MW species and DD93 has slightly more affinity for D-monomer.

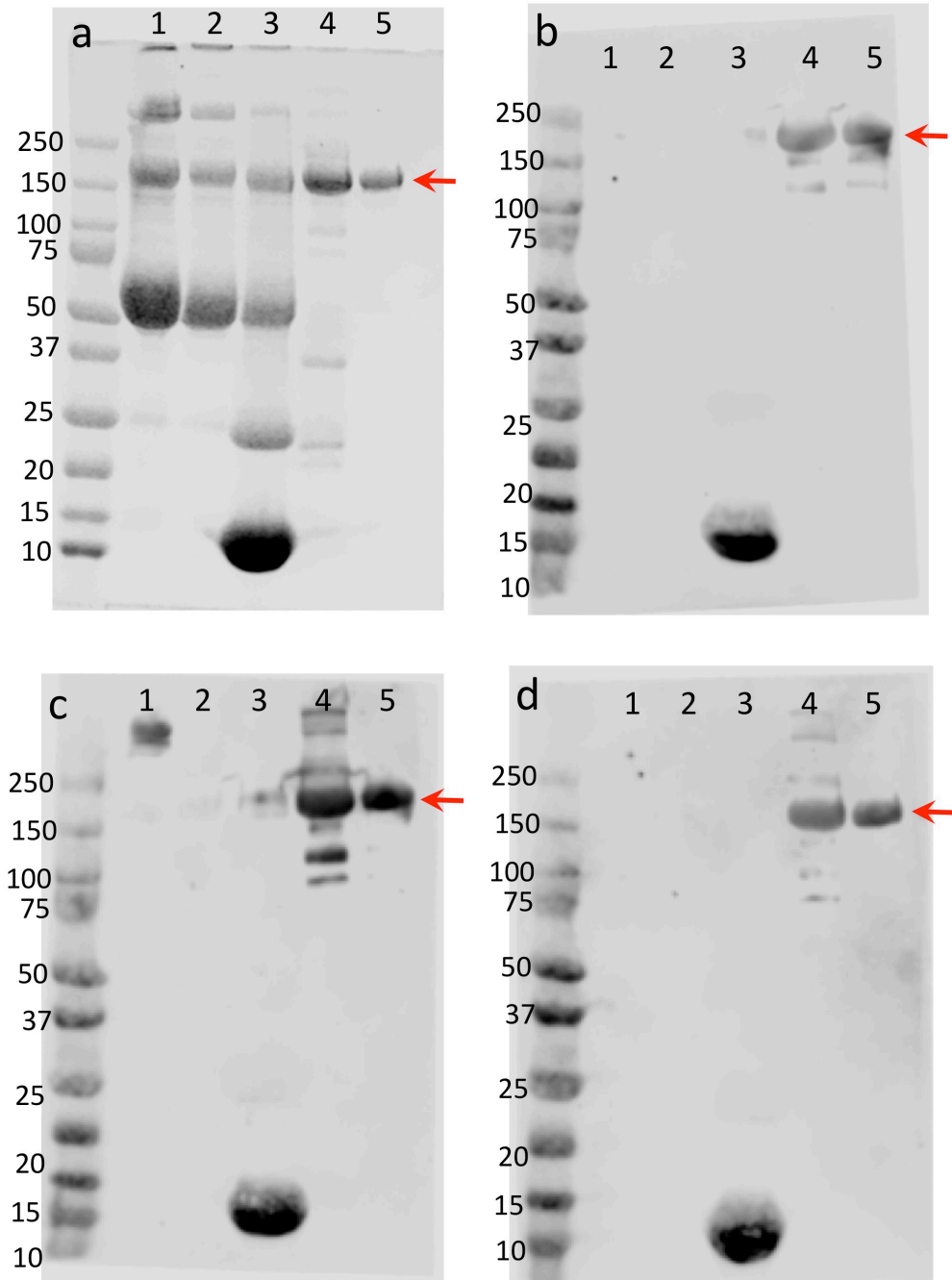


Figure II.13. A SDS-PAGE (a) and immunoblots (b, c, d) with lanes as follows: 1 – plasma, 2 – defibrinated plasma, 3 – homogenized clot, 4 – D-dimer lysate, 5 – Purified D-dimer. Immunoblots use the antibodies abcam DD93 (b), Fitzgerald 10-1752 (c) and 10-1753 (d) and are overlaid with a visible light image to provide protein size references. A non-specific hemoglobin signal can be seen in Lane 3 at <20 kDa for each immunoblot, as hemoglobin is known have peroxidase activity (Kapralov et al. 2009).

II.4.3 Discussion

The antibody pairs tested for our in-house ELISA protocol failed to be sensitive enough to detect our porcine D-dimer. No antibody pair was able to detect <500 ng/mL of D-dimer in defibrinated plasma. In homogenized clot, the Fitzgerald 10-1752/Asserachrom Anti-D-Peroxidase pair was able to detect 50 ng/mL of D-dimer and the Fitzgerald 10-1753/Asserachrom Anti-D-Peroxidase pair was able to detect 180 ng/mL of D-dimer. As expected, there was a trade-off between specificity of the antibody and sensitivity of the sandwich ELISA using the antibody. The abcam DD93/Asserachrom Anti-D-Peroxidase antibody pair did not show sufficient sensitivity to be evaluated for matrix interference, but the immunoblots (Figure II.13) showed that abcam DD93 was very specific for D-dimer with slight D-monomer reactivity. In contrast, Fitzgerald 10-1752 and 10-1753 had increased sensitivity and were able to detect D-dimer to a lower concentration, but the immunoblots showed that the antibodies were less specific for D-dimer, which may allow capture of other fibrin degradation products (FDPs).

The matrix interference studies showed that defibrinated plasma interferes with D-dimer detection when either Fitzgerald 10-1752 or 10-1753 were used as capture antibodies. This has been noted in the literature previously. Petit *et al.* measured an increase in detected D-dimer (VIDAS® D-Dimer Exclusion™II kit, bioMerieux S.A.) in citrated human plasma from 385 ± 0 ng/mL to 624 ± 97 ng/mL with the addition of 3 μ g/mL rt-PA, even without the presence of a clot. This increase is almost certainly due to nonspecific binding, as D-dimer can only arise from the breakdown of cross-linked fibrin. Non-specific binding arises from the presence of the

D-dimer antigen on different sized FDPs, leading to a great deal of variability in commercially available D-dimer assays based on the epitopes bound by the kit antibodies (Adam et al. 2009).

The ELISA protocol may be refined further to improve the sensitivity or specificity. For instance, increasing the number of PBST washes could remove proteins that are less avidly bound to the capture protein. If the capture antibody binds more avidly to D-dimer than other fibrin degradation products or plasma contaminants, D-dimer would remain bound while other proteins are knocked off, reducing the signal from the matrix blank. The Fitzgerald 10-1752/Anti-D-Peroxidase antibody pair shows a minimum detectable D-dimer concentration of <50 ng/mL with 3 PBST washes in homogenized clots, which may be further improved to desired sensitivities with an increase in the number of washes.

Additionally, consideration of the sample matrix from any given experiment is key. The Fitzgerald 10-1752/Anti-D-Peroxidase and Fitzgerald 10-1753/Anti-D-Peroxidase antibody pairs were unable to detect D-dimer in defibrinated plasma, but some experiments may not require measurement of plasma samples. For instance, evaluating thrombolysis in an intracerebral hemorrhage model (Wagner et al. 1999) would require analysis of only homogenized clot samples, and the ELISA protocol as presented may be sufficient to measure D-dimer in such samples.

Lastly, other commercially available Anti-human-D-dimer antibodies or immunoassay kits may be evaluated for cross-reactivity to porcine D-dimer. Given the wide range of products available, however, it would be cost prohibitive to evaluate all of the options. The creation of an antibody specifically against porcine D-dimer might be a more time- and cost-effective option.

II.5 Preliminary quantification of porcine D-dimer in *in vitro* thrombolysis samples

An effective porcine D-dimer immunoassay would allow quantification of thrombolytic efficacy during *in vivo* thrombolysis experiments. As a proof of concept in porcine samples, we analyzed D-dimer content in samples produced during *in vitro* experiments in a static thrombolysis system (Datta et al. 2008; Holland et al. 2008). Porcine clots created from fresh porcine blood were placed into a sample holder with defibrinated plasma and treated with plasma alone, rt-PA, or rt-PA with Definity[®] and 120 kHz ultrasound (US) for a 30 min treatment window. Clots were removed and homogenized, and aliquots of the homogenized clot and surrounding plasma were flash frozen. This static thrombolysis system has relevance to *in vivo* hematoma models, such as a porcine lobar model of intracerebral hemorrhage (Wagner et al. 1996; Wagner et al. 1999; Wagner 2007).

II.5.1 Materials and Methods

II.5.1.1 Materials

Definity[®] perflutren lipid microspheres (Lantheus Medical Imaging, North Billerica, MA, USA) were activated according to manufacturer instructions. Definity[®] was allowed to equilibrate with room temperature for 1 hr, then agitated at high shear rates using a Vial-Mix (Lantheus Medical Imaging) and allowed to cool for at least 15 minutes prior to use.

II.5.1.2 Whole Blood Clot Manufacturing

Aliquots of 1.5 mL fresh whole porcine blood were pipetted into 16 mm diameter glass tubes (366430 or 366441, BD Vacutainer[®], Franklin Lakes, NJ, USA). The 366430 Vacutainers[®] were silicone-coated and created retracted clots and the 366441 Vacutainers[®] were not silicone-coated and created unretracted clots Figure II.14. Vacutainers[®] were incubated at 37 °C for 3

hours and stored at 4 °C for between 3 and 17 days prior to use (Holland et al. 2008). Porcine blood was drawn less than 10 minutes before incubation, following a protocol approved by the UC Institutional Animal Care and Use Committee.

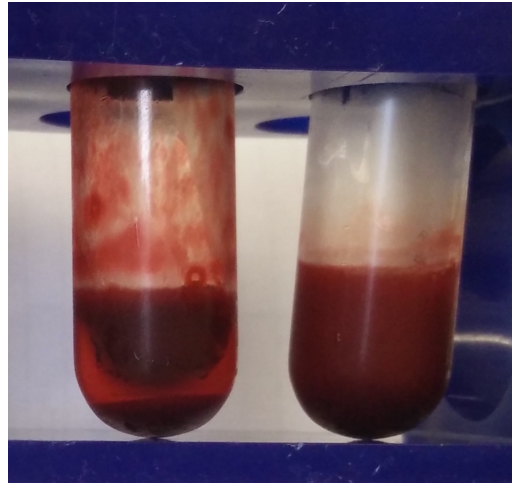


Figure II.14. A photographic image of representative retracted (left) and unretracted (right) clots

II.5.1.3 Plasma Defibrination

Pooled porcine fresh frozen plasma (Lampire Biological Laboratories, Pipersville, PA, USA) was defibrinated using bovine thrombin in order to prevent fibrin in the plasma from affecting subsequent D-dimer measurements. Bovine thrombin was added to plasma at a concentration of 5 U/mL and allowed to clot for 1 hour at room temperature. Fibrin clots were removed with a frayed bamboo skewer and plasma was retained and allowed to clot further overnight at 4 °C in the presence of glass wool in order to nucleate formation of fibrin clots. Fibrin clots were removed and the plasma was filtered through 4x4 gauze pads (Fisher Scientific). The defibrinated plasma was aliquotted and frozen at -80 °C until use.

II.5.1.4 Experimental Protocol

Experiments were conducted in a Lucite tank filled with filtered, degassed, deionized water. The water was maintained at 37 °C via a heating and circulation system. Each clot was exposed to one of three treatment protocols: plasma alone, rt-PA (96 µg/mL), or rt-PA (96 µg/mL) with 120 kHz ultrasound and Definity[®] using a previously published protocol (Holland et al. 2008). For each experiment, a whole blood clot was blotted and weighed prior to being placed into the sample holder filled with 30 mL of either defibrinated plasma alone or defibrinated plasma with rt-PA. For treatment groups exposed to rt-PA, an aliquot of rt-PA was added immediately prior to the addition of the clot so that the final rt-PA concentration in the sample holder was 96 µg/mL for porcine clots. The use of this rt-PA concentration for porcine clots compensates for reduced rt-PA susceptibility in porcine clots (Huang et al. 2017) and was chosen so that small errors in rt-PA concentration would not cause large effects on mass loss (Holland et al. 2008).

For treatment groups exposed to 120 kHz US and Definity[®] microbubbles, Definity[®] was periodically infused through an catheter surrounded by an air column to prevent premature destruction. For each run, 50 µL of Definity[®] was diluted into 4.95 mL phosphate buffered saline (PBS). A syringe pump (Harvard Apparatus Pump 11 Elite, Harvard Apparatus, Cambridge, MA, USA) was used to infuse 0.1 mL of the diluted Definity[®] solution into the sample holder directly above the clot at the beginning of each 3-min segment, for a total of 1 mL Definity[®] over the 30 minute treatment period. Each clot was treated for 30 minutes total, with or without 120 kHz ultrasound insonation. Following the completion of the treatment protocol, the thrombus was removed from the sample holder and weighed. Either 1 or 0.1 mL PBS was added to the clot in the tissue grinder (7725-13, Corning Pyrex, Corning, NY, USA) and the clot was

homogenized until no noticeable clot debris remained. The use of 0.1 mL PBS for clot homogenization was a later protocol adjustment to increase the D-dimer concentration within the homogenized clot sample and only done on unretracted clots (no D-dimer concentration data available). Liquid nitrogen was used to flash-freeze the homogenized clot and 1-mL aliquots of the surrounding fluid.

II.5.1.5 Ultrasound Set-up & Parameters

A diagram of the experimental set up can be seen in Figure II.15. In each experiment, the clot and fluid within the sample holder were insonated with a custom-designed unfocused 120 kHz transducer (61 mm diameter; Sonic Concepts, Woodburn, WA, USA). A function generator (Agilent Technologies 33250A, Santa Clara, CA, USA) was used to generate a sine-wave signal at 80% duty cycle with a 1667 Hz pulse repetition frequency (PRF). The signal was boosted 55 dB by a power amplifier (1040L, ENI, Rochester, NY, USA) and power to the transducer was maximized via a custom-built impedance matching network (Sonic Concepts). A hydrophone (TC 4038, Teledyne Reson, Slangerup, Denmark) was used to ensure that the *in situ* pressure was 0.37 MPa peak-to-peak. A single-element long-focus 2.25-MHz transducer (595516C, Picker Roentgen GmbH, Espelkamp, Germany) was used as a passive cavitation detector (PCD) to evaluate ultrasound activity throughout the insonations. The signal from the PCD was low-pass filtered (10-MHz, J73E, TTE, Los Angeles, CA, USA), augmented by a wide-band low-noise amplifier (CLC100, Cadeca Microcircuits, Loveland, CO, USA), high-pass filtered (Model 3945 Butterworth/Bessel Multi-channel filter with a cutoff frequency of 170 kHz, Krohn-Hite Corporation, Brockton, MA, USA), and digitized (1 ms duration, 10-MHz sampling frequency). The focal volume of each transducer was aligned with the clot in the sample holder using a

pulser-receiver (Olympus Panametrics Square Wave Pulser-Receiver Model 5077PR, Waltham, MA, USA) and the hydrophone (TC 4038, Teledyne Reson).

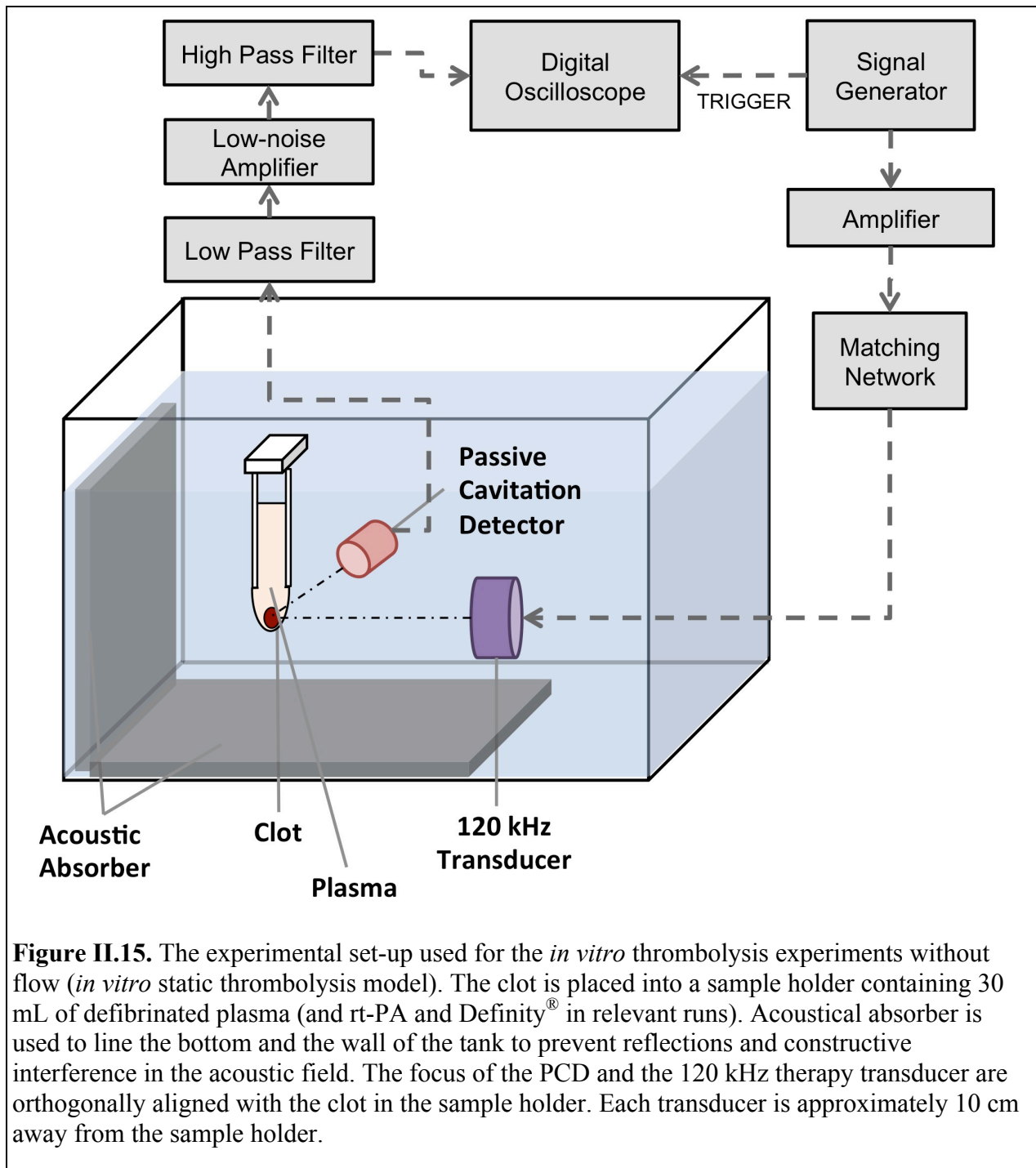


Figure II.15. The experimental set-up used for the *in vitro* thrombolysis experiments without flow (*in vitro* static thrombolysis model). The clot is placed into a sample holder containing 30 mL of defibrinated plasma (and rt-PA and Definity[®] in relevant runs). Acoustical absorber is used to line the bottom and the wall of the tank to prevent reflections and constructive interference in the acoustic field. The focus of the PCD and the 120 kHz therapy transducer are orthogonally aligned with the clot in the sample holder. Each transducer is approximately 10 cm away from the sample holder.

II.5.1.6 Evaluation of porcine D-dimer concentration

In a subset of retracted clot and fluid samples, porcine D-dimer concentration was measured using the Asserachrom D-dimer ELISA kit (Diagnostico Stago, Asnieres sur Seine, France), and the porcine D-dimer standard was acquired from Dr. Gail Pyne-Geithman in frozen aliquots (-80 °C) at a concentration of 1 mg/mL. Porcine D-dimer standard was serially diluted using the kit dilution buffer to in-well concentrations from 5 to 320 ng/mL. Porcine experimental samples (homogenized clot and defibrinated plasma in the sample holder) were thawed on ice and diluted 1:2 in kit dilution buffer. The kit protocol was otherwise followed as described in Chapter II.3.1. Briefly, the samples or standards were incubated within the wells of the test strips for 1 hr and then washed off, followed by a 1 hr Anti-D-peroxidase incubation. After a second wash, TMB solution was plated into wells and allowed to develop for 5 min, after which sulfuric acid was used to stop the reaction. Each standard or sample was evaluated in duplicate. The absolute D-dimer (ng) in the homogenized clot and surrounding fluid was calculated from the D-dimer concentration and the measured homogenized clot volume and experimental plasma volume:

$$\text{Absolute D-dimer (ng)} = [\text{D-dimer (ng/mL)}] \times [\text{Sample Volume (mL)}] \quad (\text{II.2})$$

Where "sample volume" refers to either the volume of homogenized clot or the volume of fluid surrounding the clot. Both D-dimer concentration and absolute D-dimer will be reported.

II.5.1.7 Evaluation of sample pH

In a subset of retracted clots (n = 13), the pH was measured in homogenized clot and fluid samples for undiluted sample, 1:2 diluted sample, and 1:21 diluted sample. Dilutions were done with the Asserachrom D-dimer ELISA kit dilution buffer. The 1:2 dilution reflects the

dilution used for our porcine samples as outlined above (Chapter II.5.1.6). The 1:21 dilution reflects the dilution recommended by the Asserachrom D-dimer ELISA kit protocol. A Semi-Micro pH Electrode (ThermoFisher Scientific) was used for the pH measurement due to the small size of each sample.

II.5.1.8 Statistical analysis

Data was analyzed in Graphpad Prism (Graphpad Software, La Jolla, CA, USA). Mass loss and D-dimer concentration are reported as mean and one standard deviation and are compared with one-way ANOVA between treatments for each clot type. The effect of each treatment on the two different types of clots are also compared. Tukey's method was used for post-hoc analysis of ANOVA data to identify significant differences in lytic efficacy. One-way ANOVA and a Tukey post-hoc analysis was also performed on sample pH data to evaluate the effect of dilution on pH. For clot samples for which both mass loss and D-dimer concentration data is available, linear regression was performed with Prism.

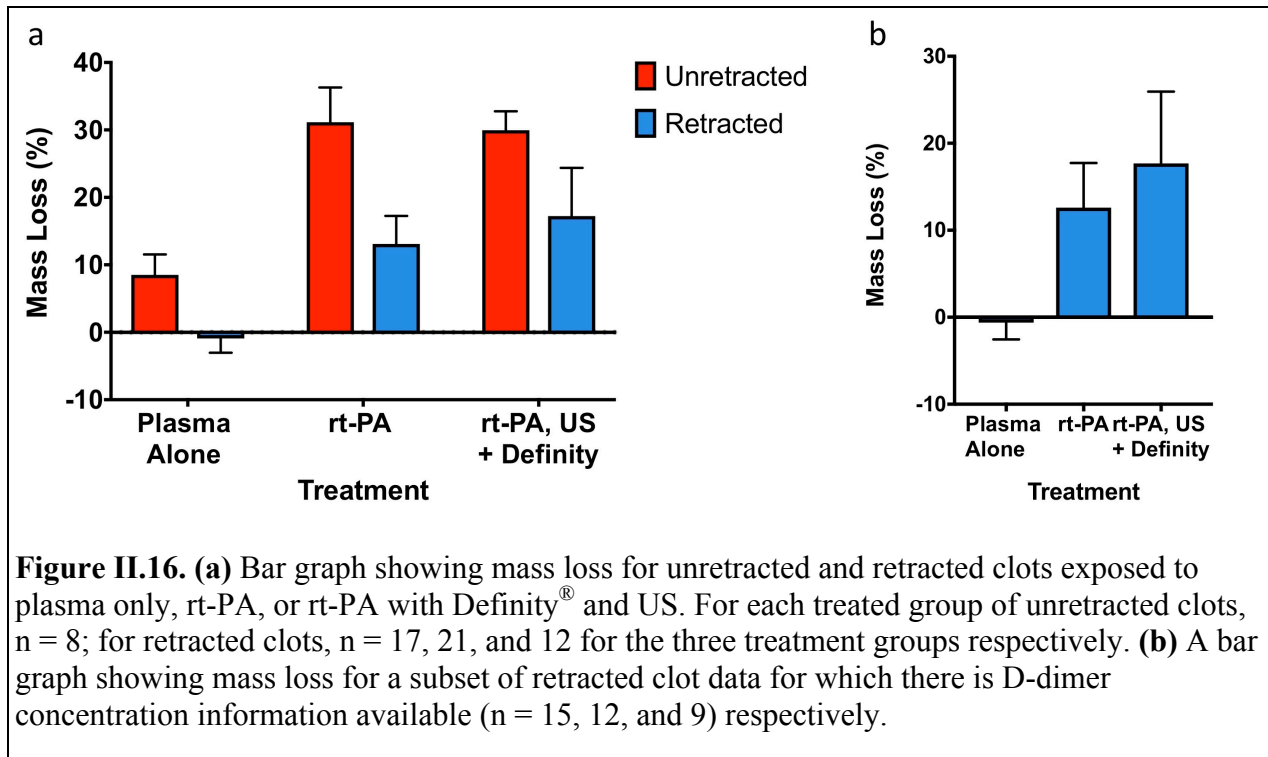
II.5.2 Results

II.5.2.1 Mass loss

The mass loss of retracted and unretracted clots exposed to plasma alone, rt-PA, and rt-PA with Definity[®] and US are shown in Figure II.16a. Exposing either type of clot to plasma alone resulted in a low degree of mass loss, $-0.9 \pm 2.1\%$ for retracted clots or $8.5 \pm 3.0\%$ for unretracted clots. Treatment with rt-PA significantly increases mass loss for both types of clots compared to treatment with plasma alone, with a mass loss of $13.1 \pm 4.1\%$ for retracted clots ($p < 0.01$) and $31.1 \pm 5.1\%$ for unretracted clots ($p < 0.01$). The adjuvant use of Definity[®] and US with rt-PA treatment significantly increases mass loss further for retracted clots, to $17.2 \pm 7.1\%$

($p = 0.03$), but there is no enhanced lysis seen in unretracted clots, which exhibit a mass loss of $30.0 \pm 2.8\%$ ($p = 0.85$). For each treatment, unretracted clots show an increased mass loss compared to retracted clots ($p < 0.01$).

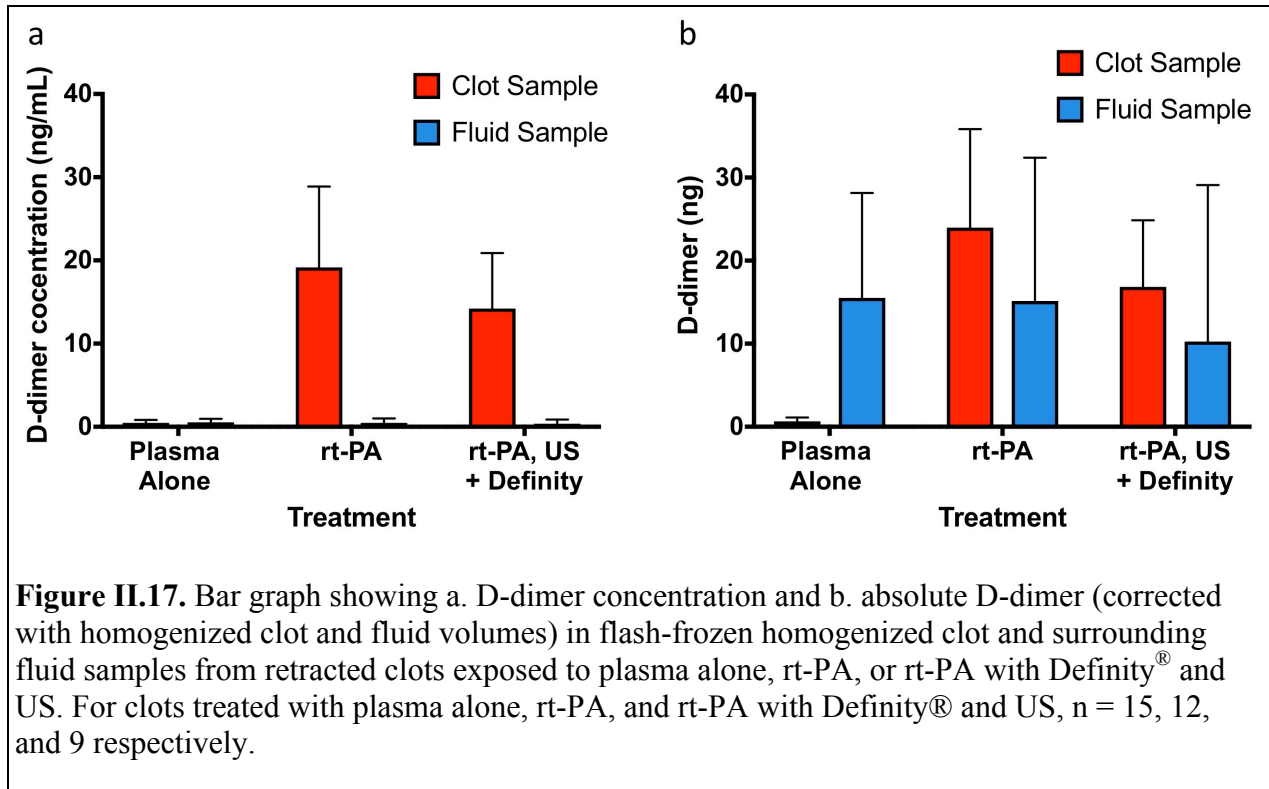
Figure II.16b shows mass loss for a subset of retracted clot data for which D-dimer concentration values are also available. For this subset of clots, the mass loss seen was $-0.62 \pm 1.9\%$ for clots treated with plasma alone, $12.6 \pm 5.1\%$ for clots treated with rt-PA, and $17.69 \pm 8.2\%$ for clots treated with rt-PA with Definity[®] and US. Clots treated with rt-PA, with or without Definity[®] and US, exhibited a significantly increased mass loss compared to clots treated with plasma alone ($p < 0.01$). However, no significant difference was seen between clots treated with Definity[®] and US as an adjuvant to rt-PA and those treated with rt-PA alone ($p = 0.08$).



II.5.2.2 D-dimer

The D-dimer concentration in homogenized clot and fluid samples of retracted clots exposed to plasma alone, rt-PA, and rt-PA with Definity[®] and US are shown in Figure II.17. Fluid samples did not contain any detectable D-dimer regardless of the treatment (0.5 ± 0.4 ng/mL, 0.5 ± 0.5 ng/mL, and 0.3 ± 0.6 ng/mL for the three treatments respectively). Homogenized clot samples treated with plasma alone similarly did not exhibit detectable D-dimer (0.5 ± 0.3 ng/mL). Homogenized clot samples treated with rt-PA showed a significant increase in D-dimer concentration compared to plasma alone, with 19.1 ± 9.7 ng/mL ($p < 0.01$). Adjuvant use of Definity[®] and US with rt-PA also significantly increased D-dimer concentration above plasma alone at 14.2 ± 6.7 ng/mL ($p < 0.01$), but did not show a significantly increased D-dimer compared to rt-PA alone ($p = 0.19$).

The mean absolute D-dimer values calculated for fluid samples for clots treated with plasma alone, rt-PA, and rt-PA with Definity[®] and US were 15.51 ± 12.63 ng, 15.14 ± 17.26 ng, and 10.2 ± 18.83 ng, respectively. No significant differences were detected between the absolute D-dimer values for any treatment group in the fluid samples. The mean absolute D-dimer values in clot samples treated with plasma alone, rt-PA, and rt-PA with Definity[®] and US were 0.65 ± 0.48 ng, 23.99 ± 11.86 ng, and 16.84 ± 8.01 ng, respectively. Clots treated with rt-PA had a higher absolute D-dimer compared to plasma alone ($p < 0.01$), but clots treated with rt-PA with Definity[®] and US did not differ in absolute D-dimer from clots treated with either plasma alone or rt-PA ($p > 0.05$).

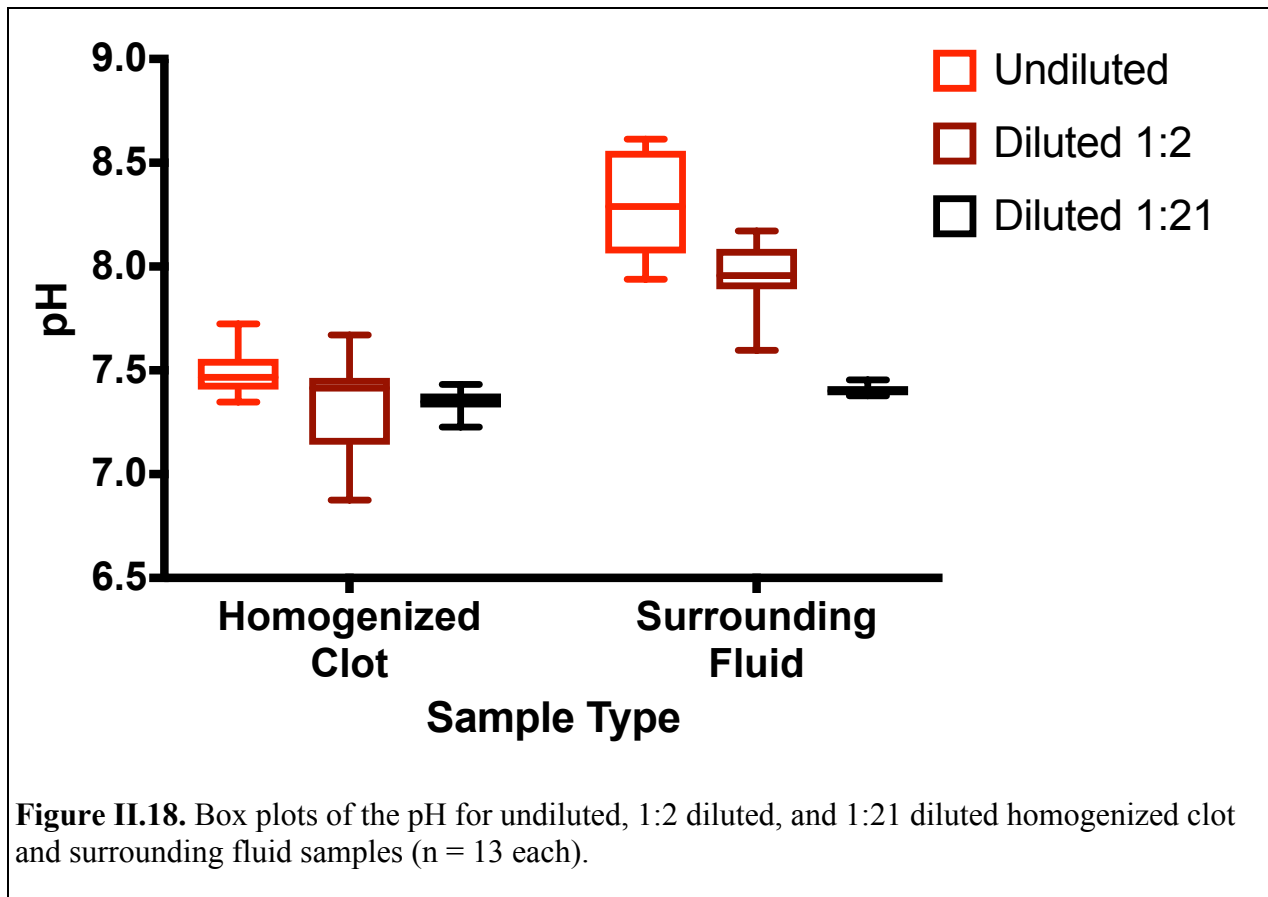


II.5.2.3 Evaluation of sample pH

The pH for homogenized clot and fluid samples at different dilutions is plotted in Figure II.18. The mean pH of both homogenized clot and fluid samples after a dilution of 1:21 was 7.35 ± 0.05 and 7.40 ± 0.03 respectively, with a very small spread in pH values. The mean pH of homogenized clot samples both undiluted and at a 1:2 dilution was also similar to the physiological pH of 7.4 at 7.49 ± 0.11 and 7.33 ± 0.21 respectively and showed an increased variability in pH values. For homogenized clot samples, the 1:2 dilution and undiluted samples had significantly different pH values ($p = 0.04$), but no significant difference was seen between 1:2 and 1:21 diluted samples ($p = 0.95$) or undiluted and 1:21 diluted samples ($p = 0.07$).

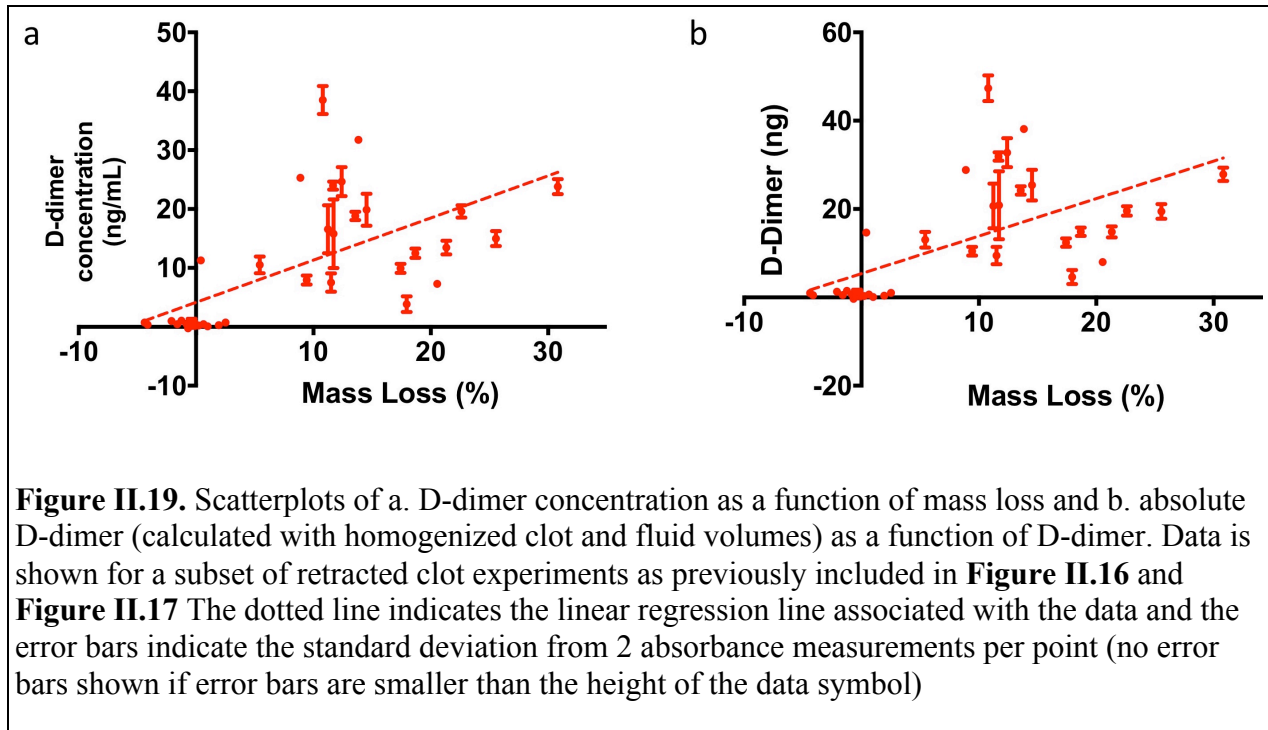
The pH of plasma samples changed much more when diluted. Undiluted plasma samples had a mean pH of 8.30 ± 0.25 and 1:2 diluted samples had a mean pH of 7.95 ± 0.16 . the

undiluted plasma sample pH was significantly higher than the 1:2 diluted sample pH ($p < 0.01$) and the 1:2 diluted sample pH was significantly higher than the 1:21 diluted sample pH ($p < 0.01$).



II.5.2.4 Correlation of D-dimer and Mass Loss

The D-dimer measured from homogenized clot samples is plotted against the mass loss of each retracted clot in Figure II.19. There is a correlation between D-dimer concentration and mass loss (Figure II.19a), with a statistically significant non-zero slope ($r = 0.64$, $p < 0.01$). There is also a correlation between absolute D-dimer and mass loss (Figure II.19b), ($r = 0.61$, $p < 0.01$).



II.5.3 Discussion

Our work shows that D-dimer concentration is significantly correlated to clot mass loss in porcine retracted clot samples. This correlation has previously been shown for human samples (Kimura et al. 1994; Pfaffenberger et al. 2003). Pfaffenberger *et al.* saw a similar spread when correlating D-dimer concentration and mass loss data ($r = 0.71$) (Pfaffenberger et al. 2003) to our correlation ($r = 0.64$). Kimura *et al.* reported that the use of D-dimer concentration as an alternative for mass loss is limited due to lack of sensitivity at the lower end. Specifically, they showed that human clots with a mass loss of $<20\%$ may still have undetectable levels of D-dimer (Kimura et al. 1994). Our porcine clots exhibited a lower amount of mass loss (approximately $-5 - 30\%$ compared to the $0 - 70\%$ seen by Kimura *et al.*), with some clots gaining mass rather than losing mass (Kimura et al. 1994). Our results are consistent with those of Kimura *et al.*, showing that clots in the lowest quarter of the mass loss range had no detectable D-dimer. The difference in the range of mass losses observed may be due to differences in clot

shape and surface area to volume ratio (Kimura *et al.* used cylindrical clots, while ours were spherical) (Kimura et al. 1994). Additionally, we did not blot the clot post-experiment to preserve D-dimer on the surface of the homogenized clots, likely leading to an overall decrease in mass loss values.

We attempted to account for differences in clot size by calculating absolute D-dimer values in clot and plasma samples using experimentally measured volumes. Unlike D-dimer concentration and mass loss, the use of absolute D-dimer as a metric of thrombolytic efficacy did not show that rt-PA with Definity[®] and US increased thrombolysis over plasma alone. This may be attributable in part to the challenge of experimentally measuring homogenized clot volume. During the clot homogenization process, bubbles are formed from the repeated motion of the pestle against the homogenizer, decreasing both the D-dimer in the sample and the volume of the homogenized clot. In the future, the addition of a centrifugation step may improve recovery of the homogenized clot. Additionally, our inability to detect D-dimer in the fluid samples limits the usefulness of an absolute D-dimer calculation, as we cannot quantify the D-dimer that was released from the clot into the surrounding plasma.

Previously published studies in which D-dimer was correlated with thrombolysis evaluated the D-dimer concentration in the fluid surrounding the clot and measured much higher D-dimer concentrations than were measured in our experiment (Kimura et al. 1994; Petit et al. 2015; Pfaffenberger et al. 2003). In a series of human thrombolysis experiments, Kimura *et al.* measured D-dimer concentrations from 154 ± 2 ng/mL for clots treated with normal saline to 1727 ± 379 ng/mL in clots treated with rt-PA (2 μ g/mL) insonated with 1 MHz US (Kimura et al. 1994). Pfaffenberger *et al.* also performed human thrombolysis experiments and did not report D-dimer concentration by treatment group but measured a range of D-dimer

concentrations from approximately 650 to 4500 ng/mL, corresponding to mass loss ranging from approximately 2 to 50% (Pfaffenberger et al. 2003). Petit *et al.* performed thrombolysis experiments in human whole blood clots in a flow phantom and measured D-dimer concentration in the effluent over time. They measured D-dimer concentrations varying from 385 ng/mL in the baseline plasma to 26 ± 1.6 $\mu\text{g/mL}$ after a 30-min treatment with rt-PA (3 $\mu\text{g/mL}$) and insonation with 1 MHz US (0.08% duty cycle, 1.3 MPa peak negative pressure) (Petit et al. 2015).

Our study contrasts the published studies of thrombolysis in human clots in a few ways. First, we did not see any measurable D-dimer in the surrounding fluid, only in the homogenized clot samples. This is likely in part due to the decreased sensitivity of anti-human antibodies to porcine D-dimer. Our protocol change to decrease the dilution factor, from the kit-recommended 1:21 for human samples to 1:2 for porcine samples reflects this expectation that the anti-human-D-dimer antibodies will bind more weakly to porcine D-dimer than their human homologues. This decreased dilution of our samples into the kit sample buffer affected the pH of our surrounding fluid samples, possibly decreasing kit sensitivity. Antibody binding is almost always pH dependent due to the effect of pH on protein conformation, and differences in pH, though small, could falsely increase or decrease the "detected" D-dimer concentration. Additionally, the use of a 1:2 dilution increases the concentration of non-D-dimer plasma proteins in the well, which may non-specifically bind to the antibodies on the surface of the assay plate and prevent D-dimer from binding. Diluting the samples further to control the pH and level of contaminants was not deemed feasible for the Asserachrom kit, as it caused the porcine D-dimer concentration to drop below the minimal detectable level (see Chapter II.3). The use of the *in vitro* thrombolysis system to evaluate the D-dimer concentration and mass loss in human clots may

help us better elucidate the distribution of D-dimer in the homogenized clot and surrounding fluid.

A few approaches to improve D-dimer detection have been discussed. One proposed protocol change was to decrease the volume of PBS added prior to the homogenization of the clot sample. Clots that have been homogenized in 0.1 mL PBS have not been analyzed for D-dimer concentration due to a lack of a functioning assay, so we cannot currently say if this change in protocol would improve D-dimer detection. Similarly, decreasing the volume of surrounding fluid used in each experiment may effectively concentrate any D-dimer within the surrounding fluid samples. Prior to D-dimer measurement, it may be feasible to remove some of the contaminants in the flash-frozen samples to reduce the possibility of competitive non-specific binding. However, this must be done with care, as we have shown that hemoglobin depletion also removes D-dimer (see Chapter II.3.1.3).

Additionally, the published studies of thrombolysis in human clots note a high baseline (385 ng/mL) or control (154 ng/mL) D-dimer concentration in untreated fluid (Kimura et al. 1994; Petit et al. 2015). All of our plasma samples, regardless of the associated treatment, showed a very low concentration of D-dimer (<1 ng/mL). This may be due to non-specific binding of the D-dimer kit to plasma components or fibrin degradation products other than D-dimer. Petit *et al.* note that the addition of rt-PA (3 µg/mL) to citrated human plasma (without the presence of a clot) approximately doubled the detected D-dimer from 385 ± 0 ng/mL to 624 ± 97 ng/mL (Petit et al. 2015), which is likely due entirely to nonspecific binding, as D-dimer can only be produced from the breakdown of cross-linked fibrin. Adam *et al.* have noted that there can be a great deal of variability in commercially available D-dimer assays because the D-dimer antigen is present on different sized FDPs and antibodies bind to different epitopes

(Adam et al. 2009). It is possible that the Asserachrom D-dimer ELISA kit is more specific for D-dimer than the commercial kits used by Kimura *et al.* and Petit *et al.*, allowing us to measure a lower baseline D-dimer concentration.

As noted, our D-dimer concentration was measured from homogenized clot samples rather than from samples of the fluid surrounding the clot. This method of D-dimer measurement has not previously been published but may be useful to evaluate static *in vivo* thrombolysis models, such intracerebral hemorrhage models (Morgan et al. 2008; Wagner et al. 1996; Wagner et al. 1999; Wagner 2007). After treatment, samples of clot may be taken and homogenized for later analysis. The generation of each clot sample is necessarily destructive, but whole, unhomogenized samples may be frozen, stored, and sampled later for analysis.

For the clots in which thrombolytic efficacy was evaluated with both mass loss and D-dimer quantification, we were able to reach the same statistical conclusions with mass loss and D-dimer concentration. The lytic rt-PA, with or without the addition of Definity[®] and US, produced significantly more thrombolysis than plasma alone. Furthermore, the exposure of Definity[®] to US did not significantly increase thrombolysis as measured by either metric. Absolute D-dimer did not show that rt-PA with adjuvant Definity[®] and US caused increased lysis over plasma alone. This lack of lytic enhancement is likely due to the limitations with the protocol used as noted previously. When comparing mass loss and D-dimer concentration, we note that the effect of Definity[®] and US shows a different trend in the two metrics, with mass loss increasing slightly with the addition of Definity[®] and US and D-dimer concentration decreasing slightly with the addition of Definity[®] and US. Ultrasound has been shown to increase rt-PA thrombolysis by both improving penetration of thrombolytics into the clot and removing fibrin degradation products away from the clot (Datta et al. 2006; Sutton et al. 2013a).

As a result, the D-dimer concentration could increase in the plasma surrounding the clot with the addition of Definity[®] and US, but decrease within the homogenized clot sample. In our system, the D-dimer in the plasma surrounding the clot seems to be too dilute to be measured by the Asserachrom D-dimer kit. For measurement of thrombolytic efficacy in the porcine ICH model, the hematoma exists within the white matter of the brain and D-dimer would likely not be able to diffuse away from the clot rapidly. However, the hematoma should be sampled in multiple areas to reflect thrombolysis throughout the volume of the clot.

II.6 Conclusions

In this chapter, we were able to develop a protocol for purification of D-dimer, with confirmation of protein identity by immunoblotting and MALDI TOF-TOF analysis. Evaluation of the commercially available Asserachrom D-dimer ELISA kit showed initial success in measurement of porcine D-dimer quantification, but the kit did not cross-react with porcine D-dimer at a later date. An initial screen of 5 commercially available D-dimer antibodies for development of an in-house ELISA protocol was completed, but no antibody pairs were found that were able to detect porcine D-dimer to a sensitivity of 10 ng/mL in contaminated samples. We found that D-dimer concentration and mass loss are correlated in a porcine model of thrombolysis and the same statistical conclusions were reached when evaluating the samples with the two separate metrics of thrombolytic efficacy. For *in vivo* experiments in which mass loss measurements are not possible, D-dimer concentration could be useful to compare different lytic therapies.

Chapter III. Initial development of a porcine arterial

thromboembolism model

III.1 Background

Conducting large-animal preclinical studies to evaluate novel thrombolytic-based therapies for ischemic stroke is necessary for their clinical translation. Models of ischemic stroke exist in many animals, including rodents, sheep, pigs, and non-human primates (Casals et al. 2011; Graham et al. 2004; Kumar et al. 2016). Many models allow the study of cerebral ischemia through methods such as surgical clamping of the carotid arteries, induction of systemic hypotension and hypoxia, or the injection of synthetic embolic material or thromboemboli (Graham et al. 2004; Kumar et al. 2016). Historically, the embolic models of stroke involved injection of embolic material into extracranial arteries which lead to variable infarcts and occlusions that often spontaneously recanalized (Kumar et al. 2016). More recently, exact placement of embolic material has been possible with the use of arterial catheters, such as through injection of thrombin at the desired site of clot formation (Chen et al. 2015) or through injection of a clot into a target artery (Culp et al. 2004; Gao et al. 2014; Gralla et al. 2006; Jahan 2010; Ringer et al. 2004). The use of thromboembolic material would allow the model to be used for evaluation of thrombolytic therapies in addition to being used for the study of cerebral ischemia (Kumar et al. 2016), and clots may be manufactured to mimic human disease based on clinical clot morphology (Liebeskind et al. 2011; Niessen et al. 2003).

Animal size and anatomy are also important when modeling human stroke conditions and treatment parameters. In 12 to 35% of human patients, the temporal bone is too thick or

inhomogeneous to allow ultrasound penetration using clinical transcranial Doppler ultrasound transducers (frequency range of 2-2.25 MHz) (Kwon et al. 2006; Postert et al. 1997; Wijnhoud et al. 2008). One proposed solution to improve ultrasound penetration is to use a lower frequency (<500 kHz) ultrasound beam (Behrens et al. 1999; Bouchoux et al. 2014b; Daffertshofer et al. 2005). At a frequency of 120 kHz, the ultrasound pressure reduction across a human temporal bone has been measured to be lower (mean of 33%, n = 5) than at a frequency of 1.03 MHz (mean of 65%, n = 5) and 2.00 MHz (mean of 86%, n = 5) (Ammi et al. 2008). Additionally, low-frequency transducers have a wider beam width compared to clinical transcranial Doppler transducers, allowing for transducer positioning based on external cranial landmarks rather than imaging-based alignment based on cranial CTs (Bouchoux et al. 2014b). Based on *in silico* analysis of clinical head CT's, an ultrasound beam would typically travel 55 mm to the M1 segment of the middle cerebral artery (MCA), at which point a 30 mm diameter unfocused 120 kHz transducer would have a -6 dB beam width of 27 mm and a 30 mm 500 kHz transducer with geometric focus at 80 mm would have a -6 dB beam width of 8 mm (Bouchoux et al. 2014b).

Large animal models such as pigs or sheep are best suited for sonothrombolysis to allow use of ultrasound equipment designed for humans in animal experiments due to the similarity of anatomical scales. Furthermore, low frequency ultrasound insonation will cover a volume that is small relative to the brain of the animal, allowing the assessment of therapeutic effects locally. In many grazing animals, including the pig, a *rete mirabile* capillary network exists between the extracranial and intracranial circulation (Daniel et al. 1953). Catheter-based placement of clots or *in situ* thrombus formation by injecting pro-coagulatory agents into intracranial vessels is difficult, if not impossible, as a catheter would not be able to bypass the capillary network. To

circumvent this limitation, previous porcine arterial thromboembolism models have utilized occlusion of the extracranial ascending pharyngeal artery for evaluation of thrombectomy devices (Gralla et al. 2006; Jahan 2010) and sonothrombolysis (Culp et al. 2004; Gao et al. 2014). Juvenile pigs (weight 30-35 kg) have been used in experiments previously to evaluate *in vivo* sonothrombolysis in the ascending pharyngeal artery (APA) with ultrasound penetration through the skull bone to mimic attenuation through human skull bone more closely (Culp et al. 2004; Gao et al. 2014). Additionally, porcine blood has commonly been used as an alternative to human blood for thrombolysis research (Chueh et al. 2011; Datta et al. 2006; Flight et al. 2006; Hitchcock et al. 2011; Holland et al. 2008; Sutton et al. 2013b) due to its availability, price, and biochemical similarity to human blood (Lewis 1996). The clots used for *in vivo* porcine sonothrombolysis studies by Culp *et al.* and Gao *et al.* were autologous, erythrocyte-rich, fresh clots formed on the day of the animal surgery (Culp et al. 2004; Gao et al. 2014). Highly retracted clots, such as those used in the evaluation of thrombectomy devices (Gralla et al. 2006; Jahan 2010), are produced to specifically resist clot fragmentation and represent a worst-case scenario in which clots are difficult to lyse with conventional thrombolytic therapy. The retracted clots used by Gralla *et al.* and Jahan *et al.* were also made radiopaque with the addition of the contrast agent barium sulfate (BaSO₄) (Gralla et al. 2006; Jahan 2010), allowing the groups to evaluate clot fragmentation and downstream embolization.

The objective of this study was to develop a porcine arterial thromboembolism model in which bilateral ascending pharyngeal arteries (APAs) were reliably occluded. A secondary objective was to assess the effect of intraarterial (IA) delivery of the FDA-approved thrombolytic recombinant tissue plasminogen activator (rt-PA) for recanalization of the occluded arteries. We hypothesized that following successful occlusion of the APA, IA delivery of rt-PA would

partially recanalize the artery over a 2 hr treatment window. Additionally, to allow for subsequent histopathological analysis of treated tissue, a tertiary objective was to create a protocol for the excision of the APAs from euthanized animals.

III.2 Materials and Methods

In each pig, occlusion of each ascending pharyngeal artery was attempted with highly-retracted, exogenously-formed clots. One occluded APA was treated with IA delivery of rt-PA and the other occluded APA was treated as an internal control with IA saline. Flow in each occluded artery was evaluated at 15 min intervals for the duration of the experiment (2 hrs).

III.2.1 Porcine whole blood clot manufacturing

Using protocols adapted from previously published studies (Gralla et al. 2006; Jahan 2010; Sutton et al. 2013b), highly retracted porcine whole blood clots were created using citrate phosphate dextrose-anticoagulated (CPD) porcine blood (Lampire Biological Laboratories, Inc., Pipersville, PA, USA). Blood was typically donor-derived, but the clots used in pig 2 were made from abattoir-derived blood. CPD blood was combined with 0.309 M calcium chloride in a 9:1 ratio and allowed to clot in borosilicate glass containers (ID 2.8-4.2 mm, Corning Pyrex, Corning, NY, USA) for 3 hours at 37 °C. To create radiopaque clots, CPD blood (4.5 mL) was combined with 0.309 M calcium chloride (0.25 mL) and powdered BaSO₄ (0.5 g) and BaSO₄-doped blood was added to borosilicate glass clotting containers (ID 2.8 – 4.2 mm, Corning Pyrex) primed with bovine thrombin (BioPharm Laboratories LLC, Bluffdate, UT, USA) solution to achieve a clot thrombin concentration of 2.5 U/mL.

Clots were incubated at 4 °C and used between 3 and 17 days following manufacture (Holland et al. 2008). Clots were trimmed to 1.5 cm in length and drawn into a large-bore 1 mL syringe (Medallion, Merit Medical, South Jordan, UT, USA) in preparation for injection.

III.2.2 Animal experiment protocol

Animal experiments were performed according to a protocol approved by the Cincinnati Children's Hospital Medical Center Institutional Animal Care and Use Committee. Nine female pigs weighing 38-80 kg were used in this study. Each pig was sedated with intramuscular (IM) ketamine (20 mg/kg) and xylazine (2 mg/kg), intubated, and general anesthesia was maintained with isoflurane (2-2.5%)/oxygen. Protocol changes were enacted over the course of the 9 pig experiments and will be highlighted in the following paragraphs. Additionally, a summary of the protocol changes enacted can be found in Table III.1.

Bilateral common carotid arteries (CCAs) were accessed with the use of 8 F transfemoral catheters introduced with 10 F introducer sheathes. Baseline digital subtraction angiography (DSA) with iodinated contrast media was used to evaluate the diameter of each APA lumen. Briefly, 8-10 mL of Optiray (Guerbet, Villepinte, France) was injected into the CCA while the Philips FD 20 Allura Clarity digital flat panel detector (Philips Healthcare, Andover, MA, USA) recorded CT images of the porcine head and neck, subtracting a baseline image from the subsequent images to provide a visualization of blood flow through the vasculature over time.

In pigs 1-5, heparin was administered in a 10 kU bolus immediately following vessel occlusion. Additional heparin (2000 U) was injected as a bolus every subsequent hour until the end of the experiment. In pigs 6-9, a baseline activated clotting time (ACT) was evaluated immediately after the establishment of vascular access. Heparin was injected in 10 kU boluses until the ACT was greater than 200 s to prevent the formation of additional clot endogenously

during the experiment (Lincoff et al. 2004). In pigs 2-9, 5 mg verapamil was injected into each APA to prevent arterial vasospasm.

For each pig, a clot of an appropriate diameter to occlude the artery (0.5-1 mm larger than the artery) was selected and injected into the APA via the 8F catheter. Arterial occlusion was confirmed with CT digital subtraction angiography. In case of unsuccessful occlusion, additional clots were injected until occlusion was successful or arterial vasospasm prevented further injections. Representative pre- and post-occlusion baseline DSA images are shown in Figure III.1.



Figure III.1. Representative CT digital subtraction angiography images of the common carotid artery and ascending pharyngeal artery (APA) (yellow arrow) a. pre-occlusion and b. following the occlusion of the APA with the exogenously formed clot.

Lytic treatment was initiated following the placement of a 0.021" microcatheter at the proximal face of each clot. Each pig served as its own internal control, with 1 mg/mL rt-PA injected into one APA while 0.9% saline was injected into the other APA following the same

protocol. To mimic clinical practice, each microcatheter was placed into the APA first crossing the clot to the distal side and used to deliver a 1 mL bolus of rt-PA or saline over 1.5 min, then withdrawn to the middle of the clot and used to deliver a second 1 mL bolus of rt-PA or saline over 1.5 min, then withdrawn to the proximal side of the clot (Lewandowski et al. 1999). At this time, CT digital subtraction angiogram was obtained for a t = 0 time point and the treatment infusion at the proximal face of the clot was initiated at a rate of 10 mL/hr. CT digital subtraction angiograms were obtained every 15 min until the conclusion of a 2 hr treatment period, at which point the pig was sacrificed. In pigs 4-7, a vascular occlusion coil (0.018", VortX, Boston Scientific, Marlborough, MA, USA) was pushed into each APA to provide a visual confirmation of APA identity upon pig head dissection immediately prior to injection of FatalPlus (20 mL, Vortech Pharmaceuticals LTD, Dearborne, MI, USA).

Table III.1 details the protocol details used in each pig experiment as noted above. For pig 5, a BaSO₄-doped clot was placed in the artery treated with saline, but not with rt-PA.

Table III.1. A summary of the 9 pig experiments performed.

Pig ID	Size (kg)	Verapamil	BaSO ₄ clots used	ACT-based Heparin dosing	# clots required for occlusion		Coil placed in APA
					Saline-treated APA	rt-PA-treated APA	
1	80	N	Y	N	unsuccessful	2	N
2	65	Y	Y	N	unsuccessful	5	N
3	52	Y	Y	N	1	1	N
4	60	Y	Y	N	1	2	Y
5	79	Y	Y saline, N rt-PA	N	1	1	Y
6	76	Y	N	Y	1	1	Y
7	62	Y	N	Y	2	1	Y
8	49	Y	N	Y	unsuccessful due to premature death		N
9	38.2	Y	N	Y	unsuccessful due to premature death		N

"Y" = yes, "N" = no

III.2.3 Thrombolytic efficacy

Our primary metric of thrombolytic efficacy was recanalization of the APA as measured by clinical perfusion scales. The Thrombolysis in Cerebral Infarction (TICI) scale allows for 5 levels of perfusion: Grade 0 indicates no perfusion, Grade 1 indicates anterograde perfusion beyond the occlusion but limited distal branch filling with slow distal perfusion, Grade 2a indicates anterograde perfusion of less than half the occluded artery ischemic territory, Grade 2b indicates anterograde perfusion of more than half of the target artery ischemic territory, and Grade 3 indicates complete anterograde perfusion of the target artery territory. Successful recanalization is achieved when an artery reaches a score of 2b or 3 on the TICI scale (Moftakhar et al. 2013). The Thrombolysis In Myocardial Infarction (TIMI) scale and Arterial Occlusive Lesion (AOL) scale scores were also recorded. The TIMI score is similar to the TICI score and the AOL score deals with recanalization of the primary lesion, largely without note on the perfusion of the affected artery (Chesebro et al. 1987; Zaidat et al. 2013b). The secondary metric for any arteries that achieved recanalization prior to the end of the 2-hr treatment window was time to recanalization.

III.2.4 APA excision

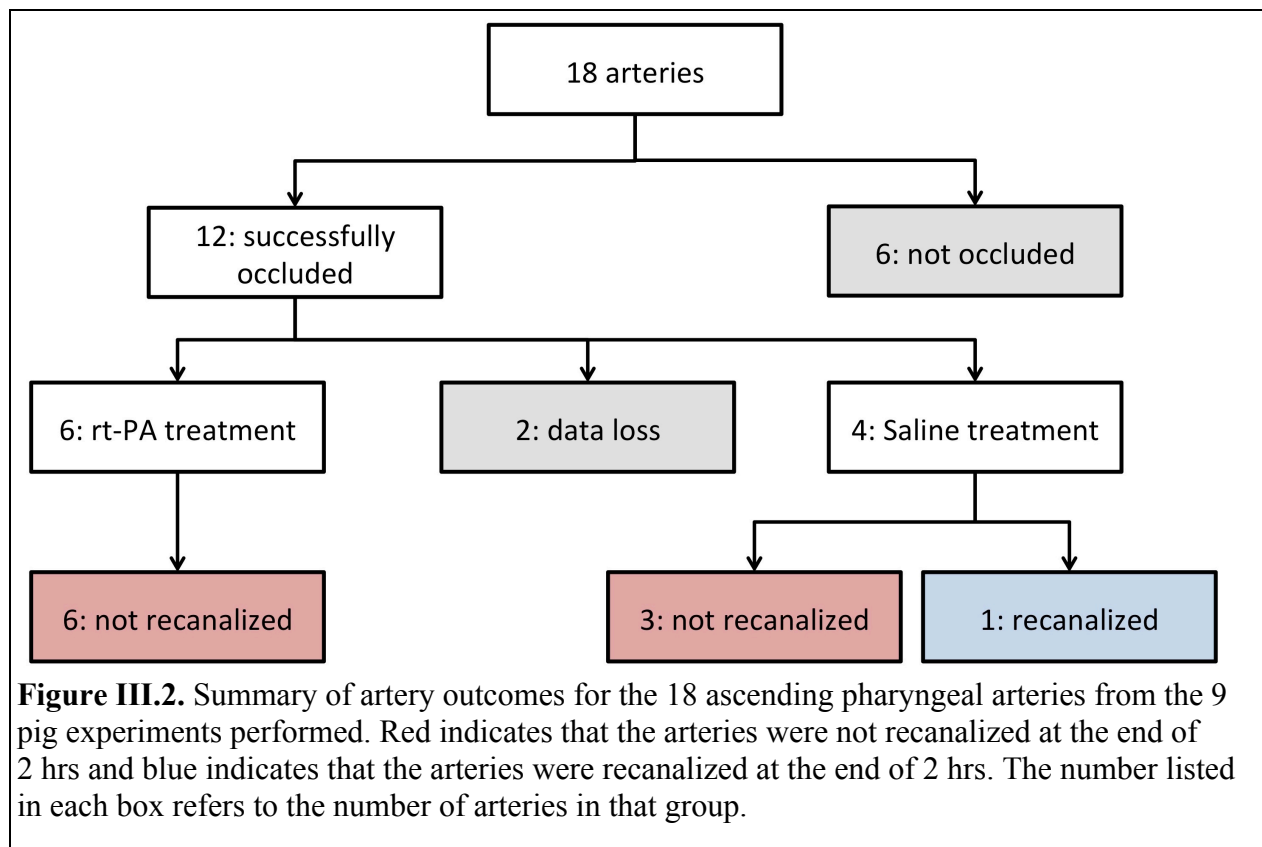
Following euthanasia, each pig was methodically dissected to establish a protocol for excision of the APAs to prepare for histopathological examination of the APAs in subsequent studies. In each animal, a 10" serrated hacksaw was used for decapitation at the cervical spine caudal to the auricles and mandible. In pig 1, decapitation was performed in the angiography suite. In pigs 2-9, the animals were transferred to a dissection room on a gurney within the veterinary services suite prior to decapitation, which began 15-30 minutes post euthanasia. In pigs 1, 2, and 7, decapitation immediately preceded exploratory dissection of the APA. In pigs 3-

6, 8, and 9, the pig head was stored at 4 °C until dissection could be performed with the aid of an Ear, Nose, and Throat surgeon, Dr. Yash Patil, up to 1 week later. Pig head 4 was discarded as it could not be dissected within the appropriate time frame. In each exploratory dissection, the CCA was identified and an ascending dissection was performed to locate the APA. As noted in Chapter III.2.2, a vascular occlusion coil was placed into each APA of pigs 4-7 immediately before euthanasia to allow for visual confirmation of APA identity. Coils could not be placed in pigs 8 and 9 due to the premature death of the animals.

III.3 Results

III.3.1 Establishment of arterial occlusion

Of the 18 ascending pharyngeal arteries, 12 were successfully occluded (bilateral occlusion in 5 pigs and unilateral in 2). Eight of our 12 successfully occluded arteries were occluded with a single clot, while 3 arteries were occluded with 2 clots and one artery required 5 clots (Table III.1). Data was acquired from 10 arteries for the full 2 hr treatment window, 6 rt-PA-treated and 4 saline-treated. Data from 2 arteries were lost due to a technical glitch. A summary of artery outcomes may be seen in Figure III.2.



III.3.2 Thrombolytic efficacy

As seen in Figure III.2, none of the 6 rt-PA treated arteries recanalized within the 2 hour treatment window. One of the 4 saline-treated arteries (pig 7) recanalized within the first 15 min of the experiment). The majority of arteries showed no change in TICI score (TICI = 0) throughout the 2 hr treatment. Two rt-PA treated arteries (pig 1 and pig 2) showed some fluctuation in the TICI score (up to a max TICI score of 2a) but had a TICI score of 0 or 1 at the end of 2 hours. Two pigs (pigs 8 and 9) died prematurely following a reaction in which the skin became red and mottled and circulation to extremities was reduced. No definitive cause of death was found for these pigs, but two possible explanations for the deaths are: 1. allergic reaction and 2. verapamil toxicity.

III.3.3 APA excision

Of the 8 pig heads dissected, 3 pigs had a vascular occlusion coil placed to aid in identification of the APA. The APA was successfully located and positively identified in 2 of the 3 pigs. Additionally, pigs 8 and 9 were dissected and the APA was believed to be successfully located based on anatomical landmarks, though this could not be confirmed with the vascular occlusion coil. Based on our experience, a protocol was finalized for excising the APA, which is described briefly in the following steps:

1. *Pig head decapitation* – An incision was made with a scalpel blade in the posterior neck, caudal to the auricles and mandible. The incision was deepened to the vertebral column and carried towards the anterior neck on either side of the vertebrae. A hacksaw was used to sever the vertebrae, after which the soft tissue in the anterior neck was severed. The head was suspended for approximately 5 minutes to allow drainage of any blood that had yet to coagulate within the vasculature.
2. *Location of the CCAs* – The trachea was identified and the CCAs were located bilaterally between the left/right sides of the trachea and more posterior soft tissues. The CCAs were the largest arteries visible in this area. For convenience, a hemostat was clipped on the severed end of each CCA to maintain artery identification.
3. *Submandibular V-incision* – At this time, two incisions were made from the anterior midline of the severed pig head to the left and right corners of the mouth, reaching approximately two-thirds to three-fourths of the way to each oral commissure. These incisions were deepened further during ascending dissection.

4. *Ascending dissection of the CCAs* – The CCA was carefully dissected away from surrounding muscles and fascia until further segments of the CCA were exposed. Muscle was excised from the pig head to maintain the field of view necessary. The CCA was progressively exposed a few centimeters at a time until the bony protrusion of the end of the styloid bone was palpable in the soft tissue lateral to the CCA. The styloid process is a critical landmark in identifying the APA, as the APA arises from the medial side of the CCA near the styloid bone and travels towards the base of the skull.
5. *APA excision* – The APA was progressively exposed by the removal of surrounding soft tissue until the skull base was exposed as well. For excision, the APA was severed at the skull base immediately proximal to the *rete mirabile* and the CCA was severed cranially to the APA.

III.4 Discussion

Throughout the porcine APA model development, the protocol was refined until bilateral APA occlusions were consistent and reproducible. Verapamil was not part of the initial protocol, but the vasospasm present in pig 1 indicated that a vasorelaxer would be needed in subsequent pigs. The clots used in pig 2 were produced from abattoir-derived rather than donor-derived CPD blood and required 5 clots to occlude a single side, suggesting that clots produced from overnight-shipped abattoir-derived blood were less firm and retracted than those produced from donor-derived blood.

For pigs 1-5, heparin was given as a set dose of a 10 kU bolus at the beginning of the experiment, followed by a 2 kU bolus every subsequent hour. Close inspection of the CT digital

subtracted angiograms and unsubtracted images indicated a mismatch between the end of the radiopaque clot and the end of the penetration of contrast into the APA. This suggested the formation of additional endogenous clot within the APA. For pigs 6-9, the heparin dosing scheme was changed to be based on an activated clotting time (ACT) measurement rather than clinical dosing to compensate for the observed porcine hypercoagulability (Lewis 1996; Velik-Salchner et al. 2006).

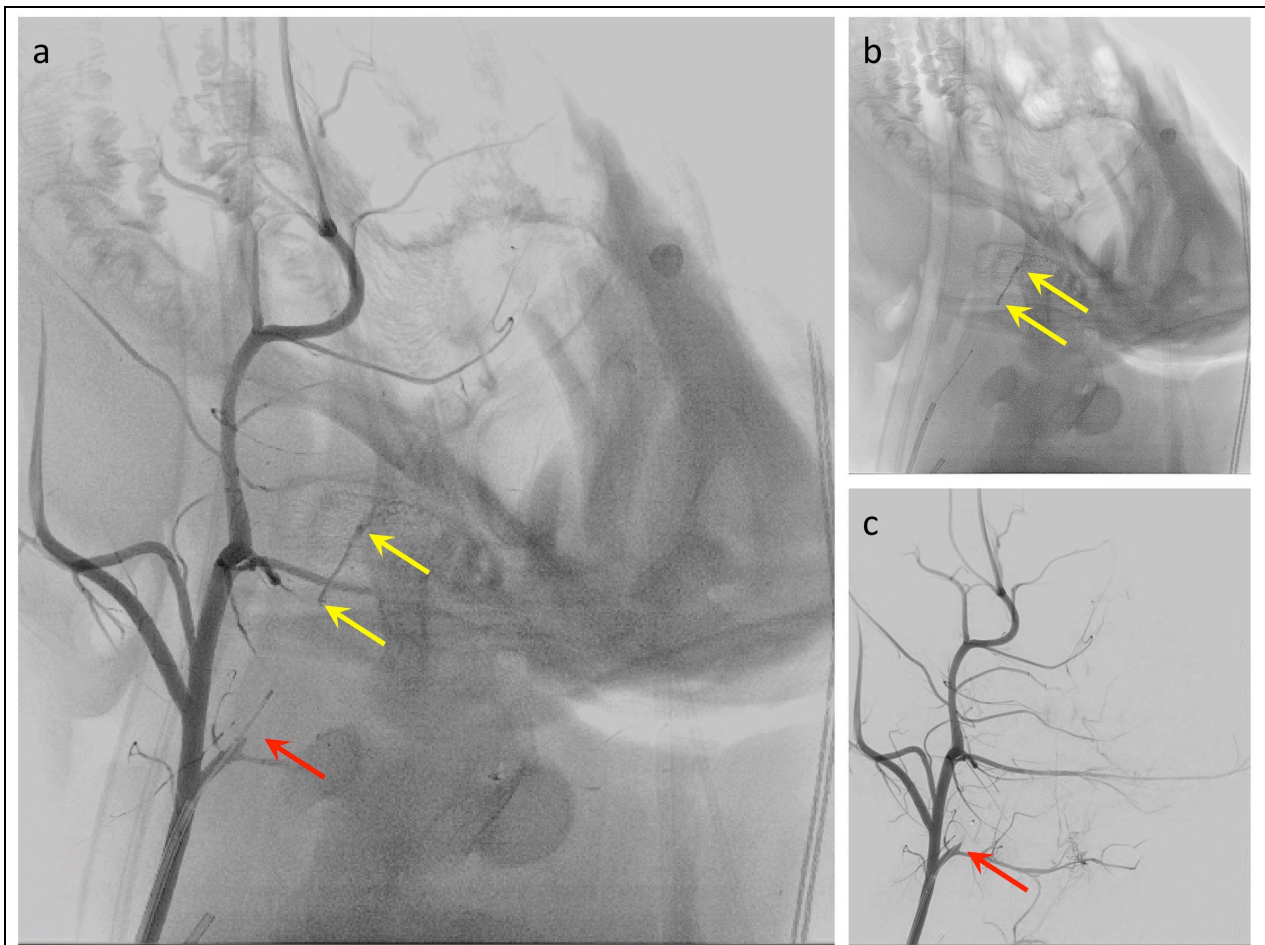


Figure III.3. (a) An overlay of a digital subtracted angiogram with corresponding unsubtracted CT image shows a mismatch between the radiopaque clot (ends denoted by the two yellow arrows) and the end of the contrast front (red arrow), **(b)** the original unsubtracted CT, **(c)** the original digital subtracted angiogram

Because of the lack of rt-PA lytic efficacy in the first 4 pigs, we hypothesized that BaSO₄ may reduce the thrombolytic susceptibility of porcine clots and used non-doped clots for the last 2 (of 6) rt-PA-treated clots and 1 (of 4) saline-treated clots. No difference was seen in degree of recanalization between the non-doped and BaSO₄-doped clots, as no rt-PA treated APAs recanalized. Other explanations for the decreased rt-PA lytic efficacy include biochemical differences in porcine and human blood, such as a reduced concentration of or activity of porcine plasminogen (Flight et al. 2006; Huang et al. 2017).

In pig 7, we observed that the first clot injected into the pig 7 saline-treated APA had traveled to a neighboring vessel rather than establishing an occlusion in the APA. The APA was successfully occluded with a second clot, but during treatment with saline, it almost immediately showed "recanalization", suggesting that the 2nd clot had also migrated to a nearby vessel rather than being lysed. It is possible that pig 7's collateral circulation was unusually strong and retrograde flow dislodged the clot early during our treatment window.

Pigs 8 and 9 died prematurely and no arteries in either pig were successfully occluded. Two possible explanations for the premature deaths have been proposed. First, it may be possible that the pigs had an allergic reaction to one or more of the compounds administered during the course of the pig experiment. However, this seems unlikely as the pigs are naïve and should not have come in contact with any medical compounds prior to our experiment. Second, pigs 8 and 9 were the smallest pigs used for our studies, at 49 kg and 38.2 kg respectively. Discussion with veterinary staff and review of veterinary textbooks suggested that the IV dose of verapamil at 10 mg in each experiment would be too high for pigs this size (0.2-0.26 mg/kg). The recommended verapamil dose in pigs is 0.15 mg/kg (Swindle 1998) and verapamil toxicity can cause low blood pressure, shock, and even death (Barry et al. 2005; Kurola et al. 2010; Tanen et al. 2000). In

order to continue verapamil use at 5 mg per artery, we should accept pigs with a minimum size of 65 kg.

We were successful in developing a general protocol for excision of the APAs following the completion of the *in vivo* thrombolysis experiment and subsequent animal euthanasia. However, some practical considerations may limit the usefulness of histopathological APA examination. The need to move the subject to a separate room for dissection increases the time elapsed between euthanasia and the successful excision of the APA by at least 10-15 minutes. Though we did not measure the time required for the full APA excision procedure, Eliyas *et al.* were able to excise the rete mirabile, the capillary network that begins where the APA meets the skull base, in 25-30 min after establishment of a focused dissection protocol (Eliyas *et al.* 2016). The closeness of the APA and the rete mirabile suggests that this time frame is a reasonable estimate for someone practiced in the APA excision protocol. This additional 35+ minutes following the conclusion of each pig experiment could impact histopathological analysis of the APA. In particular, the presence of any residual clot burden be diminished by an additional 30 min "treatment" from any rt-PA remaining in the APA (Sutton *et al.* 2013b).

Future studies in this model may use further adapted versions of the presented protocol for *in vivo* evaluation of novel thrombotic therapies. For example, to overcome deficiencies in porcine plasminogen, the introduction of human plasminogen may allow porcine clots to better mimic human hemostasis (Chapter IV and Chapter VI). Porcine clots have also been proposed to have a more retracted, less porous clot structure than human clots (Huang *et al.* 2017; Landskroner *et al.* 2005), which may be addressed by changing the clotting surface (Sutton *et al.* 2013b) or adding a compound to change clot structure, such as dextran or aspirin (Tangen *et al.* 1972; Undas *et al.* 2007)

III.5 Conclusions

In conclusion, this study showed the feasibility of bilaterally occluding the ascending pharyngeal arteries of the pig in a reliable manner. Most arteries were occluded with a single clot chosen to be about 1 mm larger than the inner diameter of the target artery. We were also able to implement a protocol for the excision of the APAs following animal euthanasia. However, the intraarterial delivery of rt-PA did not recanalize any of the occluded arteries. To investigate the possible reasons for the lack of rt-PA response, two sets of *in vitro* studies were performed. First, the differential rt-PA thrombolysis in porcine and human blood was investigated (Chapter IV). Secondly, the difference in lytic susceptibility of BaSO₄-doped and non-doped clots was investigated (Chapter V).

Chapter IV. Comparative lytic efficacy of rt-PA and ultrasound in porcine versus human clots

IV.1 Introduction

Ischemic stroke affects nearly 700,000 people each year and is the fifth most common cause of death in the United States (Mozaffarian et al. 2016). Presently, mechanical thrombectomy and intravenous administration of recombinant tissue-type plasminogen activator (rt-PA) are approved by the United States Food and Drug Administration for recanalization of arteries blocked in ischemic stroke. Although these treatments are clinically effective, ischemic stroke patients continue to experience significant morbidity and mortality. Intravenous administration of rt-PA can provide benefit within 3 to 4.5 hours of symptom onset, but treatment exclusion criteria limit administration to only 3.4-5.2% of patients (Hacke et al. 2008; Mozaffarian et al. 2016; The NINDS rt-PA Stroke Study Group 1995). Treated patients display variable outcomes dependent on clot size, site, and composition, with larger, proximal, and more fibrin-rich clots being more resistant to thrombolytic treatment (Kim et al. 2006; Linfante et al. 2002; Saqqur et al. 2007; Suarez et al. 1999; Zivin et al. 1985). Mechanical thrombectomy, the physical removal of the clot endovascularly, can be effective in treating ischemic stroke for up to 8 hours after symptom onset (Berkhemer et al. 2015; Campbell et al. 2015; Jovin et al. 2015; Nogueira et al. 2012; Saver et al. 2015; Smith et al. 2005). However, mechanical thrombectomy can only be performed when clots are located in larger cranial vessels. Only an estimated 4-14% of acute ischemic stroke patients are eligible for thrombectomy (Zaidat et al. 2013a). Furthermore, many hospitals lack the facilities and expertise to perform this advanced

interventional procedure. Patients treated with either modality exhibit similar rates of disability-free recovery (34.8% for intravenous rt-PA vs 30.4% for endovascular interventions), as well as similar rates of serious adverse reactions (6% incidence of symptomatic intracerebral hemorrhage [sICH] in both groups) (Ciccone et al. 2013). Some additional benefits have been shown with the initiation of an antiplatelet agent (e.g. aspirin) within 48 hours of symptom onset. Though antiplatelet agents prevent the formation of new thrombi, they do not promote recanalization, and, importantly can increase the incidence of sICH (Heck and Brown 2014; Jauch et al. 2013). The limitations of the existing treatment modalities motivate continued investigation of alternative strategies to improve efficacy, expand the duration of the treatment window, or increase the size of the eligible patient population.

Sonothrombolysis, the use of ultrasound (US) to promote clot lysis, has been under investigation for enhancing the efficacy of thrombolytic therapy (Adzerikho et al. 2013; Bader et al. 2015b; Culp et al. 2004; Gruber et al. 2014; Hitchcock et al. 2011; Laing et al. 2012; Suchkova et al. 2000; Sutton et al. 2013b). Clinical trials have shown that Doppler US as an adjuvant to rt-PA can moderately increase the likelihood of complete recanalization and functional independence at 3 months (Alexandrov et al. 2004; Tsivgoulis et al. 2010). Unfortunately, 2-MHz transcranial Doppler US cannot penetrate the skull in about 12-18% of the patient population, due to increased attenuation within the temporal bone (Postert et al. 1997; Wijnhoud et al. 2008).

Our group has reported enhancement of rt-PA thrombolysis with 120 kHz intermittent ultrasound using a low *in situ* peak-to-peak pressure amplitude (0.44 MPa), which avoids the limitations of temporal bone acoustic window insufficiency (Bader et al. 2015a; Bader et al. 2015b; Bouchoux et al. 2014b; Datta et al. 2008). This approach appears to expedite clot lysis by

accelerating penetration of the thrombolytic into the clot and facilitating removal of fibrin degradation products via two distinct mechanical effects: fluid mixing from microbubble activity and vibration from radiation force (Bader et al. 2015b). Sustained microbubble activity, or stable cavitation, can enhance thrombolysis by increasing the penetration of drug into clots (Bader et al. 2015b; Datta et al. 2006; Hitchcock et al. 2011). Stable cavitation can be nucleated effectively at low acoustic pressures by administration of an US contrast agent (UCA) such as Definity[®] (Lantheus Medical Imaging, North Billerica, MA, USA). These experiments employed an *in vitro* time-lapse microscopy system (Bader et al. 2015a; Bader et al. 2015b; Gruber et al. 2014) that allowed for careful control of the clot type, surrounding fluid, and US field, as well as precise quantification of thrombolysis and the degree of bubble activity.

Evaluation of US exposure parameters and treatment protocols *in vitro* and in animal models is key to the clinical translation of US as an adjuvant in ischemic stroke therapy. Previously, human and porcine clots have been treated *in vitro* and *ex vivo* (Bader et al. 2015a; Bader et al. 2015b; Hitchcock et al. 2011; Sutton et al. 2013b). In addition animal models have been developed to test sonothrombolysis (Culp et al. 2004; Gao et al. 2014; Laing et al. 2012) and thrombectomy procedures *in vivo* (Gralla et al. 2006; Jahan 2010). Highly retracted, dense clots are more resistant to rt-PA lysis and are associated with poor clinical treatment outcomes (Undas and Ariens 2011). Retracted thromboemboli can arise as a result from arterial atheromatous plaques or as a result of cardiac disease (such as atrial fibrillation, patent foramen ovale, cardiac mural thrombi) and migrate to the cerebrovasculature to cause ischemic stroke (Adams et al. 1993; Hashimoto et al. 2016; Liebeskind et al. 2011; Marder et al. 2006). Our group has reported techniques to develop highly-retracted human and porcine clots for evaluating rt-PA sonothrombolysis *in vitro* (Bader et al. 2015b; Holland et al. 2008; Sutton et al. 2013b).

Although porcine clots are employed routinely in thrombolysis research, the comparative lytic efficacy of rt-PA and intermittent US in porcine versus human clots has not been established. Porcine clots are characterized by a denser fibrin network compared to human clots, and demonstrate higher lytic resistance when treated with human plasmin (Landskroner et al. 2005). Activation of plasminogen to form plasmin relies on the presence of both rt-PA and fibrin (Gabriel et al. 1992). The activation of human and porcine plasminogen by rt-PA in the presence of same species or cross species fibrin, has been compared previously (Flight et al. 2006). The resultant porcine plasmin activity was found to be lower than human plasmin activity by almost 10-fold (Flight et al. 2006). However, the effect of this differential rt-PA activation on thrombolytic efficacy, with US exposure as an adjuvant, is still unknown.

The objective of this study was to compare thrombolytic efficacy between porcine and human clots exposed to plasma alone, rt-PA, or rt-PA with Definity[®] exposed to intermittent 120 kHz US as an adjuvant. We also exposed human and porcine clots to either porcine or human plasma to evaluate whether the type of plasminogen affected rt-PA thrombolytic efficacy. An *in vitro* flow model and time-lapse microscopy system was employed to determine lytic efficacy as reported previously (Bader et al. 2015a; Bader et al. 2015b; Gruber et al. 2014).

IV.2 Materials and Methods

IV.2.1 Preparation of plasma, rt-PA, and ultrasound contrast agents

Human or porcine fresh frozen plasma was pooled prior to experimental use to minimize the effect of individual-to-individual variability. Sodium citrate-anticoagulated fresh frozen pooled porcine plasma was procured from Lampire Biological Laboratories (Pipersville, PA, USA). Porcine plasma was thawed and filtered through 4x4 gauze pads (Fisher Healthcare,

Pittsburgh, PA, USA) to remove fibrin clots. Eight units of citrate phosphate double dextrose-anticoagulated fresh frozen human plasma were acquired from the Hoxworth Blood Center (Cincinnati, OH, USA). These units were thawed, pooled, and refrozen as 25 mL aliquots for experimental use. Prior to each experiment, either porcine or human plasma was thawed and warmed to 37 °C and allowed to equilibrate to atmospheric gas saturation.

The FDA approved lytic agent rt-PA (Activase, Genentech, San Francisco, CA, USA) was reconstituted with sterile water according to manufacturer instructions to a concentration of 1 mg/mL. One-milliliter aliquots were created and stored at -80 °C until use. Aliquots of rt-PA stored according to this protocol have been shown to have stable activity for at least 7 years (Shaw et al. 2009b). Definity[®] perflutren lipid microspheres were activated according to manufacturer instructions. Specifically, vials of Definity[®] stored at 4 °C were equilibrated at room temperature for 1 hour prior to agitation using a Vial-Mix (Lantheus Medical Imaging) for 45 s, and used at least 15 min after agitation.

IV.2.2 Preparation of human whole blood clots

In accordance with previously reported protocols, cylindrical human clots (initial mean clot width of 302.3 ± 41.8 μm) were formed around silk sutures in micropipettes (Bader et al. 2015a; Bader et al. 2015b; Shaw et al. 2009a). Briefly, borosilicate micropipettes (1.12 mm inner diameter, World Precision Instruments, Sarasota, FL, USA) were cut to a length of 2.5 cm and each was threaded with a 10 cm long 7-0 silk suture (Ethicon Industries, Cornelia, GA, USA). The threaded micropipettes were placed into 10 x 75mm disposable borosilicate glass culture tubes (VWR, West Chester, PA, USA). Following a protocol approved by the University of Cincinnati Institutional Review Board, written consent was obtained from four healthy volunteers and venous human blood was drawn from each volunteer into 10-mL BD plastic

syringes (Franklin Lakes, NJ, USA). A 500 μL aliquot of donor blood was pipetted into each of the disposable glass culture tubes containing a threaded micropipette and allowed to clot at 37 $^{\circ}\text{C}$ for 3 hrs, followed by a minimum of 3 days at 4 $^{\circ}\text{C}$ to allow for retraction (Shaw et al. 2009a). The use of this clot model allowed direct comparison with previously published experiments which investigated mechanisms of thrombolysis in human clots (Bader et al. 2015b).

IV.2.3 Preparation of porcine whole blood clots

The protocol used to prepare human blood clots (Bader et al. 2015b) was combined with a protocol for preparing porcine blood clots (Sutton et al. 2013b) to produce porcine whole blood clots around silk sutures. Borosilicate micropipettes (1.12 mm inner diameter, World Precision Instruments, Sarasota, FL, USA) were cut to a length of 2.5 cm, threaded with 10 cm long 7-0 silk sutures (Ethicon Industries, Cornelia, GA, USA), and placed into 10x75mm disposable borosilicate glass culture tubes (VWR, West Chester, PA, USA). Porcine clots were created using whole porcine blood anti-coagulated with citrate phosphate dextrose (CPD) solution from Lampire Biological Laboratories, Inc. (Pipersville, PA, USA). The CPD blood was recalcified with 309 mM calcium chloride (Sigma-Aldrich, St. Louis, MO, USA) solution in a 9:1 ratio. Aliquots of 500 μL recalcified blood were pipetted into each glass culture tube. The recalcified blood was allowed to clot for 3 hours in a 37 $^{\circ}\text{C}$ water bath and was stored at 4 $^{\circ}\text{C}$ for a minimum of 3 days to allow for clot retraction. The initial mean clot width of porcine clots was $384.6\pm 41.8 \mu\text{m}$.

IV.2.4 Comparison of rt-PA susceptibility in porcine and human clots using time-lapse microscopy *in vitro*

IV.2.4.1 Experimental set-up

Following previously published protocols (Bader et al. 2015a; Bader et al. 2015b; Gruber et al. 2014), an *in vitro* capillary flow system (Fig 1) was used to measure the thrombolytic efficacy and cavitation activity in human and porcine whole blood clots. An acrylic tank (16 x 33 x 9 cm) lined with 1-cm-thick acoustically absorbent material (Aptflex F48, Precision Acoustics, Dorchester, Dorset, UK) was filled with reverse-osmosis water. The water was heated to 37 ± 1 °C, degassed ($20\pm 5\%$ dissolved oxygen), and filtered ($0.2\ \mu\text{m}$) via a custom recirculation system for the duration of each experiment. The cylindrical clots adherent to sutures were gently removed from the micropipettes, placed into a larger glass micropipette (2.15-mm inner diameter; Drummond Scientific, Broomall, PA, USA), and attached to the flow channel with latex tubing that allowed the clot to be held securely during the experiments. Low-density polyethylene tubing (inner diameter 1.6 mm; Freelin Wade, McMinnville, OR, USA) formed the flow channel connecting the glass micropipette to the perfusate reservoir upstream and the syringe-pump downstream. A syringe-pump (Model 44, Harvard Apparatus, South Natick, MA, USA) was used in continuous withdrawal mode to maintain a flow rate of 0.65 mL/min, which is consistent with physiologic flow rates in ischemic stroke (Alexandrov et al. 2010). The clot within the micropipette was positioned 1 mm from the bottom of the tank and imaged with an inverted microscope (IX71, Olympus, Center Valley, PA, USA). Images were recorded with a charge-coupled device (CCD) camera (Regita-2000 R, Q Imaging, Surrey, BC, Canada) at a rate of 2.33 Hz throughout each 30-min experiment.

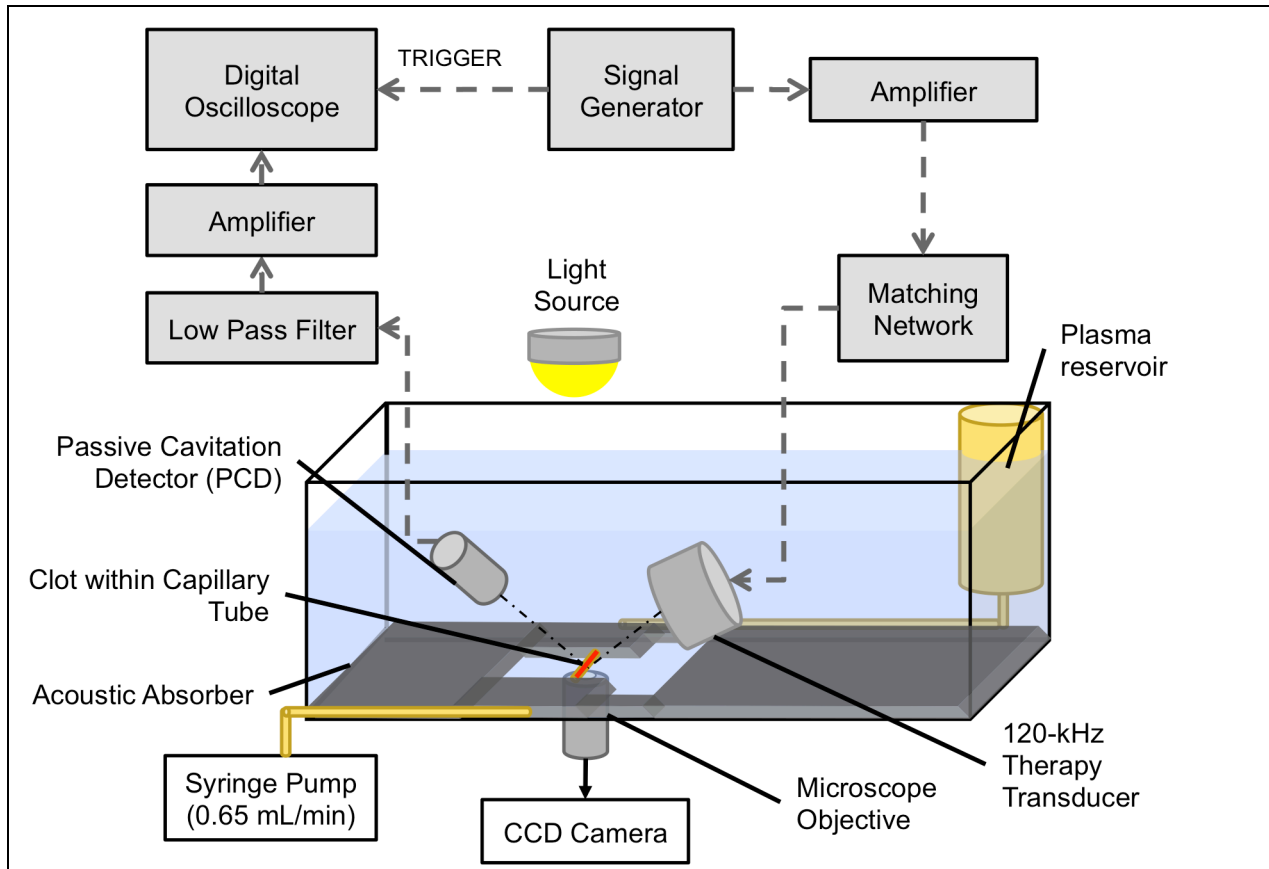


Figure IV.1. The experimental set-up for the in vitro flow system. In a water tank held at 37 °C, the clot is mounted within a capillary tube through which plasma is drawn from an upstream plasma reservoir to a downstream syringe pump. Acoustic absorber was used to line the 4 vertical walls of the water tank (not shown) and the bottom of the tank (shown), with approximately 3 cm of the capillary tube visible through a window in the acoustic absorber. From: Huang *et al.* Comparative lytic efficacy of rt-PA and ultrasound in porcine versus human clots. *PLoS One*. 2017;12(5):e0177786.

IV.2.4.2 Clot Diameter

Using the images recorded with the CCD camera, the clot width as a function of time was determined based on an edge-detection routine published previously (Meunier et al. 2007). The detected clot width was verified visually following the completion of the routine and adjusted in a few cases to correct algorithmic errors (3.7% of experimental runs). These algorithmic errors arose from issues such as debris flowing in the field of view. The clot diameter in each frame

was defined as the average distance between the detected edges over all pixel rows minus the diameter of the suture ($58.5 \pm 12.0 \mu\text{m}$) (Bader et al. 2015b; Shaw et al. 2009a). The fractional clot loss (FCL) and average lytic rate (ALR) were computed to evaluate the thrombolytic efficacy. The fractional clot loss was defined as:

$$\text{FCL} = \frac{CW_0 - CW_f}{CW_0} \times 100\%, \quad (1)$$

where CW represents the clot width after the suture has been subtracted. CW_0 represents the initial clot width, and CW_f represents the final clot width after the completion of treatment (30 min).

The average lytic rate was defined as:

$$\text{ALR} = \frac{\text{FCL}}{t_d}, \quad (2)$$

where t_d represents the treatment duration. For clots that lysed completely before 30 minutes, t_d was set to the time at which 100% FCL was achieved. The ALR was used as a secondary metric to improve assessment of groups in which 100% FCL was achieved prior to the end of the treatment period.

IV.2.4.3 Ultrasound Insonation and Detection

For trials involving US exposure, clots and perfusate were insonated using a custom-designed unfocused 120 kHz transducer (30-mm diameter aperture; H160, Sonic Concepts, Woodburn, WA, USA) (Bader et al. 2015a; Bader et al. 2015b; Gruber et al. 2014). A function generator (33250A, Agilent Technologies, Santa Clara, CA, USA) was used to generate tone-bursts that were boosted by 55 dB by a power amplifier (1040L, ENI, Rochester, NY, USA). The transducer was excited at 120 kHz, and the power transfer to the transducer was maximized via a custom-built impedance matching network (Sonic Concepts, Woodburn, WA, USA). A peak-to-

peak pressure of 0.44 MPa (*in situ*) was employed using an intermittent insonation scheme (50 s continuous wave insonation followed by a 30 s quiescent period) for the duration of the 30-min experiment (Hitchcock et al. 2011). The 50-s on-time was found to maximize ultraharmonic (UH) emissions, indicative of stable cavitation (Datta et al. 2006), throughout the 30-min treatment period (Bader et al. 2015b). A 30s off-time allowed for replenishment of Definity[®] within the microscope field of view for the flow rate employed in this study (0.65 mL/min). An intermittent exposure scheme also prevented transducer overheating during the 30-min treatment period.

The acoustic field within the acrylic tank was measured and the transducer was calibrated previously (Gruber et al. 2014). No standing waves or constructive interference were detected at the location of the clot. A single-element long-focus 2.25-MHz transducer (595516C, Picker Roentgen GmbH, Espelkamp, Germany) was used as a passive cavitation detector (PCD) to measure ultraharmonic and broadband emissions, which are characteristic of stable (Datta et al. 2008; Hitchcock et al. 2011) and inertial cavitation (Datta et al. 2008) respectively. The signal from the PCD was low-pass filtered (10-MHz, J73E, TTE, Los Angeles, CA, USA), boosted by a wide-band low-noise amplifier (CLC100, Cadeca Microcircuits, Loveland, CO, USA), and digitized (10-ms duration, 31.25-MHz sampling frequency). Custom MATLAB scripts were used to analyze the power spectra of the PCD signal. To quantify stable cavitation emissions, the UH energy bands between 250 kHz and 1 MHz were summed over a 2-kHz bandwidth centered around each UH frequency, which were previously shown to have a signal-to-noise ratio greater than 3 dB (Gruber et al. 2014). To quantify inertial cavitation emissions, the BB energy was summed in 4-kHz bands centered around the UH bands (± 10 kHz and ± 30 kHz).

IV.2.4.4 Experimental Protocol

Porcine and human clots were exposed to one of three experimental protocols in the presence of human or porcine plasma, respectively. Each clot was exposed to one of three treatment protocols: plasma alone; plasma with rt-PA (3.15 $\mu\text{g}/\text{mL}$); and plasma with rt-PA (3.15 $\mu\text{g}/\text{mL}$) and Definity[®] (2 $\mu\text{L}/\text{mL}$) exposed to intermittent 120 kHz US as described above. We also compared the thrombolytic efficacy against previously published studies from our laboratory that exposed human clots to human plasma, rt-PA, Definity[®], and intermittent 120 kHz US (Bader et al. 2015b). We employed the same experimental system, utilized the same treatment protocols and analysis scripts, obtained human blood from the same volunteer donor pool, and plasma from the same source as Bader *et al.* (2015). Additionally, porcine clots were also exposed to each of the 3 experimental protocols in porcine plasma for comparison. The rt-PA concentration of 3.15 $\mu\text{g}/\text{mL}$ is consistent with steady-state rt-PA concentration in the bloodstream after an intravenous injection of rt-PA in a patient with ischemic stroke (Tanswell et al. 1991). The concentration of Definity[®] (2 $\mu\text{L}/\text{mL}$, or 2.4×10^7 microspheres/mL [The particle concentration at a 2 $\mu\text{L}/\text{mL}$ dilution of Definity[®] was previously erroneously cited as 1×10^4 particles/mL (Bader et al. 2015a; Bader et al. 2015b).]) was based on our previous studies (Bader et al. 2015b). In each trial, one clot was mounted in the capillary tube, connected to the flow system, submerged in the water tank, and positioned over the microscope objective. The PCD focus was aligned with the capillary tube and used to record US emissions over the 30 min treatment period. The CCD camera recorded images at a rate of 2.3 Hz, which were transferred to a desktop computer for offline analysis.

IV.2.5 Histology

Human whole blood clots and porcine whole blood clots were fixed in 10% formalin, embedded in paraffin, and stained with hematoxylin and eosin (H&E) before being analyzed histologically. An Olympus IX-71 research inverted microscope and DP72 camera (Olympus Scientific Solutions Americas Inc., Waltham, MA, USA) were used to observe and image the clot sections.

IV.2.6 Electron Microscopy

Clots were processed and subjected to routine scanning electron microscopy (SEM) to visualize the fibrin mesh. After the 3-day retraction period, clots were removed from the capillary tubes and rinsed with cold PBS. Clots were placed in 2.0% paraformaldehyde and 2.5% gluteraldehyde in 0.1 M sodium-cacodylate buffer, pH 7.4, for an overnight fixation. Samples were rinsed 3 times with 0.1 M sodium-cacodylate buffer and post-fixed with 1% osmium tetroxide. Samples were again rinsed 3 times with 0.1 M sodium cacodylate buffer and dehydrated in a graded series of ethanol steps for 30-min each (v/v: 25, 50, 75, 95, 100, 100, and 100%). Finally, clots were dehydrated on a Leica EM CPD300 Critical Point Dryer (Leica Microsystems, Buffalo Grove, IL, USA) and sputter-coated with gold-palladium on a Leica EM ACE600 High Vacuum Sputter Coater. High-resolution SEM images (800-7000x magnifications) were acquired from the surfaces of six clot samples (three human and three porcine).

Three blinded observers evaluated the fibrin fiber diameter of the human and porcine clots using ImageJ (National Institutes of Health, Bethesda, MD, USA), based on previously published methods (Sutton et al. 2013b). Each observer was presented with a SEM image

(3500x, 8 μm square), on which 5 randomly chosen locations were marked. The diameters of the fibers closest to each location were measured and recorded by the observer.

IV.2.7 Statistical Analysis

All data were analyzed in MATLAB (Mathworks, Natick, MA, USA). Lilliefors's test was performed on each data set to assess data for normality. Lytic efficacy, assessed via FCL and ALR, was compared using one-way ANOVA between treatment protocols for each combination of clot and plasma type (porcine clots in porcine plasma, human clots in porcine plasma, and porcine clots in human plasma). Within each treatment (plasma only, rt-PA, or rt-PA and Definity[®] exposed to US), the lytic efficacy of each combination of clot and plasma type was also compared. The lytic efficacy for human clots in porcine plasma, porcine clots in human plasma, and porcine clots in porcine plasma was directly compared to previously reported lytic efficacy of human clots in human plasma in the same time-lapse microscopy system (Bader et al. 2015b). ALR was calculated for cross-species experiments to improve analysis of groups that achieved 100% FCL prior to the end of the 30-min treatment period. Post-hoc analysis was done using the Tukey method to identify significant differences in lytic efficacy. Lilliefors's test revealed that the fiber diameter data deviated from normality for both types of clots ($p < 0.05$). Fiber diameter was compared using the Wilcoxon rank sum test.

IV.3 Results

IV.3.1 Comparison of rt-PA susceptibility in porcine and human clots

The fractional clot loss (FCL) at the end of the 30-min treatment period for porcine clots in porcine plasma, porcine clots in human plasma, and human clots in porcine plasma exposed to

either plasma alone, rt-PA (3.15 $\mu\text{g}/\text{mL}$), or rt-PA (3.15 $\mu\text{g}/\text{mL}$) and Definity[®] with intermittent 120 kHz US is shown in Fig 2a. For comparison, previously published data with human clots in human plasma exposed to the same treatment protocols are also plotted (Bader et al. 2015b). For all clots treated with plasma alone, negligible reduction in clot width was observed ($0.67\pm 2.52\%$, $2.56\pm 2.56\%$, and $5.27\pm 3.03\%$ for porcine clots in porcine plasma, porcine clots in human plasma, and human clots in porcine plasma, respectively). Porcine clots in porcine plasma treated with rt-PA (3.15 $\mu\text{g}/\text{mL}$) or rt-PA (3.15 $\mu\text{g}/\text{mL}$) and Definity[®] with intermittent 120 kHz US exposure showed equivalent FCL to clots treated with plasma only ($2.56\pm 3.19\%$ and $3.05\pm 8.04\%$ respectively). Additionally, increased thrombolysis was not observed in human clots exposed to porcine plasma treated with rt-PA (3.15 $\mu\text{g}/\text{mL}$) compared to clots in plasma alone ($p>0.05$).

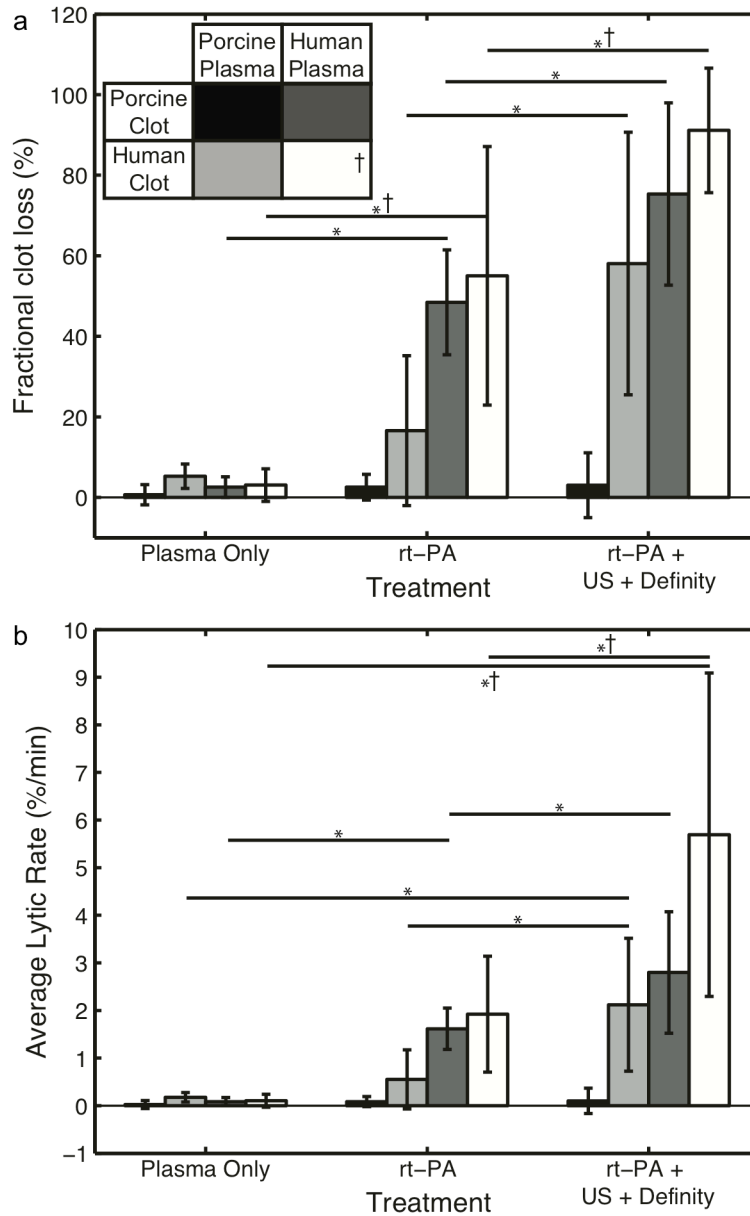


Figure IV.2. Thrombolysis of human and porcine clots. a. Fractional clot loss (FCL) for porcine clots in porcine plasma (n=5, black), human clots in porcine plasma (n=12, light grey), and porcine clots in human plasma (n=12, dark grey) exposed to plasma alone, rt-PA (3.15 $\mu\text{g}/\text{mL}$), and rt-PA (3.15 $\mu\text{g}/\text{mL}$) with Definity[®] and intermittent 120 kHz ultrasound (US). Statistically significant differences in FCL ($p < 0.05$) across treatments are denoted by (*). No difference ($p > 0.05$) in FCL was observed for porcine clots in porcine plasma exposed to rt-PA without or with the use of Definity[®] and US as an adjuvant compared to plasma alone. b. Average lytic rate (ALR) for the same clots and treatments shown in 2(a). Statistically significant differences in ALR ($p < 0.05$) across treatments are denoted by (*). † Data with human clots in human plasma (n=12, white) was reproduced from (Bader et al. 2015b). From: Huang *et al.* Comparative lytic efficacy of rt-PA and ultrasound in porcine versus human clots. *PLoS One*. 2017;12(5):e0177786.

Porcine clots in human plasma treated with either rt-PA (3.15 µg/mL) or rt-PA (3.15 µg/mL) and Definity[®] with intermittent 120 kHz US exhibited a significantly higher FCL than clots treated with plasma alone (48.44±13.01% and 75.35±22.63%, respectively). Human clots in porcine plasma treated with rt-PA (3.15 µg/mL) and Definity[®] with intermittent 120 kHz US also exhibited significantly higher FCL than clots treated with plasma alone (58.08±32.61%). For both porcine clots in human plasma and human clots in porcine plasma, treatment with rt-PA (3.15 µg/mL) and Definity[®] exposed to intermittent 120 kHz US exhibited a significantly higher FCL than treatment with rt-PA (3.15 µg/mL) alone. A full analysis of statistical significance across clot types and treatments may be found in Tables 1 and 2.

Table IV.1. Tukey p-values for cross-species thrombolysis experiments within each combination of clot/plasma

A. Porcine Clots, Porcine Plasma			
	Plasma Only	rt-PA	rt-PA, US, Definity
Plasma Only	--		
rt-PA	0.665	--	
rt-PA, US, Definity	0.527	0.981	--
B. Human Clots, Porcine Plasma			
	Plasma Only	rt-PA	rt-PA, US, Definity
Plasma Only	--		
rt-PA	0.432	--	
rt-PA, US, Definity	0.000*	0.000*	--
C. Porcine Clots, Human Plasma			
	Plasma Only	rt-PA	rt-PA, US, Definity
Plasma Only	--		
rt-PA	0.000*	--	
rt-PA, US, Definity	0.000*	0.000*	--

* indicates p<0.05.

From: Huang *et al.* Comparative lytic efficacy of rt-PA and ultrasound in porcine versus human clots. *PLoS One*. 2017;12(5):e0177786.

Table IV.2. Tukey p-values for cross-species thrombolysis experiments within each treatment protocol

A. Treatment: Plasma Alone					
		Porcine Plasma		Human Plasma	
		Porcine clots	Human clots	Porcine clots	Human clots [†]
Porcine Plasma	Porcine clots	--			
	Human clots	0.002*	--		
Human Plasma	Porcine clots	0.394	0.149	--	
	Human clots [†]	0.196	0.308	0.977	--
B. Treatment: rt-PA (3.15 µg/mL)					
		Porcine Plasma		Human Plasma	
		Porcine clots	Human clots	Porcine clots	Human clots [†]
Porcine Plasma	Porcine clots	--			
	Human clots	0.637	--		
Human Plasma	Porcine clots	0.002*	0.006*	--	
	Human clots [†]	0.000*	0.000*	0.874	--
C. Treatment: rt-PA (3.15 µg/mL), Definity (2 µL/mL), & 120 kHz US					
		Porcine Plasma		Human Plasma	
		Porcine clots	Human clots	Porcine clots	Human clots [†]
Porcine Plasma	Porcine clots	--			
	Human clots	0.000*	--		
Human Plasma	Porcine clots	0.000*	0.278	--	
	Human clots [†]	0.000*	0.007*	0.373	--

* indicates $p < 0.05$.

[†] Data with human clots in human plasma data previously published (Bader et al. 2015b)
From: Huang *et al.* Comparative lytic efficacy of rt-PA and ultrasound in porcine versus human clots. *PLoS One*. 2017;12(5):e0177786.

Fig 2b shows the average lytic rate (ALR) for porcine clots in porcine plasma, porcine clots in human plasma, and human clots in porcine plasma, treated with plasma alone, rt-PA, or rt-PA with Definity[®] exposed to 120 kHz US. Previously published data with human clots in human plasma exposed to the same treatment protocols are also plotted for comparison (Bader et al. 2015b). The ALR for plasma treated clots irrespective of clot or plasma type was very low, as was the ALR for porcine clots in porcine plasma exposed to any treatment. Increased ALR was not observed in human clots in porcine plasma treated with rt-PA ($p > 0.05$), but was observed in

porcine clots in human plasma treated with rt-PA ($p < 0.01$). An increased ALR was observed for both combinations treated with rt-PA and Definity[®] exposed to 120 kHz US ($p < 0.01$).

The ultraharmonic (UH) and broadband (BB) energy detected by the PCD during trials with US exposure are shown in Fig 3. Again, previously published data with human clots in human plasma are plotted for comparison (Bader et al. 2015b). The amount of UH energy detected is not significantly different ($p > 0.05$) for porcine clots in porcine plasma, porcine clots in human plasma, or human clots in porcine plasma.

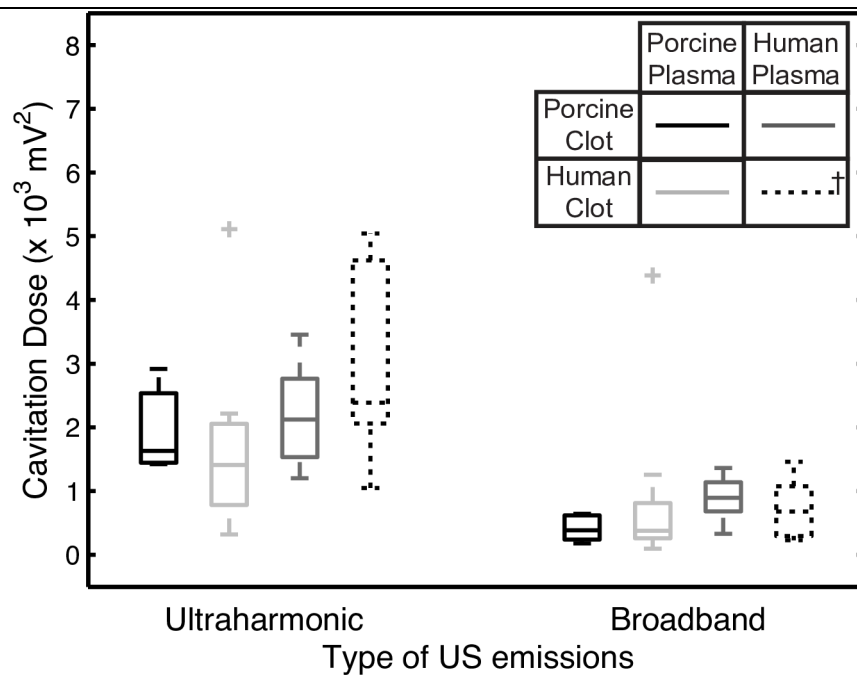


Figure IV.3. Measured ultraharmonic and broadband emissions for trials involving US exposure. Cavitation dose is shown for porcine clots in porcine plasma (black), human clots in porcine plasma (light grey), and porcine clots in human plasma (dark grey) when treated with rt-PA, Definity[®], and 120 kHz US. † Data with human clots in human plasma (dashed line) was reproduced from (Bader et al. 2015b). From: Huang *et al.* Comparative lytic efficacy of rt-PA and ultrasound in porcine versus human clots. *PLoS One.* 2017;12(5):e0177786.

IV.3.2 Histological Examination of the clots

Histological examination of the human whole blood clots (Fig 4a) sectioned axially revealed erythrocyte-rich clots with a dense central region and a porous outer layer. Examination of the porcine blood clots (Fig 4b) revealed a similar appearance as the human blood clots: erythrocyte-rich with a similar degree of porosity near the surface of the clots. Porcine clots also had a central region of increased clot density that was surrounded by a region of increased porosity.

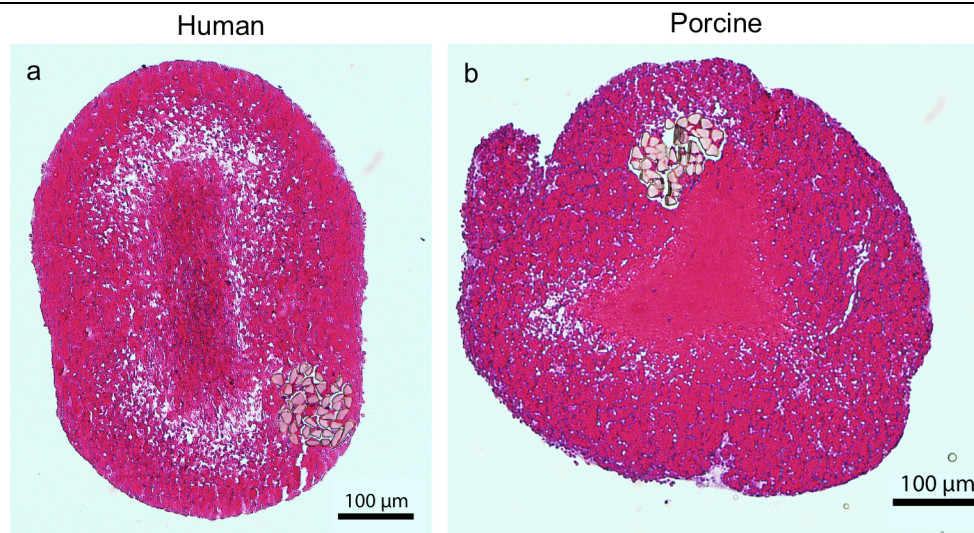


Figure IV.4. Representative human (a) and porcine (b) clots with standard H&E staining. From: Huang *et al.* Comparative lytic efficacy of rt-PA and ultrasound in porcine versus human clots. *PLoS One.* 2017;12(5):e0177786.

IV.3.3 SEM Examination of the clots

Scanning electron microscopy revealed both qualitative and quantitative differences in clot structure and composition between human and porcine clots. Representative SEM images of the surface of each clot are shown in Fig 5. Porcine clots had fewer visible erythrocytes on the surface of clots compared to human clots (Fig 5 a-b) and exhibit a denser fibrin mesh composed

of thinner fibrin fibers compared to human clots (Figs 5-6). Porcine clots had a median fibrin fiber diameter of 0.114 μm , which is significantly different from the median human fiber diameter of 0.144 μm ($p < 0.01$) (Fig 6).

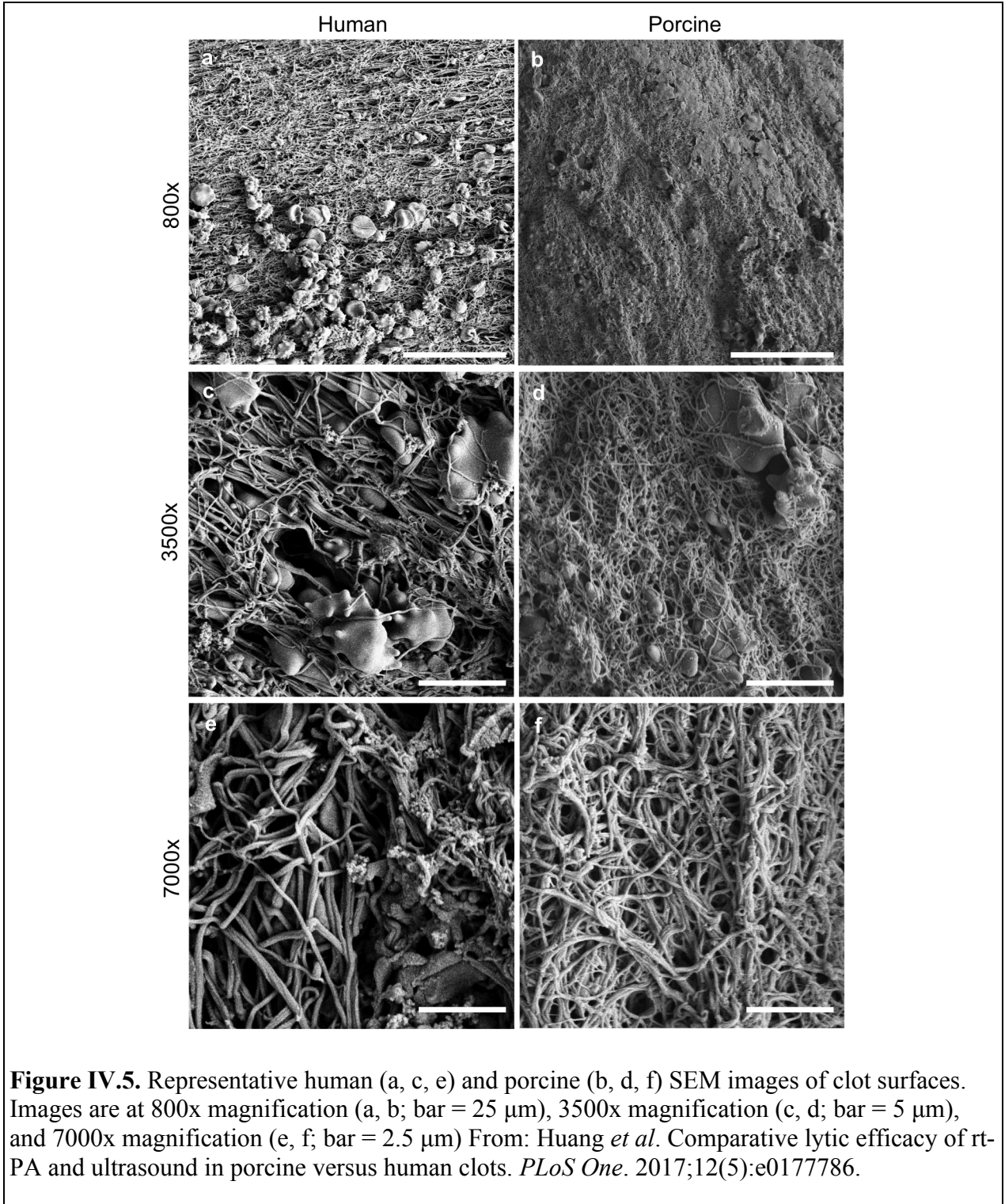


Figure IV.5. Representative human (a, c, e) and porcine (b, d, f) SEM images of clot surfaces. Images are at 800x magnification (a, b; bar = 25 μm), 3500x magnification (c, d; bar = 5 μm), and 7000x magnification (e, f; bar = 2.5 μm) From: Huang *et al.* Comparative lytic efficacy of rt-PA and ultrasound in porcine versus human clots. *PLoS One.* 2017;12(5):e0177786.

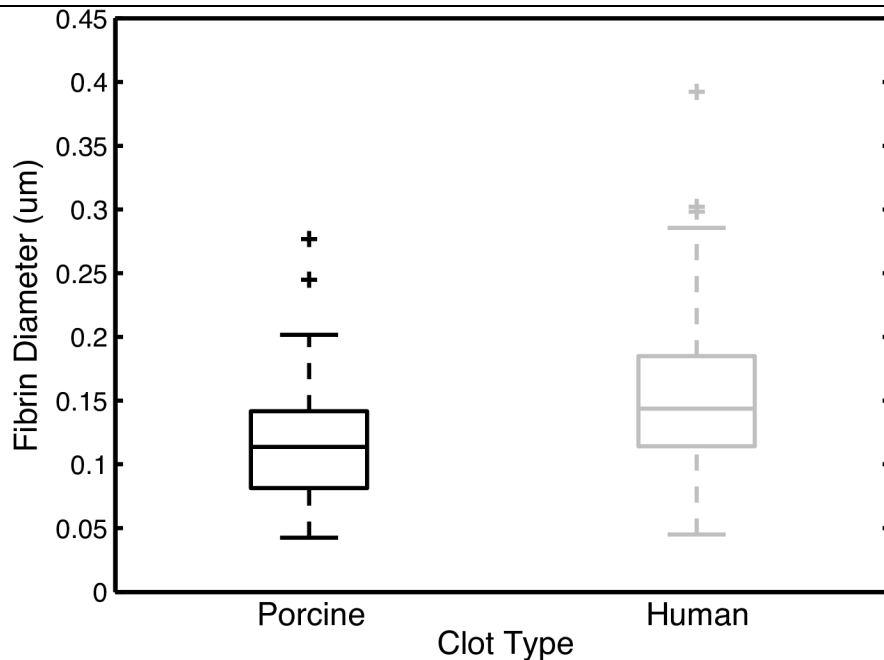


Figure IV.6. Clot fibrin fiber diameter. Box plots showing the range, median, 25th quartile, and 75th quartile of measured fiber diameter for human (n = 130) and porcine (n = 140) clots as measured by blinded observers from SEM images. Outliers are represented by the symbol "+" and statistically significant differences are denoted with a "*". From: Huang *et al.* Comparative lytic efficacy of rt-PA and ultrasound in porcine versus human clots. *PLoS One*. 2017;12(5):e0177786.

IV.4 Discussion

In this study we evaluated thrombolysis in human and porcine clots in the presence of flow treated with rt-PA and Definity[®] exposed to intermittent 120 kHz US. The flow rate used in this study is within the range observed in the middle cerebral artery during ischemic stroke (Alexandrov et al. 2010). The presence of flow is known to impact both cavitation activity and duration as well as thrombolytic activity. Specifically, flow allows the constant replenishing of Definity[®] as well as the removal of fibrin degradation products, which makes the drug delivery setting different compared to experiments without flow (Jadhav et al. 2007). Further, the peak-to-peak pressure used in this study was low (0.44 MPa) and sustained stable cavitation activity was

observed (Figs 3 and 5). Shimizu *et al.* investigated the effect of 490-kHz continuous wave US (peak-to-peak pressure of 0.25 MPa) on monkey brains and did not observe tissue damage or neurological deficits (Shimizu et al. 2012). A 2005 clinical trial employing 300-kHz continuous wave US at an intended peak to peak pressure of 0.12 to 0.26 MPa noted an increased rate of sICH (Daffertshofer et al. 2005). A post-hoc analysis revealed that the increased sICH rate was likely caused by the presence of US standing waves within the cranium with *in situ* peak to peak pressures between 0.54 and 2.4 MPa (Baron et al. 2009). Clearly careful selection of US exposure parameters is required to promote enhanced thrombolysis and mitigate adverse bioeffects.

The types of thrombi that cause ischemic stroke *in vivo* are highly variable in both their composition and susceptibility to rt-PA lysis (Liebeskind et al. 2011; Mutch et al. 2010; Undas and Ariens 2011). Hashimoto *et al.* found that of 83 stroke patients with thrombectomy, 41% had erythrocyte-rich thrombi (Hashimoto et al. 2016). Liebeskind *et al.* found that 56% of clots retrieved from 50 stroke patients were either predominantly erythrocytic or had a mixture of fibrin and erythrocytes (Flint et al. 2007). Marder *et al.* (2006) provided a qualitative description of clots removed from 25 stroke patients, of which 12% were predominantly erythrocytic, 12% were fibrin-rich, and 76% were a mixture of fibrin and erythrocytes.

Our experiments showed that porcine clots exposed to porcine plasma treated with rt-PA (3.15 µg/mL), without or with Definity[®] and US, exhibited negligible thrombolysis. However, porcine clots exposed to human plasma treated with rt-PA (3.15 µg/mL) exhibited a similar FCL as human clots in human plasma exposed to rt-PA at the same concentration. Furthermore, the addition of Definity[®] and 120 kHz US increased FCL for both porcine clots in human plasma

and human clots in porcine plasma. US-enhanced thrombolysis is thus observed for human clots in human plasma, but not for porcine clots in porcine plasma (Fig 2).

Previously in our lab, Hitchcock *et al.* and Sutton *et al.* both showed that unretracted porcine clots lysed in response to 3.15 $\mu\text{g/mL}$ rt-PA, with an increase in lysis with adjuvant Definity[®] and US (Hitchcock *et al.* 2011; Sutton *et al.* 2013b). However, the clots used in this study were highly retracted. Sutton *et al.* showed that retracted clots formed in borosilicate glass lyse in response to rt-PA, but that there is not an enhancement of rt-PA lysis with adjuvant Definity[®] and US (Sutton *et al.* 2013b). Though we do not see significant lysis with rt-PA, this may be due to the limitation of our metric of thrombolytic efficacy. Clot width is evaluated in a 2D plane and cannot provide any information about clot lysis in the direction perpendicular to the plane of view. Sutton *et al.* used mass loss as a metric of thrombolytic efficacy (Sutton *et al.* 2013b), which evaluates clot lysis in all dimensions.

Our results shown in Fig 2a are consistent with the work of Flight *et al.*, which revealed a higher activation of human plasminogen in response to rt-PA than porcine plasminogen (Flight *et al.* 2006). If porcine clots are exposed to porcine plasma, only porcine plasminogen is present, which produces a substantially lower concentration of active plasmin, leading to lower thrombolytic efficacy relative to human clots in human plasma exposed to the same concentration of rt-PA. The reduced rt-PA thrombolysis for human clots in porcine plasma appears to be caused by the lack of human plasminogen in the surrounding fluid, despite the presence of human plasminogen intercalated within the clots. The presence of human plasminogen in the surrounding fluid enables rt-PA thrombolytic efficacy, regardless of the type of clot (human or porcine).

The adjuvant use of Definity[®] and 120 kHz US improved rt-PA thrombolytic efficacy for human clots in porcine plasma over rt-PA alone. Previous studies have concluded that the addition of Definity[®] and 120 kHz US exposure enhances the penetration of thrombolytic into the clot (Datta et al. 2008; Hitchcock et al. 2011). Acoustically activated Definity[®] microbubbles likely serve as micropumps which increase the transport of rt-PA further into the clot allowing activation of the human plasminogen within the clot. The UH dose measured during exposure to US (Fig 3) was comparable to that reported previously by Bader *et al.* (Bader et al. 2015a). We observed a similar degree of US enhancement of rt-PA thrombolysis (increase in FCL of 41.5%) for human clots in porcine plasma as Bader *et al.* observed for human clots in human plasma (increase in FCL of 36.1%) (Fig 2a).

Equivalent rt-PA lytic efficacy was measured for porcine clots in human plasma and human clots in porcine plasma exposed to rt-PA with Definity[®] and US (Fig 2a) despite the large difference in the amount of human plasminogen present in the system. The amount of human plasminogen in the human clots given their volume is estimated to have on the order of 0.002-0.004 U of activity, which is 4 orders of magnitude smaller than amount of human plasminogen in the human plasma flowing by either type of clot (18-28 U). The co-localization of plasminogen and rt-PA at the site of fibrin is likely key in producing rt-PA thrombolysis. Definity[®] and US exposure improves the penetration of both proteins. Site-specific delivery of plasmin to the clot is an alternative strategy to reduce the dependence on the *in situ* availability of plasminogen (Kandadai et al. 2014). Our group has reported thrombolysis using plasmin that was encapsulated into echogenic liposomes to prevent inhibition in the bloodstream (Kandadai et al. 2014).

In studies by Landskroner *et al.* (2005), 5 mg human plasmin produced $50\pm 4\%$ mass loss from porcine clots, compared to $80\pm 2\%$ mass loss from human clots after a 60-min treatment period (Landskroner *et al.* 2005). Landskroner *et al.* attributed this decreased thrombolysis in porcine clots to a denser fibrin network as observed on scanning electron microscopy (Landskroner *et al.* 2005). Our study also showed that porcine clots have a denser fibrin network (Fig 5) with smaller diameter fibrin diameters than human clots (Fig 6). In addition, the ALR for porcine clots in human plasma treated with rt-PA with Definity and US was also significantly lower than the ALR for human clots in human plasma (Fig 2b, $p < 0.01$). A denser fibrin network, characterized by decreased strand thickness and increased fibrin density, has been correlated with decreased rt-PA susceptibility in human thrombi *ex vivo* and clots *in vitro* (Collet *et al.* 2000; Gabriel *et al.* 1992). The denser fibrin network in porcine clots may be attributable to the increased levels of coagulation factors in swine blood (Table 3) (Lewis 1996). Platelets are known to inhibit fibrinolysis (Moore *et al.* 2015). Therefore, the higher number of platelets in porcine blood (Lewis 1996) could also have contributed to the lower rt-PA thrombolytic efficacy in porcine blood clots observed in this study.

The SEM data presented in our work is consistent with Landskroner *et al.*'s qualitative observations that the human fibrin network is less dense than the porcine fibrin network (Landskroner *et al.* 2005). Other groups have also quantified fiber diameter through measurement from SEM images (Collet *et al.* 2000; Ryan *et al.* 1999; Sutton *et al.* 2013b). Sutton *et al.* quantified the diameter of porcine fibrin fiber diameters, showing that porcine clots had a mean fiber diameter of $0.169\ \mu\text{m}$ and $0.173\ \mu\text{m}$ for superficial fibers in unretracted and retracted clots respectively (Sutton *et al.* 2013b), larger than our porcine clot fiber diameters (median of $0.114\ \mu\text{m}$). Collet *et al.* have observed that fiber diameters in human plasma clots have a mean of

$0.299 \pm 0.070 \mu\text{m}$ with a high thrombin concentration or $0.376 \pm 0.104 \mu\text{m}$ with a low thrombin concentration (Collet et al. 2000). Ryan *et al.* combined different concentrations of fibrinogen, thrombin, calcium chloride, and a Factor XIII inhibitor to create clots with a large range of fibrin fiber diameters, with mean diameters ranging from $0.044 \pm 0.015 \mu\text{m}$ (high-thrombin clots) to $0.147 \pm 0.059 \mu\text{m}$ (high-calcium chloride clots) (Ryan et al. 1999). We measured a median human fibrin fiber diameter of $0.144 \mu\text{m}$, which is intermediate between the values seen by Ryan *et al.* and Collet *et al.* This wide range of reported fibrin diameters in both porcine and human clots is likely attributable to both differences in fiber diameter measurement techniques and the use of different clot models. In order to compare two types of clots, one must control for the variability between the individuals measuring the fibrin diameters, such as by using the same group of blinded observers to evaluate images of the two types of clots (Huang et al. 2017; Sutton et al. 2013b).

The technique for measurement of fibrin fiber diameters is useful for characterization of clot structure, but would have limited use in post hoc evaluation of thrombolytic efficacy. Fibrin diameter appears to indicate susceptibility of a clot to lysis. However, no studies have shown that the structure of the fibrin network changes as clots are lysed. It has been observed using confocal microscopy that rt-PA mediated clot lysis happens with a gradual loss of fibrin fibers from the clot surface, with deeper clot structure largely preserved (Collet et al. 2000; Sakharov et al. 1996). Fibrin fibers do not lyse radially from the outside in, but are instead cleaved transversely (Collet et al. 2000; Veklich et al. 1998). Analysis of SEM images would not be able to distinguish between lysed fibers and fibers which have not undergone lysis. Additionally, SEM sample preparation is necessarily consumptive and analysis of the same clot before and after rt-PA lysis is impossible. Furthermore, as mentioned in the previous paragraph, the variety in

published fibrin diameters even within the same species would likely preclude the establishment of any absolute metric based on fibrin diameter.

Collet *et al.* have noted a difference in diffusion between coarse and fine fibrin networks in plasma clots, where diffusion is measured as progression of the rt-PA binding front (Collet et al. 2000). Individual thin fibrin fibers are lysed more quickly than individual thick fibrin fibers, but the rt-PA binding front in the coarse fibrin network ($0.38 \pm 0.10 \mu\text{m}$ mean \pm SD fibrin diameter) advances at a 14-fold higher rate than the binding front in the fine fibrin network ($0.30 \pm 0.07 \mu\text{m}$ mean fibrin diameter) (Collet et al. 2000). Collet *et al.* notes that rt-PA binding depends on the fibrin conformation and thicker fibers allow formation of a looser fibrin network resulting in a faster rate of rt-PA binding and faster lytic rate (Collet et al. 2000). The results of Collet *et al.* cannot be directly extrapolated to our system, due to our use of whole blood clots in which formed elements (particularly red blood cells) can further modify the rate of rt-PA penetration into clots. We did not see a difference in average lytic rate between human and porcine clots perfused with human plasma and treated with rt-PA. This similarity may indicate the progression of the rt-PA binding front in whole blood clots is less affected by fibrin mesh structure than plasma clots. Our lab has previously shown that adjuvant Definity[®] and US increases rt-PA penetration into clots (Datta et al. 2008). We noted that the human clots treated with rt-PA with adjuvant Definity[®] and US had an approximately 2-fold higher average lytic rate compared to porcine clots that underwent the same treatment. This pattern is consistent with that seen by Collet *et al.*

Table IV.3. Human and porcine blood composition and coagulation characteristics.

Coagulation parameter	Human (normal range)	Porcine (n=6)
Factor I (mg/dL)	150 – 450	348 ± 78
Factor II (U/mL)	0.70 - 1.30	0.68 ± 0.3
Factor V (U/mL)	0.65 – 1.45	2.80 ± 0.6
Factor VII (U/mL)	0.50 – 1.30	1.92 ± 0.4
Factor VIII (U/mL)	0.75 – 1.40	6.42 ± 0.8
Factor IX (U/mL)	0.65 – 1.0	3.20 ± 0.3
Factor X (U/mL)	0.75 – 1.25	2.54 ± 0.9
Factor XII (U/mL)	0.50 – 1.45	5.65 ± 1.4
Plasminogen (U/mL)	0.80 – 1.20	0.50 ± 0.1 (n = 2)
Platelet count (x 10 ³ /mm ³)	150 – 450	580 ± 115 (n = 9)
Clotting Time (min)	6 – 12	6 ± 3.8
Hematocrit (%)	37 – 52	38 ± 2.1

Values were compiled from Lewis' *Comparative Hemostasis in Vertebrates* (Lewis 1996)

From: Huang *et al.* Comparative lytic efficacy of rt-PA and ultrasound in porcine versus human clots. *PLoS One*. 2017;12(5):e0177786.

The effect of clot structure on rt-PA thrombolytic susceptibility as also been previously investigated by our laboratory. Sutton *et al.* found that the structure of porcine whole blood clots is affected by the type of glass used to initiate clotting (Sutton et al. 2013b). Specifically, unretracted clots manufactured in flint glass have lower fibrin content and are less dense and more porous than the highly retracted clots formed in borosilicate glass. The higher charge or hydrophilicity of borosilicate glass may contribute to a higher degree of platelet activation and increased clot retraction. Unretracted clots exhibited significantly more mass loss than retracted clots, and rt-PA thrombolysis was enhanced with the addition of Definity[®] and intermittent 120 kHz US (Sutton et al. 2013b).

This study possesses a few notable limitations. Our experiments were completed in an *in vitro* flow system, which limits direct applicability to either *in vivo* animal studies or human trials. For example, the *in vitro* flow model used in this study lacked physiological pulsatile

blood pressures, and the flow rate was fixed for the entire treatment period (Bader et al. 2015b). However, the *in vitro* experiments reported in our paper allowed direct quantitation of the differential rt-PA efficacy and the combination of blood products from different species.

The human and porcine whole blood clots used in this study were formed using equivalent protocols, but the human clots were produced using fresh blood, and the porcine clots were produced using recalcified anticoagulated blood. There is evidence that a high concentration of citrate reduces the levels of Factor V, VIII, and IX in human fresh frozen plasma (Hellstern and Haubelt 2002). However, the 3 hr incubation of our clots at 37 °C to allow clotting should provide sufficient time for the activation of the coagulation cascade, as the activated partial thromboplastin time in pigs is <30 s (Lewis 1996).

The human clots produced from venous blood donated from healthy volunteers may not completely model thrombi occurring in stroke (Shaw et al. 2006; Shaw et al. 2007), which can vary in composition and morphology (Singh et al. 2013). Our human clot model, though erythrocytic, is allowed to retract for 3 days, which leads to a decrease in rt-PA thrombolytic susceptibility (Shaw et al. 2006) and is consistent with a tighter fibrin network (Collet et al. 2000). Porcine clots are further resistant to rt-PA thrombolysis and the dilution of whole blood with an anticoagulant and calcium chloride decreases effective hematocrit, noticeable as a decrease in surface erythrocytes on SEM (Fig 5). Additionally, we did not investigate any possible immune reactions that might arise from the combination of blood products from two different species (human and porcine). However, porcine plasmin has formerly been administered to human patients repeatedly without allergic problems (Hedner et al. 1978), demonstrating significant homology between the proteins. Additionally, histology and SEM imaging was performed only on untreated clots.

Although retracted porcine thrombi have been used to model ischemic stroke (Gralla et al. 2006; Jahan 2010; Ringer et al. 2004), porcine studies that have evaluated the efficacy of microbubbles and ultrasound have thus far only used fresh thrombi (Culp et al. 2004; Gao et al. 2014). Retracted porcine thrombi may represent a “worst case” scenario for rt-PA treatment and could serve as an excellent model for certain subtypes of thrombi responsible for ischemic stroke, chronic deep vein thrombosis, and pulmonary emboli. In order to mimic the rt-PA efficacy of human clots, porcine clots may be altered biochemically to model the thrombolytic susceptibility of human clots more closely. Human clots exposed to porcine plasma and rt-PA demonstrated increased lytic susceptibility over porcine clots in porcine plasma (Fig 2a), likely because of co-localization of human plasminogen at the site of lytic activity. In this scenario, the only source of human plasminogen was intercalated in the clot. One approach to "humanize" porcine clots to model human thrombus rt-PA susceptibility may be to dope the porcine whole blood with human plasminogen during the manufacturing process. Alternatively, platelet activation could be modulated to reduce the retraction of clots (Sutton et al. 2013a), either chemically or by changing the surface properties of container used to form clots (Sutton et al. 2013b).

IV.5 Conclusions

The results of this study demonstrate that treating porcine clots in porcine plasma with rt-PA *in vitro* produces 22-fold lower lytic efficacy than treating human clots in human plasma with rt-PA. Including human plasminogen, either at the time of clot formation or in the surrounding plasma, produces more humanoid thrombolysis. Porcine clots in human plasma showed equivalent fractional clot loss for all treatment protocols compared to human clots in human plasma. Human clots in porcine plasma did not demonstrate rt-PA lysis, but the addition

of Definity[®] and 120 kHz US exposure significantly increased lytic efficacy. The use of porcine clot models to test new human thrombolytic therapies may necessitate modulation of coagulation and thrombolytic factors to reflect human hemostasis accurately.

Chapter V. Lytic efficacy of tissue plasminogen activator and ultrasound in porcine clots doped with barium sulfate *in vitro*

V.1 Background

Occlusion of the swine ascending pharyngeal artery (APA) with thromboemboli has been used in evaluation of mechanical thrombectomy devices (Gralla et al. 2006; Jahan 2010) and sonothrombolysis, the use of ultrasound (US) to enhance clot breakdown (Culp et al. 2004; Gao et al. 2014). For mechanical thrombectomy studies, clots have been made radiopaque with a radiocontrast agent, barium sulfate (BaSO_4), to allow direct visualization of emboli that may become dislodged and travel distally (Gralla et al. 2006; Jahan 2010). This doped clot model is also useful for investigating sonothrombolysis *in vivo*, to explore the presence of downstream emboli, an important step for evaluating biosafety.

It is unknown whether BaSO_4 affects rt-PA thrombolytic efficacy. Zucker *et al.* have shown that "treating" plasma with a short BaSO_4 incubation (30 min) lowers the concentrations of Factor V and Factor VIII, producing an incoagulable plasma without removal of plasma calcium (Zucker and Owen 1982). However, without physical removal of BaSO_4 , it is unknown whether this anti-coagulant effect would be present in sonothrombolysis studies. Additionally, the creation of BaSO_4 -doped clots has relied on the use of bovine thrombin to hold the BaSO_4 within the clot matrix (Gralla et al. 2006; Jahan 2010). BaSO_4 is insoluble in aqueous solutions and settles out of suspension if it is not quickly trapped within the clot matrix by the addition of the pro-coagulant thrombin. Increased thrombin concentrations produce clots with a thinner, denser fibrin network which is less permeable and more difficult to lyse (Wolberg and Campbell

2008). However, studies on the effect of thrombin concentration on clot permeability and resistance to lysis have only been performed on fibrin clots and thus it is not known whether the effect of thrombin concentration would be the same on whole blood clots thrombolysis, particularly for BaSO₄-doped clots.

The objective of this study was to determine the effect of BaSO₄ in porcine whole-blood clots on rt-PA lytic susceptibility with and without the adjuvant exposure to 120-kHz continuous wave US. Based on the results from Chapter IV indicating resistance to rt-PA lysis in porcine clots, higher concentrations of rt-PA will be used. Established protocols for manufacturing porcine clots with and without BaSO₄-doping (Gralla et al. 2006; Holland et al. 2008; Sutton et al. 2013b) were followed. An *in vitro* time-lapse microscopy system with flow was employed to determine rt-PA lytic efficacy (Bader et al. 2015a; Bader et al. 2015b; Gruber et al. 2014). The FDA-approved US contrast agent Definity[®] (Lantheus Medical Imaging, North Billerica, MA, USA) was used as a source of microbubbles for nucleation of cavitation.

V.2 Materials and Methods

V.2.1 Preparation of porcine plasma, rt-PA, and Definity[®] microbubbles

Porcine plasma was acquired and prepared as previously described in Chapter IV.2. All porcine clots were created with donor-derived whole porcine blood anti-coagulated with citrate phosphate dextrose (CPD) solution from Lampire Biological Laboratories, Inc. (Pipersville, PA, USA). Our lab has observed that abattoir-derived CPD blood has resulted in clots with an atypical response to rt-PA lysis (not published). The lytic rt-PA and Definity[®] microbubbles were prepared as noted previously in Chapter IV.2.

V.2.2 Preparation of non-doped and BaSO₄-doped porcine whole-blood clots

Two sizes of whole blood clots were prepared according to previously published protocols: ~500 micron clots around silk sutures in micropipettes (Bader et al. 2015b; Shaw et al. 2008) and ~4-5 mm diameter clots in Pasteur pipettes (Sutton et al. 2013b). Both types of pipettes were made of borosilicate glass, which has been previously shown to trigger robust retraction of the clot over 3 days at 4 °C (Sutton et al. 2013b). Clots at both sizes were prepared with and without the use of BaSO₄ as a dopant (Gralla et al. 2006).

V.2.2.1 Preparation of porcine whole-blood clots adherent to sutures

Borosilicate micropipettes were prepared as described in Chapter IV.2 for both non-doped and BaSO₄-doped clots. Non-doped porcine whole blood clots were prepared as described in Chapter IV.2. To produce radiopaque, BaSO₄-doped clots, each threaded micropipette was injected with 2.5 μL of 50 U/mL bovine thrombin solution (BioPharm Laboratories, Bluffdale, UT, USA). CPD blood was combined with calcium chloride solution and BaSO₄ and a 47.5 μL aliquot of recalcified, BaSO₄-doped blood was injected through each threaded micropipette. Recalcified blood (0.4 mL) was pipetted into each glass culture tube to improve temperature coupling. The final concentrations of thrombin and BaSO₄ in the clot were 2.5 IU/mL and 0.1 g/mL respectively, similar to that presented in previously published studies (Gralla et al. 2006; Jahan 2010). Clots were allowed to form for 3 hours at 37 °C and stored at 4 °C for a minimum of 3 days before use (Bader et al. 2015b; Holland et al. 2008).

V.2.2.2 Preparation of porcine whole-blood clots in Pasteur pipettes

To create clots in Pasteur pipettes, 5.75" disposable borosilicate Pasteur pipettes (Fisher Scientific, Pittsburgh, PA, USA) were prepared by sealing off the tip using an open flame, and placed in 16x100mm Pyrex test tubes (Corning, Corning, NY, USA) for ease of handling

throughout the manufacturing process. For non-doped clots, 2 mL of recalcified CPD blood (9:1 blood:calcium chloride solution as above) was pipetted into each Pasteur pipette. For BaSO₄-doped clots, sealed Pasteur pipettes were primed with 100 µL of the bovine thrombin solution and 1.9 mL of recalcified, BaSO₄-doped blood was added to each Pasteur pipette. Again, the concentrations of thrombin and BaSO₄ in the BaSO₄-doped clots were 2.5 IU/mL and 0.1 g/mL respectively. Blood was allowed to clot for 3 hours at 37 °C, and stored at 4 °C for a minimum of 3 days before use to allow for retraction (Bader et al. 2015b; Holland et al. 2008).

V.2.3 Histology

Porcine whole blood clots prepared without and with BaSO₄ were fixed in 10% formalin, embedded in paraffin, and stained with hematoxylin and eosin (H&E) before histological analysis.

V.2.4 *In vitro* static thrombosis experiments

V.2.4.1 Experiment protocol

Based on a previously published protocols (Holland et al. 2008), clot mass loss in static pooled porcine plasma was measured to established whether the addition of BaSO₄ affected rt-PA susceptibility. Briefly, sample holders were filled with 10 mL porcine plasma prepared as described in V.2.1 (Lampire Biological Laboratories) and warmed to 37 °C. Tissue plasminogen activator (rt-PA) was added to the sample holders to achieve a range of concentrations (0 µg/mL, 3.15 µg/mL, 6.20 µg/mL, 15.75 µg/mL, 31.5 µg/mL, 63 µg/mL, and 100 µg/mL), chosen to include 50 µg/mL. Previously published data established that the thrombolytic efficacy of rt-PA in non-doped porcine clots saturates at a concentration of ~50 µg/mL (Holland et al. 2008). The 4-5 mm diameter clots were removed from Pasteur pipettes, trimmed to 1.5 cm in length, blotted,

weighed, placed into the sample holder, and treated with either plasma alone or rt-PA. At the conclusion of a 30 min treatment window, clots were removed, blotted, and weighed again.

Percent mass loss was calculated for each clot.

V.2.4.2 Statistical Analysis

All data were analyzed in MATLAB (Mathworks, Natick, MA, USA). The mean and standard deviation of mass loss for each clot was calculated for each concentration and clot type. The percent mass loss for BaSO₄-doped and non-doped clots was compared with a 2-tailed t-test at each concentration at a significance level of $p = 0.05$.

V.2.5 *In vitro* thrombolysis experiments with flow and time-lapse microscopy

An *in vitro* time-lapse microscopy system was used to evaluate rt-PA thrombolysis with and without 120 kHz intermittent US in non-doped and BaSO₄-doped porcine clots. The system is described in detail in Chapter IV.2. Images were analyzed post-hoc and thrombolytic efficacy was measured as fractional clot loss (FCL) at the end of the 30-min treatment period as described in Chapter IV.2.4. The ultrasound insonation and detection scheme is described in detail in Chapter IV.2.4.3. For the experiments presented here in non-doped and BaSO₄-doped clots, each clot was exposed to one of three treatment protocols: porcine plasma alone; plasma with rt-PA (15.75 µg/mL); and plasma with rt-PA (15.75 µg/mL) and Definity[®] (2 µL/mL) exposed to 120 kHz intermittent ultrasound as described above. This concentration of Definity[®] is consistent with previously reported studies (Bader et al. 2015b). However, the concentration of rt-PA is 5 times higher than the clinical steady state concentration that was used previously in Chapter IV (Tanswell et al. 1991).

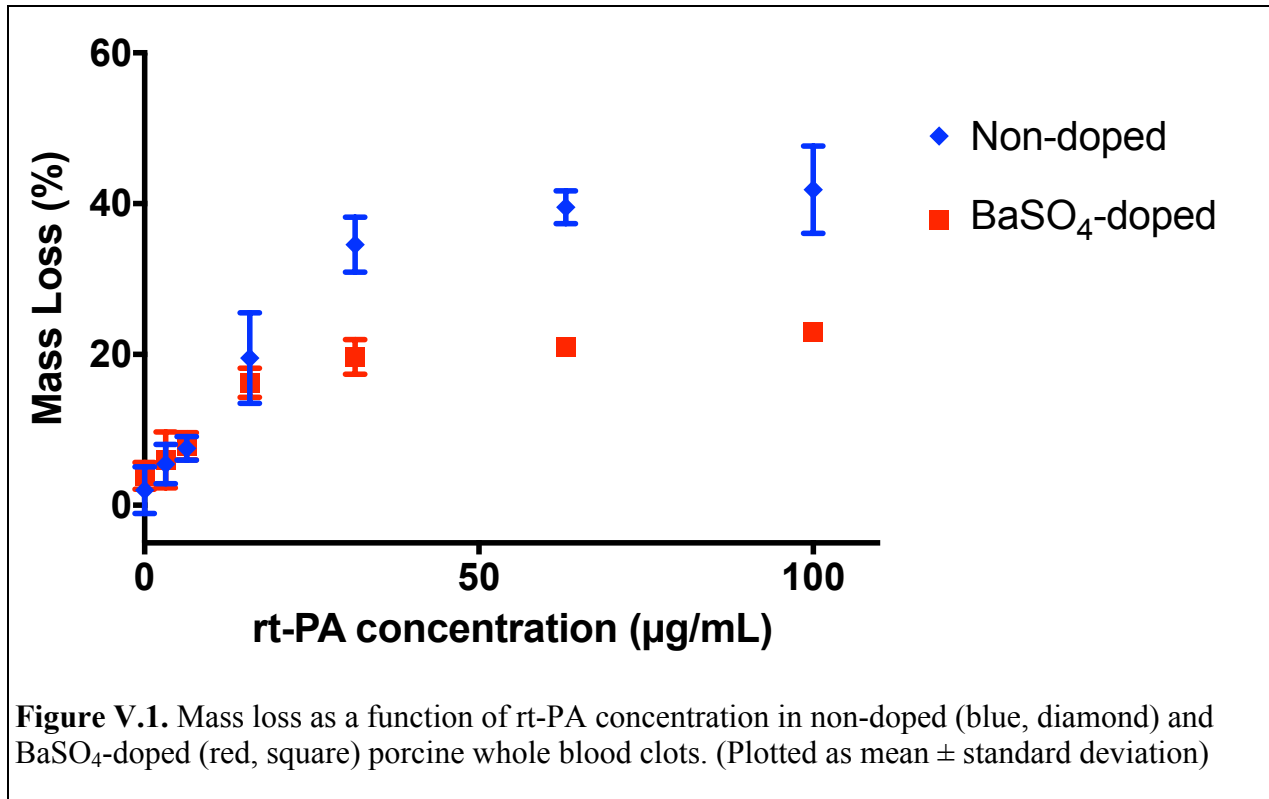
V.2.5.1 Statistical Analysis

The FCLs measured in the different treatment protocols and clot types were compared with a one-way ANOVA. The Tukey-Kramer method was used to identify significant differences in FCL. Following the application of a 4-s moving average, the relationship between UH energy and the change in clot width was assessed using Spearman's rank correlation coefficient in MATLAB (Bader et al. 2015b).

V.3 Results

V.3.1 *In vitro* static thrombosis experiments

Figure V.1 shows the mass loss as a function of rt-PA concentration for non-doped and BaSO₄-doped porcine clots. Both types of clot show an increase in mass loss as a function of rt-PA concentration at lower concentrations. However, the mass loss appears to saturate at rt-PA concentrations of 31.5 µg/mL and higher. The BaSO₄-doped clots have a maximum mass loss of approximately 20% and non-doped clots have a maximum mass loss of approximately 40%. For rt-PA concentrations less than or equal to 15.75 µg/mL, the lytic efficacy of rt-PA is similar for the two types of clots ($p > 0.05$). For rt-PA concentrations higher than 15.75 µg/mL, percent mass loss in non-doped clots is significantly higher than in BaSO₄-doped clots ($p < 0.01$).

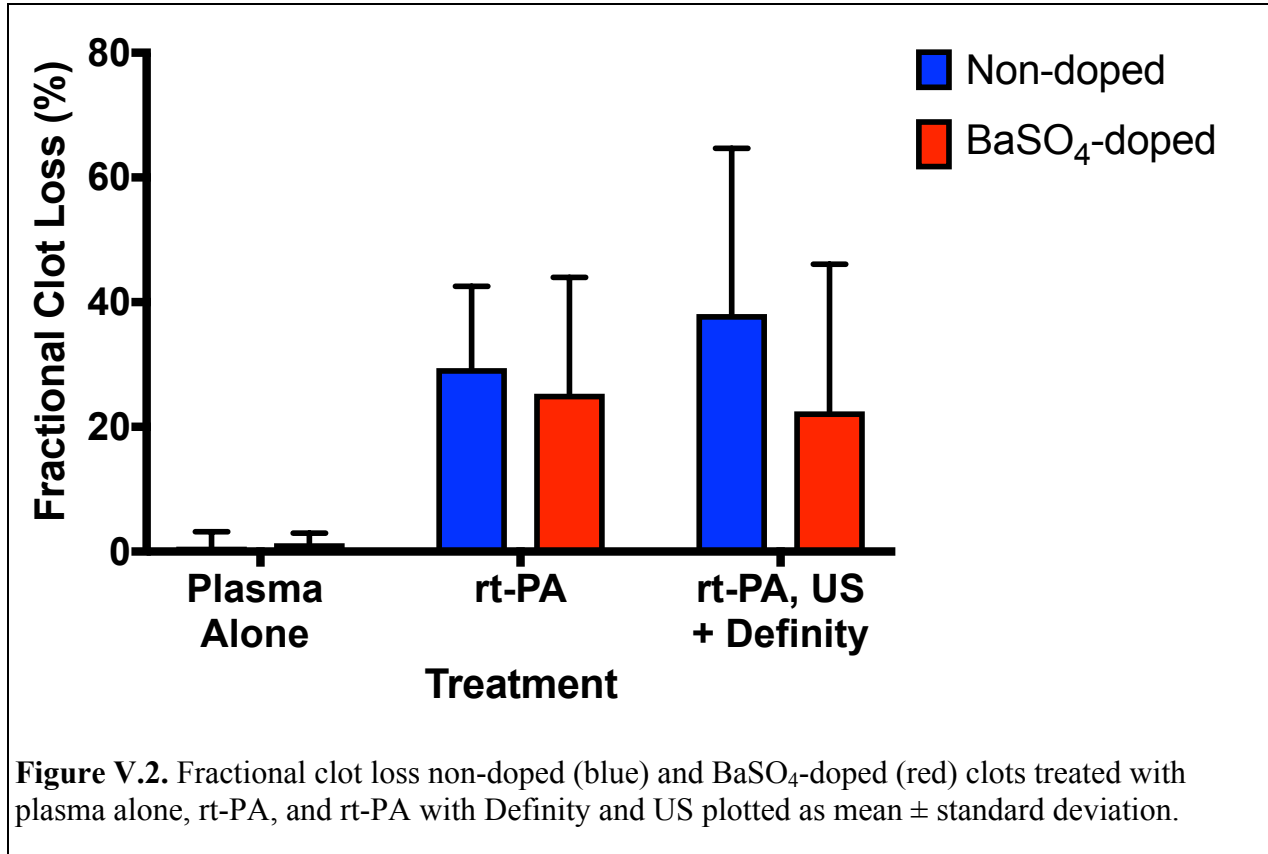


V.3.2 *In vitro* thrombolysis with flow

Figure V.2 shows the fractional clot loss (FCL) at the end of the 30 min treatment period for non-doped and BaSO₄-doped porcine clots. No clot lysis was seen for clots treated with plasma alone, with a FCL of $0.67 \pm 2.52\%$ [$n = 15$] and $1.35 \pm 1.61\%$ [$n = 15$] for non-doped and BaSO₄-doped clots respectively). Clots treated with 15.75 µg/mL rt-PA had a significantly higher FCL than those treated with plasma alone: $29.45 \pm 13.11\%$ ($p < 0.01$, $n = 15$) for non-doped clots and $25.33 \pm 18.63\%$ ($p < 0.01$, $n = 15$) for BaSO₄-doped clots. Non-doped and BaSO₄-doped clots did not demonstrate statistically significant differences in lytic efficacy when subjected to treatment with rt-PA ($p = 0.49$).

Clots treated with rt-PA and Definity[®] exposed to intermittent 120 kHz US also had a significantly higher FCL than those treated with plasma alone ($37.61 \pm 25.92\%$ [$p < 0.01$, $n = 19$]

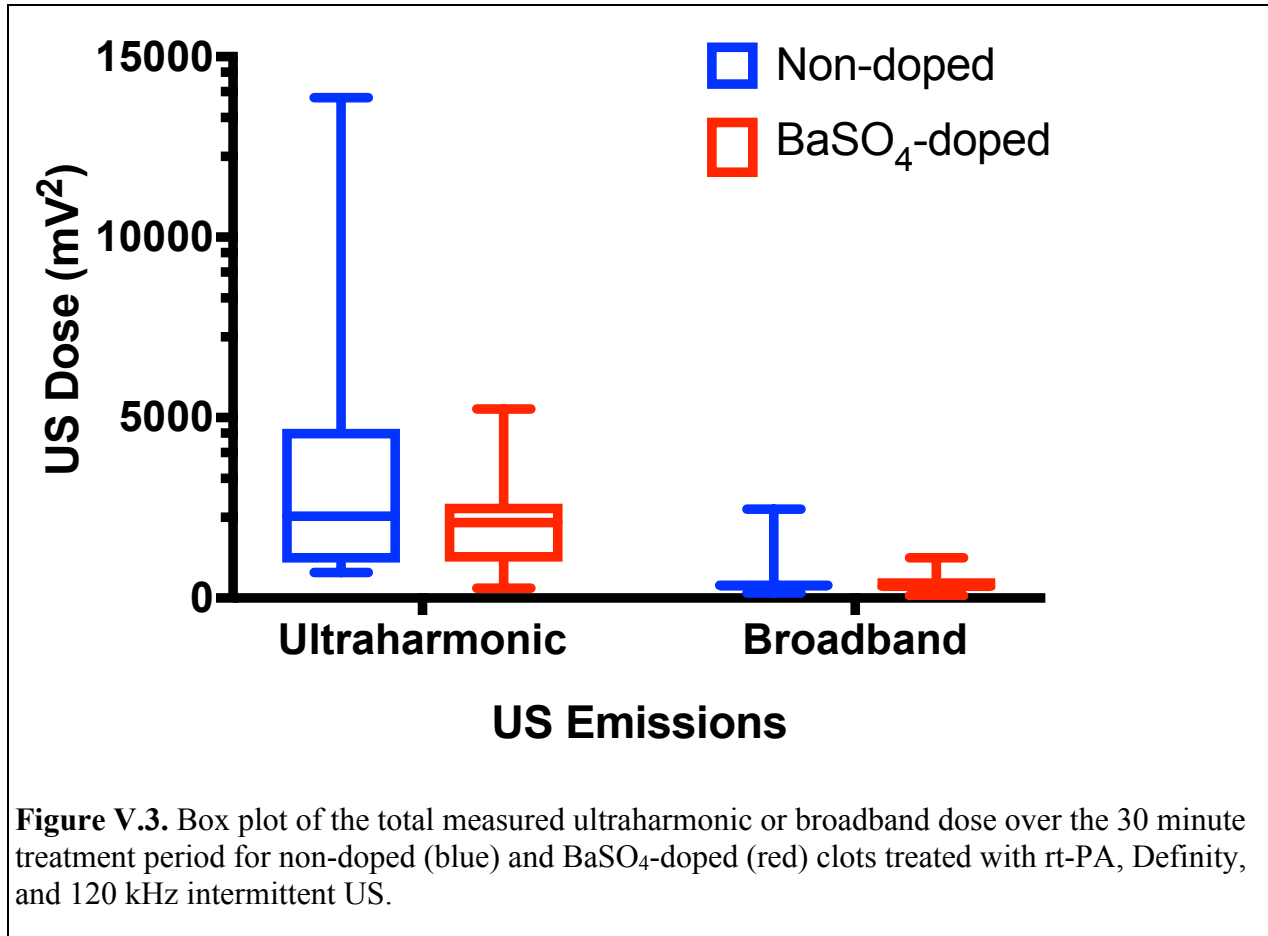
for non-doped clots and $22.49 \pm 23.57\%$ [$p < 0.01$, $n = 18$] for BaSO₄-doped clots). However, treatment with rt-PA and US and Definity® did not significantly increase the FCL compared to treatment with rt-PA for either type of clot ($p = 0.27$ and $p = 0.71$ for non-doped and BaSO₄-doped clots respectively). Non-doped and BaSO₄-doped clots also did not show a difference in lysis when treated with rt-PA, Definity®, and US ($p = 0.07$).



V.3.3 Ultrasonic content of passively detected US emissions

The mean cavitation dose measured during the rt-PA, Definity®, and US runs is shown in Figure V.3. The ultraharmonic (UH) dose detected was $3436.1 \pm 3436.1 \text{ mV}^2$ and $1974.85 \pm 1204.11 \text{ mV}^2$ for non-doped and BaSO₄-doped clots, respectively. The broadband (BB) dose detected was $347.59 \pm 326.83 \text{ mV}^2$ and $194.11 \pm 143.63 \text{ mV}^2$, for non-doped and BaSO₄-doped clots, respectively. Spearman's rank correlation was calculated for the

instantaneous clot width loss and detected UH energy for clots treated with rt-PA, Definity[®], and US. No significant correlation between percent clot width loss and UH energy existed for either non-doped clots ($\rho = 0.020$, $p < 0.01$) or BaSO₄-doped clots ($\rho = -0.003$, $p = 0.53$).



V.3.4 Histological Examination of the clots

Histological images of the non-doped and BaSO₄-doped clots can be seen in Figure V.4. Histological examination of the non-doped and BaSO₄-doped clots revealed erythrocyte-rich clots with a similar degree of porosity near the surface of the clots. Non-doped clots exhibited scant amounts of fibrin on the outside of the clot, which were not seen in BaSO₄-doped clots. Both types of clots had a central region of increased clot density that was surrounded by a region of increased porosity. Non-doped clots had a larger dense region, and BaSO₄-doped clots

exhibited a larger porous region around the dense area. The BaSO₄ was visible as a granular material intercalated within the clot, with a few larger deposits near the surface on one side (yellow arrow in Figure V.4) in addition to smaller particles more evenly distributed throughout the clots.

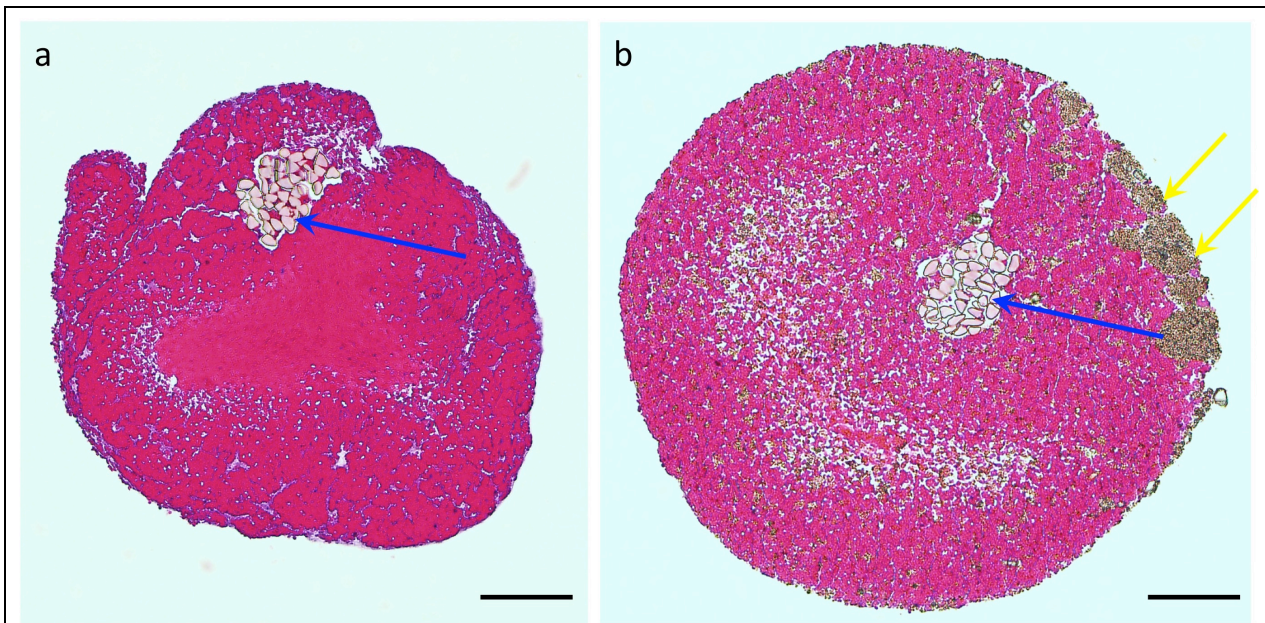


Figure V.4. Histological images (4x magnification) of a. non-doped and b. BaSO₄-doped porcine clots on sutures. The suture is noted with a blue arrow on each clot. The BaSO₄ is pointed out with yellow arrows. The non-doped porcine clot image (a) is from: Huang *et al.* Comparative lytic efficacy of rt-PA and ultrasound in porcine versus human clots. *PLoS One*. 2017;12(5):e0177786.

V.4 Discussion

Our experiments have shown that the lytic efficacy of rt-PA does not differ statistically between non-doped and BaSO₄-doped porcine clots for rt-PA concentrations up to 15.75 µg/mL. However, at rt-PA concentrations at 31.5 µg/mL and above, the addition of BaSO₄ and thrombin appears to increase the lytic resistance of the clots, likely due to the effect of thrombin on clot structure. Fibrin clots formed with added thrombin have thinner, more tightly packed fibrin

strands on scanning electron micrographs (Wolberg 2007) and decreased rates of fibrinolysis (Collet et al. 2000; Gabriel et al. 1992). In Chapter IV, we noted that porcine clots have thinner fibrin fibers and a denser fibrin mesh than human clots. The use of thrombin in the BaSO₄-doped clots may have created fibrin mesh that is even finer, denser, and difficult to lyse than normal porcine clots, leading to reduced mass loss in the BaSO₄-doped clots at higher rt-PA concentrations.

The addition of BaSO₄ may also have an effect on thrombosis and thrombolysis. It has been hypothesized that BaSO₄ has a small anti-coagulant effect (Kan et al. 2010; Yuki et al. 2012) due to its adsorption of vitamin K-dependent clotting factors, particularly Factor V and VIII (Zucker and Owen 1982). Shafrir and de Vries showed that plasma without with BaSO₄ clotted more quickly than plasma with BaSO₄ (15.75±2.96 and 25.38±9.46 min respectively) (Shafrir and de Vries 1956). However, the BaSO₄-doped clots had clotted by the time of the experiment. The 3 hr, 37 °C incubation followed by our 3 day, 4 °C incubation likely allowed a more than adequate time frame for clotting to occur, even if there was a reduction in the amount or function of Factor V or VIII.

The *in vitro* flow system used in these experiments was well established previously using human clots and plasma (Bader et al. 2015a; Bader et al. 2015b; Gruber et al. 2014), allowing direct comparison of our data with published data. We treated our porcine whole blood clots with 15.75 µg/mL of rt-PA and achieved around 30% lysis for both non-doped and BaSO₄-doped clots. In contrast, human clinical steady state is 5 times lower (Tanswell et al. 1991), and Bader *et al.* showed that human clots in this *in vitro* flow system treated with 3.15 µg/mL rt-PA exhibited an average FCL of 55% (Bader et al. 2015b).

The decreased lytic susceptibility of porcine clots compared to human whole blood clots (Bader et al. 2015b) may be due to any number of mechanisms. Pigs have an increased level of many pro-thrombotic coagulation factors compared to humans, namely Factors V, VII, VII, IX, X, XII, and high molecular weight kininogen (Lewis 1996). These increased levels may hasten coagulation or create a denser fibrin network compared to human clots. Rt-PA lytic efficacy relies on the conversion of plasminogen to plasmin in order to enact thrombolysis. Porcine plasma has a lower concentration of plasminogen compared to human plasma (Lewis 1996) and porcine plasminogen has been shown to be approximately 10-fold less responsive to rt-PA than human plasminogen (Flight et al. 2006). This differential rt-PA susceptibility is consistent with the data presented in Chapter IV, in which the use of human plasma as a physiological source of human plasminogen allowed porcine clots perfused with human plasma to lyse similarly to human clots. We also observed in Chapter IV that porcine and human clot structure differed, with porcine clots having finer fibrin fibers and a denser fibrin mesh than human clots.

Sutton *et al.* showed that the mass loss in response to rt-PA at a concentration of 3.15 $\mu\text{g/mL}$ was much lower in porcine clots created in borosilicate glass (8.8%) than those created in flint glass (17.1%) (Sutton et al. 2013b). The two different glass types were hypothesized to activate platelets to different degrees, changing the degree of clot retraction and allowing for differential responses to rt-PA, with or without the adjuvant US exposure (Sutton et al. 2013b). Histological examination showed that porcine clots formed in flint glass were more porous than clots formed in borosilicate glass (Sutton et al. 2013b). Our clots adherent to sutures were qualitatively similar to the clots from Sutton *et al.* made in borosilicate pipettes (Sutton et al. 2013b), though the clots on sutures used in our study had a central region with increased porosity, possibly due to the addition of the suture during clot formation process. Borosilicate

glass capillaries and micropipettes are widely available, which makes their use more convenient than flint glass materials. Other types of glass could also be investigated for to determine the affect on clot retraction. Alternatively, borosilicate glass may be treated prior to use as a clotting container to reduce fibrinogen absorption and decrease platelet activation (Park et al. 1990).

Bader *et al.* found that the addition of Definity[®] and US exposure had a significant, positive effect on lytic rate in human clots, with increasing UH dose correlated to an increasing lytic rate (Bader et al. 2015b). In contrast, neither non-doped clots nor BaSO₄-doped clots showed a significant increase in FCL in our experiments with the addition of Definity and US exposure. Bader *et al.* suggested that the UH emissions may be linked to the formation of resonance-sized bubbles in the clot matrix via coalescence of smaller microbubbles (Bader et al. 2015b). The use of an US exposure pressure within the stable cavitation regime allowed these resonance-sized bubbles to oscillate stably over time (over 100 sec) and cause visible lysis in the adjacent clot (Bader et al. 2015b). Fifty such bubbles were observed among 36 clots treated with rt-PA, US, and Definity[®], a mean of 1.39 bubbles per clot (Bader et al. 2015b). Bader *et al.* suggested that resonance-sized bubbles were a key component of enhanced rt-PA clot lysis (Bader et al. 2015b)

Comparatively, in the experiments performed here with porcine clots and plasma, only 2 such bubbles were noted among the 18 non-doped clots treated with rt-PA, Definity[®], and US exposure, or 0.13 bubbles per clot and no resonance-sized microbubbles were observed in the experiments performed with BaSO₄ clots. In our study, there may have been less coalescence of gas liberated from Definity[®] (mean diameter range 1.1 μm – 3.3 μm , Lantheus Medical Imaging) into larger resonance-sized bubbles. The same concentration of Definity[®] was used as that used by Bader *et al.*, which should maintain a similar mean free path between bubbles. However, a

less porous or flexible clot matrix may have inhibited microbubble coalescence. In BaSO₄-doped clots, the presence of the BaSO₄ may have confounded visual detection of resonance-sized microbubbles due to increased clot opacity or decreased clot porosity, preventing microbubble penetration. Despite the lack of visible bubbles in the recorded microscopy images, the UH and BB dose detected in our study was not significantly different from Bader *et al.*'s published studies ($p>0.05$) (Bader et al. 2015a). Thus we would not expect the amount of stable and inertial cavitation experienced by the porcine clots and the previously published human clots to differ.

Our study invites future experiments to investigate the differential lytic susceptibility in porcine and human clots. It is possible – even likely – that the reduced lytic susceptibility seen in the porcine clots compared to their human counterparts is multifactorial. Multiple studies may be required to understand porcine hemostasis as a model of human hemostasis, from investigating a biochemical factor such as plasminogen to evaluating structural differences in porcine and human clots.

V.5 Conclusions

Porcine clots doped with BaSO₄ demonstrated a similar response to rt-PA compared to clots that were not doped with BaSO₄ for rt-PA concentrations up to 15.75 µg/mL. Above this concentration, BaSO₄ doped clots exhibited lower rt-PA lytic efficacy. The development of porcine thrombotic stroke models for testing lytic treatments must acknowledge the poor lytic efficacy of rt-PA relative to clinical applications. Porcine blood clots are less susceptible to rt-PA than human clots and do not show enhancement of thrombolysis with the addition of Definity[®] exposed to intermittent 120 kHz US.

Chapter VI. Development of a "humanized" porcine thromboembolism model

VI.1 Background

To evaluate novel thrombolytic therapies, a porcine ischemic stroke model (such as that discussed in Chapter III) would ideally mimic human hemostasis. Perfusing porcine clots with human plasma produced an equivalent degree of thrombolysis to human clots (Huang et al. 2017), but replacing pig's plasma volume with human plasma is impractical for both cost and immunological reasons. Porcine plasma-perfused human clots had rt-PA lysis between that of porcine clots in porcine plasma and that of porcine clots in human plasma (Huang et al. 2017), suggesting that the presence of human plasminogen within the target clot may allow for improved rt-PA thrombolysis. While there are still immunological concerns when introducing a human protein into porcine circulation, porcine plasmin has repeatedly been administered to patients without an adverse immunological reaction (Hedner et al. 1978).

Additionally, the clot structure of porcine clots also contributes to decreased rt-PA lytic susceptibility. Aspirin is a commonly prescribed, widely available pharmaceutical with antithrombotic effects (Undas et al. 2007). Aspirin has been largely thought to inhibit thrombosis via modulation of platelet activity but may also decrease thrombin generation and inhibit fibrin cross-linking (Undas et al. 2007). Furthermore, aspirin has been shown to increase the plasma clot permeability, as well as increase fibrin diameter and rate of fibrinolysis (He et al. 2006; Williams et al. 1998).

The objective of this study was to evaluate two methods for "humanizing" porcine clots and to test the hypothesis that the presence of human plasminogen affects rt-PA thrombolytic efficacy in porcine clots *in vitro*. We will create porcine clots adherent to sutures doped with human plasminogen and aspirin. The lytic efficacy will be measured in our previously published *in vitro* time lapse microscopy system and compared to published data in porcine and human clots (Bader et al. 2015b; Huang et al. 2017). Our hypothesis is that the plasminogen-doped and aspirin-doped porcine clots will have increased rt-PA susceptibility to non-doped porcine clots.

VI.2 Materials and Methods

VI.2.1 Materials

Porcine blood and plasma were acquired and prepared as described previously in Chapter IV.2. Human plasminogen was acquired from Athens Research & Technology (Athens, GA, USA) and reconstituted with nanopure water (ddH₂O) to a stock concentration of 4 mg/mL. Acetylsalicylic acid (aspirin) was acquired from Acros Organics (Geel, Belgium) and a stock solution at 1.5 mg/mL with 60 mM sodium bicarbonate, pH adjusted to 8.0 with 60 μ L of 1 M sodium hydroxide. Calcium chloride dihydrate was acquired from Sigma-Aldrich (St. Louis, MO, USA) and dissolved in ddH₂O to make a 618 mM stock solution. The lytic rt-PA and Definity[®] microbubbles were prepared as described previously in Chapter IV.2

VI.2.2 Preparation of human plasminogen-doped and aspirin-doped porcine whole blood clots

Borosilicate micropipettes were prepared as described previously in Chapter IV.2. Previously published protocols were adapted to create plasminogen-doped and aspirin-doped porcine clots (Huang et al. 2017; Sutton et al. 2013b). In 15 mL centrifuge tubes, CPD blood was

combined with calcium chloride stock solution and either plasminogen stock solution or aspirin stock solution in a 18:1:1 ratio and mixed thoroughly with a pipette. Aliquots of 0.35 mL recalcified, doped blood were pipetted into each glass culture tube. Clots were allowed to form for 3 hours in a 37 °C water bath and then were stored at 4 °C for a minimum of 3 days to allow for clot retraction (Bader et al. 2015b).

The resultant concentrations of aspirin and plasminogen in doped clots were 0.075 mg/mL and 0.2 mg/mL, respectively. This concentration of aspirin is higher than the concentration of 0.009 mg/mL needed to maximally inhibit platelet activity (Roth and Majerus 1975), but lower than the clinical steady state concentration of 0.15-0.30 mg/mL (Levy 1978). The final clot concentration of aspirin is limited by the low solubility of aspirin in aqueous solutions (Ajjan et al. 2009). The concentration of human plasminogen has been reported as 0.146 – 0.2 mg/mL in plasma (Cederholm-Williams 1981; DeFilippis et al. 2016). For this initial investigation, we chose to use a concentration of plasminogen that was slightly higher than this human physiological level. The clot concentration of 0.2 mg/mL is equivalent to 0.3 mg/mL in non-erythrocyte blood volume in our clots, assuming a hematocrit of 38% (Lewis 1996).

VI.2.3 *In vitro* thrombolysis experiments with flow and time-lapse microscopy

The experimental set-up for the *in vitro* time-lapse microscopy experiments with flow is described in detail in Chapter IV.2. Images were analyzed post-hoc and the thrombolytic efficacy was measured as fractional clot loss (FCL) at the end of the 30-min treatment period as described in Chapter IV.2.4. The ultrasound insonation and detection scheme is described in detail in Chapter IV.2.4.3. Each human-plasminogen-doped or aspirin-doped clot was exposed to one of three treatment protocols: porcine plasma alone; porcine plasma with rt-PA (3.15 µg/mL); and porcine plasma with rt-PA (3.15 µg/mL) and Definity[®] (2 µL/mL) exposed to 120 kHz

intermittent ultrasound as described above. This concentration of Definity[®] is consistent with previously reported studies (Bader et al. 2015b).

VI.2.4 Statistical Analysis

Lytic efficacy of the different treatment protocols in the doped clots was compared with a one-way ANOVA. Tukey post-hoc analysis was used to identify significant differences in FCL.

VI.3 Results

VI.3.1 Lytic efficacy

The fractional clot loss in aspirin-doped and plasminogen-doped clots are shown in Figure VI.1. Aspirin-doped clots treated with plasma showed a FCL of $1.10 \pm 0.66\%$. Compared to plasma alone, rt-PA treatment increased FCL to $6.40 \pm 11.26\%$ ($p = 0.52$) and the addition of Definity[®] and US exposed to rt-PA treatment increased FCL to $10.67 \pm 6.36\%$ ($p = 0.15$), but neither increase in FCL was statistically significant. In plasminogen-doped clots, plasma alone produced $3.23 \pm 1.75\%$ FCL and the addition of rt-PA increased the FCL to $16.80 \pm 7.79\%$ ($p = 0.04$). Treatment of plasminogen-doped clots with rt-PA, US, and Definity[®] further increased FCL to $34.23 \pm 11.16\%$ ($p = 0.01$).

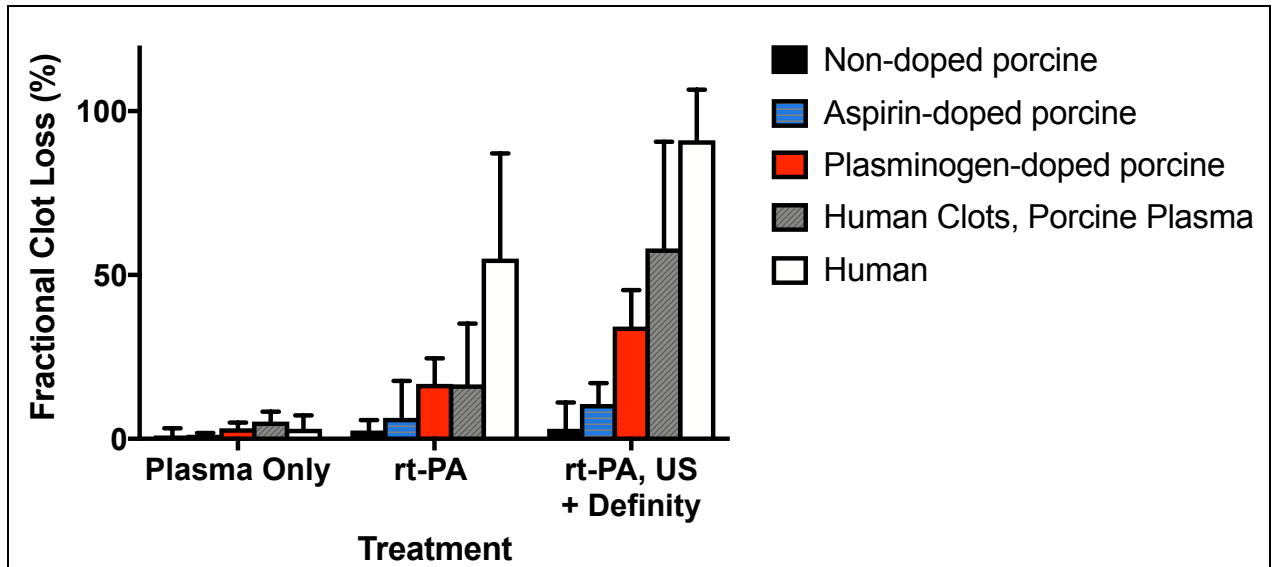


Figure VI.1. Fractional clot loss for aspirin-doped (blue) and plasminogen-doped (red) clots in response to plasma only (n = 5), rt-PA (n = 5), and rt-PA with US and Definity[®] (n = 5 for aspirin-doped, n = 4 for plasminogen-doped). For convenience, previously published data in non-doped porcine clots (black), human clots (white), and human clots perfused with porcine plasma (grey) is also plotted (Bader et al. 2015b; Huang et al. 2017).

VI.3.2 Cavitation activity

The ultraharmonic (UH) and broadband (BB) energy detected by the PCD during trials with US exposure are shown in Figure VI.2. Though variability can be seen in the cavitation dose measured between different types of clots, no significant difference was measured between the UH doses delivered to aspirin-doped and plasminogen-doped clots compared to previously published UH doses ($p > 0.05$) (Huang et al. 2017).

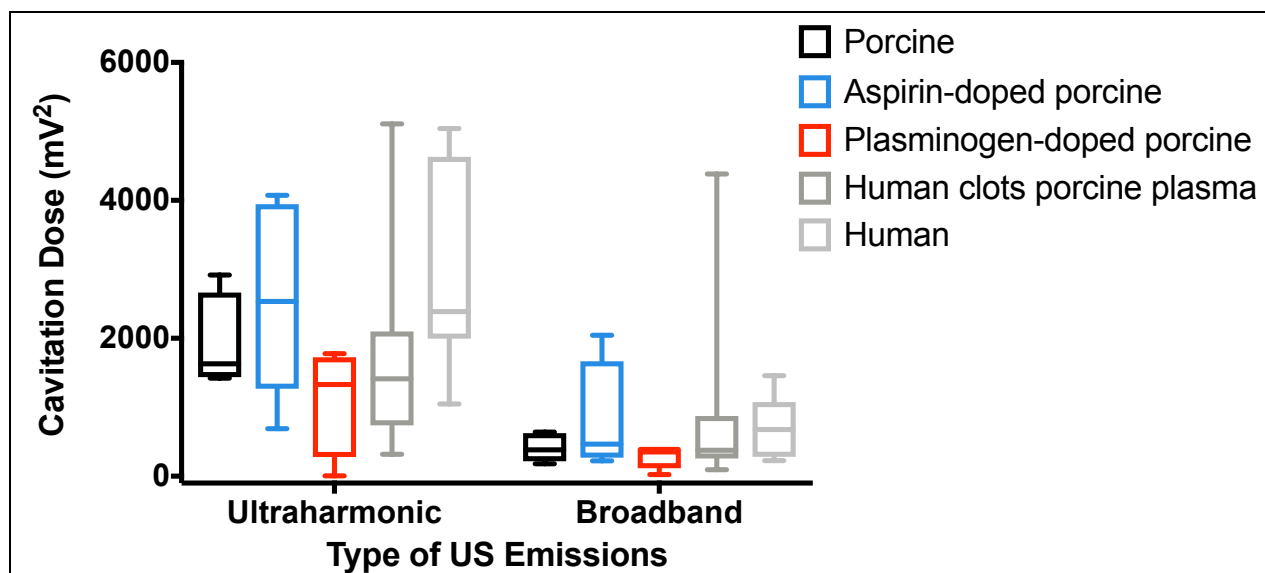


Figure VI.2. Measured ultraharmonic and broadband emissions for aspirin-doped (blue) and plasminogen-doped (red) clots. For convenience, previously published data in non-doped porcine clots (black), human clots (light grey), and human clots perfused with porcine plasma (dark grey) is also plotted (Bader et al. 2015b; Huang et al. 2017).

VI.4 Discussion

The preliminary studies presented here show that plasminogen-doped porcine clots have increased rt-PA lysis with and without rt-PA, Definity[®], and US compared to non-doped porcine clots. However, doping porcine clots with plasminogen does not increase rt-PA lytic susceptibility to levels similar to that seen in human clots (perfused with human plasma). The concentration of human plasminogen in our doped clots is relatively high compared to human plasma concentrations but may be insufficiently activated to affect the same level of rt-PA lysis as in native human plasminogen. Upon binding to fibrin, plasminogen undergoes a large ligand-based change from a "closed", difficult-to-activate conformation to an "open", more easily activated conformation (Mangel et al. 1990). The human plasminogen may have a stronger binding affinity for human fibrin than porcine fibrin, though no supporting evidence for this hypothesis has been seen in either previously published chromogenic assays of plasminogen

activation (Flight et al. 2006) or our previous cross-species rt-PA thrombolysis experiments (Huang et al. 2017). We had hypothesized that the presence or lack of human plasminogen was the main factor affecting rt-PA thrombolysis in the cross-species experiments done previously (Huang et al. 2017), but it is possible that other blood components also contribute to lytic susceptibility. For instance, the inactivation of plasmin may be faster with porcine plasma proteins than with human plasma proteins. The isolated addition of even high concentrations of human plasminogen was not sufficient to increase porcine rt-PA susceptibility that seen in human clots.

Aspirin-doped porcine clots showed a trend of increased lysis with rt-PA administration with and without Definity[®] and US, but the increase was not statistically significant compared to plasma alone for either group. It may be possible that the current concentration of aspirin in clots was insufficient to change clot structure to affect mass loss significantly. The protocol may be refined to reach a higher aspirin concentration in the doped clots, e.g. by creating a higher concentration stock solution or by preparing a combination calcium chloride and aspirin stock solution. Alternately, clinical formulations of aspirin have been developed for increased solubility and may be used instead of pure acetylsalicylic acid (Leonards 1963). It is also possible that aspirin has been engineered to be extremely efficacious in humans, but lacks the same activity in pigs.

In these preliminary studies, no histology or electron microscopy was performed on the doped porcine clot samples to evaluate any structural differences. Future studies should evaluate whether aspirin is effective in altering the clot structure of porcine clots through electron microscopy. Future studies could also consider the effect of doping porcine clots with multiple

dopants, e.g. with both human plasminogen and aspirin, to evaluate whether multiple dopants may synergize to better mimic human hemostasis.

VI.5 Conclusions

Porcine clots doped with human plasminogen showed an increased rt-PA lysis compared to plasma alone, and US exposure adjuvant to rt-PA treatment showed US enhancement of rt-PA lysis. The degree of rt-PA lysis seen in human-plasminogen-doped porcine clots is intermediate between porcine and human clots. While more studies must be completed, our results suggest that biochemically altered porcine clots may serve as model of thrombolysis that better mimics human hemostasis than non-doped porcine clots. Aspirin clots did not show any significant rt-PA lysis with or without adjuvant US exposure. Further studies must be done to investigate whether aspirin is suitable for biochemical modification of porcine clot structure.

Chapter VII. Conclusions and Future Work

VII.1 Summary

In this dissertation, we evaluated porcine *in vitro* and *in vivo* thrombosis models for similarity to human hemostasis. In Chapter II, we were able to develop a protocol for purification of D-dimer, with confirmation of protein identity by immunoblotting and MALDI TOF-TOF analysis. Evaluation of the commercially available Asserachrom D-dimer ELISA kit showed initial success in measurement of porcine D-dimer quantification, but the kit did not cross-react with porcine D-dimer at a later date. An initial screen of 5 commercially available D-dimer antibodies for development of an in-house ELISA protocol was completed, but no antibody pairs were found that detected porcine D-dimer at a sensitivity of 10 ng/mL in samples contaminated with porcine plasma proteins. We found that D-dimer concentration and mass loss were correlated in a porcine clot *in vitro* model. With both metrics of thrombolytic efficacy, statistical comparison of lysis associated with each treatment groups concluded that treatment with rt-PA increased lysis over plasma alone, but the addition of Definity[®] and 120-kHz ultrasound exposure did not enhance lysis further. For *in vivo* experiments in which mass loss measurements are not possible, D-dimer concentration could be useful to compare different lytic therapies. However, no D-dimer assay was developed with adequate sensitivity so far.

In Chapter III, we showed the feasibility of bilateral occlusion of the porcine ascending pharyngeal arteries reliably. Most arteries were occluded with a single clot chosen to be about 1 mm larger than the inner diameter of the target artery. We were also able to establish a protocol for the excision of the APAs following animal euthanasia. However, the intraarterial delivery of rt-PA did not recanalize any of the occluded arteries. The preliminary results in the *in vivo*

arterial thromboembolism model motivated *in vitro* experiments which are presented in Chapter IV and Chapter V.

In Chapter IV, we demonstrated that rt-PA has a 22-fold lower lytic efficacy in porcine clots in porcine plasma compared to human clots in human plasma. The presence of human plasminogen either intercalated within the clot or in the surrounding plasma allows for more humanoid rt-PA thrombolytic efficacy. When perfused with human plasma, porcine clots and human clots showed equivalent fractional clot loss for all treatment protocols. Human clots perfused with porcine plasma did not show rt-PA lysis, but adjuvant 120 kHz US exposure significantly increased rt-PA lysis (Huang et al. 2017). The results seen in these cross-species studies motivated the creation of human plasminogen-doped porcine clots, which were evaluated experiments described in Chapter IV.

In Chapter V, porcine clots doped with BaSO₄ demonstrated a similar response to rt-PA compared to clots that were not doped with BaSO₄ for rt-PA concentrations up to 15.75 µg/mL. Above this concentration, BaSO₄ doped clots exhibited lower rt-PA lytic efficacy. The development of porcine thrombotic stroke models for testing lytic treatments should take into account the poor lytic efficacy of rt-PA relative to clinical dosing. Porcine blood clots are less susceptible to rt-PA than human clots and do not show enhancement of thrombolysis with the addition of Definity[®] exposed to intermittent 120-kHz US.

In Chapter IV, rt-PA lytic efficacy was evaluated in human plasminogen-doped porcine clots and aspirin-doped porcine clots. Porcine clots doped with human plasminogen showed an increased rt-PA lysis compared to plasma alone, and US exposure adjuvant to rt-PA treatment showed US enhancement of rt-PA lysis. The degree of rt-PA lysis observed in human plasminogen-doped porcine clots (16.8% with rt-PA alone) was intermediate between non-doped

porcine clots (2.6%) and human clots (approximately 55%). While more studies must be completed, our results suggest that biochemically altered porcine clots may serve as model of thrombolysis that better mimic human hemostasis than non-doped porcine clots. Aspirin-doped porcine clots did not show any significant rt-PA lysis with or without adjuvant US exposure. Further studies must be done to investigate whether aspirin is suitable for biochemical modification of porcine clot structure.

VII.2 Summary of Clot Models

Overview of clot models

In this dissertation, four porcine clot models were employed in three experimental thrombolysis systems. A summary of the clot model and experimental system combinations are listed by chapter in Table VII.1. Two *in vitro* systems were employed: the *in vitro* static thrombolysis system and the *in vitro* time-lapse microscopy system. *In vitro* experiments allowed quantification of thrombolytic efficacy as mass loss or fractional clot loss.

Table VII.1. A summary of clot models and thrombolysis systems used in this dissertation

Chapter	Experimental System	Borosilicate Clotting Container Description	Blood source	Dopant	rt-PA used
II.5	<i>in vitro</i> static thrombolysis model	Vacutainers [®] , silicone-coated and non-silicone-coated	Porcine (fresh)	n/a	96 µg/mL
III	Porcine APAs	Tube (2.8-4.2 mm inner diameter)	Porcine (CPD*)	BaSO ₄	2 mg bolus, then IA at 10 mg/hr
				n/a	
IV	<i>in vitro</i> time-lapse microscopy system	Micropipettes Micropipettes	Porcine (CPD*)	none	3.15 µg/mL
			Human volunteers	none	
V	<i>in vitro</i> static thrombolysis model	Pasteur pipettes (5-6 mm inner diameter)	Porcine (CPD*)	BaSO ₄	3.15 to 100 µg/mL
				n/a	
	<i>in vitro</i> time-lapse microscopy system	Micropipettes	Porcine (CPD*)	BaSO ₄	15.75 µg/mL
				n/a	
VI	<i>in vitro</i> time-lapse microscopy system	Micropipettes	Porcine (CPD*)	aspirin	3.15 µg/mL
				human plasminogen	

* CPD indicates blood was citrate phosphate dextrose-anticoagulated

The majority of the *in vitro* thrombolysis experiments (Chapter IV - Chapter VI) presented were completed in the *in vitro* time-lapse microscopy system with flow, in which clots adherent to sutures were placed into a flow system and imaged over the course of a 30-min treatment period. One key advantage of this system is that time-dependent thrombolysis data is gathered for analysis of lytic rate. In Chapter IV, we used this time-dependent data to differentiate porcine and human clots perfused with human plasma, noting that more human clots had achieved a fractional clot loss of 100% by the end of our 30 min treatment period. However, the detection of clot width from an image takes into account only 2 dimensions. The *in vitro* static thrombolysis system allows measurement of mass loss, which accounts for clot loss in all 3 dimensions, but does not allow us to measure thrombolytic efficacy over time. The *in vitro* time-lapse microscopy system was used for thrombolysis experiments using cross-species

combinations of clots and plasma (described in Chapter IV), which revealed the importance of the presence of human plasminogen in rt-PA lytic efficacy.

The porcine *in vivo* arterial thromboembolism model (Chapter III) is similar to the *in vitro* time-lapse microscopy flow system. Thrombolytic efficacy is measured as a function of time as angiograms are recorded every 15 min. Additionally, the angiogram is also a 2-dimensional image with limited information about clot width. Additional information about clot lysis is obtained through the degree of perfusion of distal territories. The *in vitro* static thrombolysis system (Chapter II.5) is similar to the porcine intracerebral hemorrhage (ICH) model, in which blood is treated rt-PA without the presence of flow. The *in vitro* static thrombolysis system allows measurement of mass loss, which is not possible in the ICH model. The quantitative porcine D-dimer assay was developed to determine thrombolytic efficacy in the ICH model (Chapter II).

All of the clotting containers used in this dissertation were made of borosilicate glass, which is noted to cause strong clot retraction, likely through platelet activation (Sutton et al. 2013b). Borosilicate glass was used due to its wide availability in a variety of diameters and container types. However, other types of glass or container materials have been used to modulate clot retraction (Sutton et al. 2013b). Additionally, plasma treatment or silicone coatings on borosilicate glass decreases platelet activation and would likely modulate clot retraction (Park et al. 1990). In Chapter II.5, we noted that silicone-coated borosilicate BD Vacutainers[®] triggered robust clot retraction, but non-silicone-coated Vacutainers[®] did not. However, the specific product line used in Chapter II.5 for clot production has been discontinued and currently commercially available products would need to be evaluated for the effect on clot retraction.

The clots produced for this dissertation were made with recalcified citrate phosphate dextrose-anticoagulated (CPD) porcine blood. This previously published clot model (Collet et al. 1993; Gersh et al. 2009; Prokop et al. 2007; Sutton et al. 2013b) uses a convenient source of blood. However, the anticoagulation and subsequent recalcification of the blood decreases the hematocrit of the blood, and the overnight shipment of at 4 °C may affect the stability of platelets and red blood cells. The use of fresh blood (porcine fresh blood in Chapter II.5 and human fresh blood in Chapter IV) eliminates the overnight storage and reduces concerns about formed element stability. The main advantage of using CPD anticoagulated blood for clot formation is the ability to modify clot elements during the clot-making process, such as the addition of a dopant to cause radiopacity (BaSO₄, Chapter III & Chapter V) or increase clot lysis (human plasminogen and aspirin, Chapter VI). Additionally, it might be possible to modify the degree of blood clotting through removal of platelets, red blood cells, or clotting factors (Kunitada et al. 1992; Pieters et al. 2004), though this was not done in the experiments presented here.

One additional consideration when choosing a clot model is the volume of blood required per clot. Clots formed in the micropipette only require 0.35 mL per clot, but clots in Pasteur pipettes and Vacutainers[®] require 1.5-2 mL per clot. Clots formed in borosilicate glass tubes for the porcine *in vivo* arterial thromboembolism model vary in the blood volume required (0.19-0.43 mL). Note that multiple sizes of clots must be prepared for each porcine experiment to allow for a variety of APA sizes.

Lastly, rt-PA concentrations of 3.15 to 100 µg/mL were used in the studies presented in this dissertation. In Chapter II.5, an rt-PA concentration of 96 µg/mL was used. This concentration was chosen to be similar to previously published studies from our lab (Datta et al.

2006; Datta et al. 2008) and so that small changes in rt-PA concentration have minimal effect on the mass loss (Holland et al. 2008). However, the experiments presented in Chapter II.5 show that the addition of Definity® and US did not enhance lysis in unretracted clots. This may be due to the resistance of porcine clots to ultrasound enhancement of rt-PA lysis, as we saw in Chapter III, IV, and V. In Chapter III, we used a protocol previously used in clinical trials for intraarterial rt-PA delivery (2 mg bolus, followed by 10 mg/hr for 2 hours) without determining a local rt-PA concentration (Lewandowski et al. 1999). There have been other published intraarterial rt-PA delivery protocols using higher rt-PA doses which may better elucidate recanalization in an *in vivo* porcine model (Berkhemer et al. 2015; Ciccone et al. 2013; Poncyłjusz et al. 2007). However, the inherent resistance to rt-PA lysis with pigs and porcine blood must be recognized.

In Chapter IV and Chapter VI, we used a concentration of 3.15 $\mu\text{g/mL}$ to mimic human steady state after intravenous rt-PA injection (Tanswell et al. 1991), which allowed us to compare rt-PA lysis in porcine and human clots directly. We observed that porcine clot lysis was 20-fold lower than human clot lysis in response to 3.15 $\mu\text{g/mL}$ rt-PA. This resistance to rt-PA lysis led us to use a higher rt-PA concentration (15.75 $\mu\text{g/mL}$) for the experiments designed to compare rt-PA lysis of BaSO₄-doped and non-doped clots (Chapter V). In future studies, a 3.15 $\mu\text{g/mL}$ rt-PA concentration should be utilized to allow direct comparison of our porcine clot models with human clots.

VII.3 Future Directions

In Chapter II, quantification of porcine D-dimer was ultimately unsuccessful with both the Asserachrom D-dimer ELISA kit and in-house ELISA protocol using commercially available antibodies. Our experience with the Asserachrom D-dimer ELISA kit showed that though human

and porcine D-dimer are homologous, "off-label" use of a human kit to quantitate porcine protein can be unreliable. Several other anti-human D-dimer antibodies are commercially available and could be evaluated for cross-reaction to porcine D-dimer. Immune-based quantification of porcine D-dimer may best be achieved, however, through creation of antibodies specific to the porcine protein.

In Chapter III, we were able to occlude the ascending pharyngeal arteries in the pigs bilaterally, but intraarterial delivery of rt-PA did not recanalize the arteries. The subsequent *in vitro* studies (Chapter IV - Chapter VI) highlighted the difference in rt-PA lytic susceptibility of porcine clots and human clots (Huang et al. 2017). Further work must be done to evaluate human plasminogen, aspirin, and other dopants, either singly or in combination, as modifiers of porcine hemostasis to allow porcine clots to better mimic human thromboses. The development of sonothrombolysis as a therapy for ischemic stroke relies on the pig as a large-animal model for human ischemic stroke. As a result, the creation of a porcine clot that exhibits humanoid rt-PA susceptibility has value. An alternate approach would be to introduce human blood clots or human plasma into swine to reduce the effect of porcine rt-PA resistance on evaluation of novel ischemic stroke therapies. The use of human blood clots and human plasma may serve as a time- and cost-effective solution to the challenge of how to create humanoid porcine clots. However, studies must be done to determine the degree of adverse immunological reactions that would occur in such a system.

References

- Adam SS, Key NS, Greenberg CS. D-dimer antigen: current concepts and future prospects. *Blood* 2009 [cited 2014 Sep 8];113:2878–2887. Available from: <http://bloodjournal.hematologylibrary.org/content/113/13/2878.short>
- Adams H., Adams H., Bendixen B., Bendixen B., Kappelle L., Kappelle L., Biller J, Biller J, Love B., Love B., Gordon D., Gordon D., Marsh E., Marsh E. Classification of Subtype of Acute Ischemic Stroke. *Stroke* 1993;23:35–41.
- Adzerikho I, Shantsila E, Minchenya V, Kulak A. Ultrasound-assisted thrombolysis with streptokinase improves thrombus resolution with minimal distal embolisation. *J Thromb Thrombolysis* 2013;36:263–70. Available from: <http://www.ncbi.nlm.nih.gov/pubmed/23180283>
- Ajjan RA, Standeven KF, Khanbhai M, Phoenix F, Gersh KC, Weisel JW, Kearney MT, Ari??ns RAS, Grant PJ. Effects of aspirin on clot structure and fibrinolysis using a novel in vitro cellular system. *Arterioscler Thromb Vasc Biol* 2009;29:712–717.
- Alexandrov AWA V., Tsivgoulis G, Rubiera M, Vadikolias K, Stamboulis E, Molina CA, Alexandrov AWA V., Investigators for the T. End-Diastolic Velocity Increase Predicts Recanalization and Neurological Improvement in Patients With Ischemic Stroke With Proximal Arterial Occlusions Receiving Reperfusion Therapies. *Stroke* 2010;41:948–952. Available from: <http://stroke.ahajournals.org/content/41/5/948.abstract>
- Alexandrov A V, Barlinn K. Taboos and opportunities in sonothrombolysis for stroke. *Int J Hyperthermia* 2012 [cited 2012 Aug 8];28:397–404. Available from: <http://www.ncbi.nlm.nih.gov/pubmed/22621740>
- Alexandrov A V, Molina CA, Grotta JC, Garami Z, Ford SR, Alvarez-Sabin J, Montaner J, Saqqur M, Demchuk AM, Moyé LA, Hill MD, Wojner AW. Ultrasound-enhanced systemic thrombolysis for acute ischemic stroke. *N Engl J Med* 2004 [cited 2013 Mar 13];351:2170–8. Available from: <http://www.ncbi.nlm.nih.gov/pubmed/15548777>
- Amiral J, Grosley B, Mimilla F. Measurement of D. dimer with a monoclonal enzyme immuno assay. *Ultin, Vinazzer, H Thromb Hemorrhagic Dis Gozlem Matbaacilik Koll Sti, Istanbul* 1986;363–369.
- Ammi AY, Mast TD, Huang IH, Abruzzo TA, Coussios CC, Shaw GJ, Holland CK. Characterization of Ultrasound Propagation Through Ex-vivo Human Temporal Bone. *Ultrasound Med Biol* 2008;34:1578–1589.
- Bader KB, Bouchoux G, Holland CK. Sonothrombolysis. *Ther Modalities* 2016. pp. 339–362. Available from: http://link.springer.com/10.1007/978-3-319-22536-4_19
- Bader KB, Bouchoux G, Peng T, Klegerman ME, Mcpherson DD, Holland CK. Thrombolytic efficacy and enzymatic activity of rt-PA-loaded echogenic liposomes. *J Thromb*

- Thrombolysis Springer US, 2015a;:144–155. Available from:
<http://dx.doi.org/10.1007/s11239-015-1204-8>
- Bader KB, Gruber MJ, Holland CK. Shaken and Stirred: Mechanisms of Ultrasound-Enhanced Thrombolysis. *Ultrasound Med Biol* 2015b;41:187–196. Available from:
<http://linkinghub.elsevier.com/retrieve/pii/S0301562914005705>
- Baron C, Aubry JF, Tanter M, Meairs S, Fink M. Simulation of Intracranial Acoustic Fields in Clinical Trials of Sonothrombolysis. *Ultrasound Med Biol* 2009;35:1148–1158.
- Barry JD, Durkovich D, Cantrell L, Richardson W, Tong T, Offerman S, Clark RE, Tanen DA, Williams S. Vasopressin treatment of verapamil toxicity in the porcine model. *J Med Toxicol* Springer-Verlag, 2005 [cited 2017 Aug 12];1:3–10. Available from:
<http://link.springer.com/10.1007/BF03160898>
- Behrens S, Daffertshofer M, Spiegel D, Hennerici M. Low-frequency, low-intensity ultrasound accelerates thrombolysis through the skull. *Ultrasound Med Biol* 1999 [cited 2014 Oct 12];25:269–273. Available from:
<http://linkinghub.elsevier.com/retrieve/pii/S0301562998001586>
- Benjamin EJ, Blaha MJ, Chiuve SE, Cushman M, Das SR, Deo R, de Ferranti SD, Floyd J, Fornage M, Gillespie C, Isasi CR, Jimenez MC, Jordan LC, Judd SE, Lackland D, Lichtman JH, Lisabeth L, Liu S, Longenecker CT, Mackey RH, Matsushita K, Mozaffarian D, Mussolino ME, Nasir K, Neumar RW, Palaniappan L, Pandey DK, Thiagarajan RR, Reeves MJ, Ritchey M, Rodriguez CJ, Roth GA, Rosamond WD, Sasson C, Towfighi A, Tsao CW, Turner MB, Virani SS, Voeks JH, Willey JZ, Wilkins JT, Wu JH, Alger HM, Wong SS, Muntner P. Heart Disease and Stroke Statistics--2017 Update: A Report From the American Heart Association. *Circulation*. 2017.
- Berkhemer OA, Fransen PSS, Beumer D, van den Berg LA, Lingsma HF, Yoo AJ, Schonewille WJ, Vos JA, Nederkoorn PJ, Wermer MJH, van Walderveen MAA, Staals J, Hofmeijer J, van Oostayen JA, Lycklama à Nijeholt GJ, Boiten J, Brouwer PA, Emmer BJ, de Bruijn SF, van Dijk LC, Kappelle LJ, Lo RH, van Dijk EJ, de Vries J, de Kort PLM, van Rooij WJJ, van den Berg JSP, van Hasselt BAAM, Aerden LAM, Dallinga RJ, Visser MC, Bot JCJ, Vroomen PC, Eshghi O, Schreuder THCML, Heijboer RJJ, Keizer K, Tielbeek A V., den Hertog HM, Gerrits DG, van den Berg-Vos RM, Karas GB, Steyerberg EW, Flach HZ, Marquering HA, Sprengers MES, Jenniskens SFM, Beenen LFM, van den Berg R, Koudstaal PJ, van Zwam WH, Roos YBWEM, van der Lugt A, van Oostenbrugge RJ, Majoie CBLM, Dippel DWJ. A Randomized Trial of Intraarterial Treatment for Acute Ischemic Stroke. *N Engl J Med* 2015;372:11–20. Available from:
<http://www.nejm.org/doi/abs/10.1056/NEJMoa1411587>
- Böhm-Weigert M, Wissel T, Muth H, Kemkes-Matthes B, Peetz D. Long- and short-term in vitro D-dimer stability measured with INNOVANCE D-Dimer. *Thromb Haemost* 2009;103:461–465. Available from: <http://www.schattauer.de/index.php?id=1214&doi=10.1160/TH09-04-0230>
- Bouchoux G, Shivashankar R, Abruzzo TA, Holland CK. In silico study of low-frequency transcranial ultrasound fields in acute ischemic stroke patients. *Int Soc Ther Ultrasound*

2014a.

- Bouchoux G, Shivashankar R, Abruzzo TA, Holland CK. In silico study of low-frequency transcranial ultrasound fields in acute ischemic stroke patients. *Ultrasound Med Biol* 2014b;40:1154–1166.
- Campbell BCV, Mitchell PJ, Kleinig TJ, Dewey HM, Churilov L, Yassi N, Yan B, Dowling RJ, Parsons MW, Oxley TJ, Wu TY, Brooks M, Simpson M a, Miteff F, Levi CR, Krause M, Harrington TJ, Faulder KC, Steinfort BS, Priglinger M, Ang T, Scroop R, Barber PA, McGuinness B, Wijeratne T, Phan TG, Chong W, Chandra R V., Bladin CF, Badve M, Rice H, de Villiers L, Ma H, Desmond PM, Donnan G a, Davis SM. Endovascular Therapy for Ischemic Stroke with Perfusion-Imaging Selection. *N Engl J Med* 2015;372:1009–1018. Available from: <http://www.nejm.org/doi/10.1056/NEJMoa1414792>
- Casals JB, Pieri NCG, Feitosa MLT, Ercolin ACM, Roballo KCS, Barreto RSN, Bressan FF, Martins DS, Miglino MA, Ambrósio CE. The use of animal models for stroke research: A review. *Comp Med* 2011;61:305–313.
- Cederholm-Williams S a. Concentration of plasminogen and antiplasmin in plasma and serum. *J Clin Pathol* 1981;34:979–981.
- Chen Y-H, Yang JT, Chau KH. Determination of the helix and β form of proteins in aqueous solution by circular dichroism. *Biochemistry* 1972;13:3350–3359.
- Chen Y, Zhu W, Zhang W, Libal N, Murphy SJ, Offner H, Alkayed NJ. A novel mouse model of thromboembolic stroke. *J Neurosci Methods* 2015 [cited 2017 Aug 11];256:203–211. Available from: <http://linkinghub.elsevier.com/retrieve/pii/S0165027015003465>
- Chesebro JH, Knatterud G, Roberts R, Borer J, Cohen LS, Dalen J, Dodge HT, Francis CK, Hillis D, Ludbrook P. Thrombolysis in Myocardial Infarction (TIMI) Trial, Phase I: A comparison between intravenous tissue plasminogen activator and intravenous streptokinase. Clinical findings through hospital discharge. *Circulation* 1987;76:142–154.
- Chueh JY, Wakhloo AK, Hendricks GH, Silva CF, Weaver JP, Gounis MJ. Mechanical characterization of thromboemboli in acute ischemic stroke and laboratory embolus analogs. *AJNR Am J Neuroradiol* 2011;32:1237–1244.
- Ciccone A, Valvassori L, Nichelatti M, Sgoifo A, Ponzio M, Sterzi R, Boccardi E. Endovascular Treatment for Acute Ischemic Stroke. *N Engl J Med* 2013;368:904–913. Available from: <http://www.nejm.org/doi/abs/10.1056/NEJMoa1213701>
- Collet JP, Park D, Lesty C, Soria J, Soria C, Montalescot G, Weisel JW. Influence of fibrin network conformation and fibrin fiber diameter on fibrinolysis speed: dynamic and structural approaches by confocal microscopy. *Arterioscler Thromb Vasc Biol* 2000;20:1354–1361.
- Collet JP, Soria J, Mirshahi M, Hirsch M, Dagonnet FB, Caen J, Soria C. Dusart syndrome: a new concept of the relationship between fibrin clot architecture and fibrin clot degradability: hypofibrinolysis related to an abnormal clot structure. *Blood* 1993;82:2462–

9. Available from: <http://www.ncbi.nlm.nih.gov/pubmed/7691261>

Culp WC, Porter TR, Lowery J, Xie F, Roberson PK, Marky L. Intracranial clot lysis with intravenous microbubbles and transcranial ultrasound in swine. *Stroke* 2004 [cited 2013 Sep 28];35:2407–11. Available from: <http://www.ncbi.nlm.nih.gov/pubmed/15322299>

Daffertshofer M, Gass A, Ringleb P, Sitzer M, Sliwka U, Els T, Sedlaczek O, Koroshetz WJ, Hennerici MG. Transcranial low-frequency ultrasound-mediated thrombolysis in brain ischemia: Increased risk of hemorrhage with combined ultrasound and tissue plasminogen activator - Results of a phase II clinical trial. *Stroke* 2005;36:1441–1446.

Daniel PM, Dawes JDK, Prichard MML. Studies of the Carotid Rete and Its Associated Arteries. *Philos Trans R Soc B Biol Sci* 1953 [cited 2013 Oct 4];237:173–208. Available from: <http://rstb.royalsocietypublishing.org/cgi/doi/10.1098/rstb.1953.0003>

Datta S, Coussios C-C, Ammi AY, Mast TD, de Courten-Myers GM, Holland CK. Ultrasound-enhanced thrombolysis using Definity as a cavitation nucleation agent. *Ultrasound Med Biol* 2008 [cited 2012 Jul 31];34:1421–33. Available from: <http://www.pubmedcentral.nih.gov/articlerender.fcgi?artid=2945910&tool=pmcentrez&rendertype=abstract>

Datta S, Coussios C, McAdory LE, Tan J, Porter T, De Courten-Myers G, Holland CK. Correlation of cavitation with ultrasound enhancement of thrombolysis. *Ultrasound Med Biol* 2006 [cited 2013 Feb 15];32:1257–67. Available from: <http://www.pubmedcentral.nih.gov/articlerender.fcgi?artid=1937506&tool=pmcentrez&rendertype=abstract>

DeFilippis AP, Chernyavskiy I, Amraotkar AR, Trainor PJ, Kothari S, Ismail I, Hargis CW, Korley FK, Leibundgut G, Tsimikas S, Rai SN, Bhatnagar A. Circulating levels of plasminogen and oxidized phospholipids bound to plasminogen distinguish between atherothrombotic and non-atherothrombotic myocardial infarction. *J Thromb Thrombolysis* Springer US, 2016;42:61–76.

Demchuk a. M, Burgin WS, Christou I, Felberg R a., Barber P a., Hill MD, Alexandrov a. V. Thrombolysis in Brain Ischemia (TIBI) Transcranial Doppler Flow Grades Predict Clinical Severity, Early Recovery, and Mortality in Patients Treated With Intravenous Tissue Plasminogen Activator. *Stroke* 2001 [cited 2014 Aug 25];32:89–93. Available from: <http://stroke.ahajournals.org/cgi/doi/10.1161/01.STR.32.1.89>

Di Tommaso P, Moretti S, Xenarios I, Orobitz M, Montanyola A, Chang JM, Taly JF, Notredame C. T-Coffee: A web server for the multiple sequence alignment of protein and RNA sequences using structural information and homology extension. *Nucleic Acids Res* 2011;39:13–17.

Eliyas JK, Niekrasz M, Wardrip C, Lee S-K. Focused post mortem dissection technique for harvest of rete mirabile in domestic swine (*Sus scrofa*). *J Neurointerv Surg* 2016;8:973–976. Available from: <http://jn.is.bmj.com/lookup/doi/10.1136/neurintsurg-2015-011949>

Ferguson EW, Fretto LJ, McKee PA. A re-examination of the cleavage of fibrinogen and fibrin

- by plasmin. *J Biol Chem* 1975;250:7210–8. Available from:
<http://www.ncbi.nlm.nih.gov/pubmed/126232>
- Flight SM, Masci PP, Lavin MF, Gaffney PJ. Resistance of porcine blood clots to lysis relates to poor activation of porcine plasminogen by tissue plasminogen activator. *Blood Coagul Fibrinolysis* 2006;17:417–420. Available from:
<http://content.wkhealth.com/linkback/openurl?sid=WKPTLP:landingpage&an=00001721-200607000-00013>
- Flint AC, Duckwiler GR, Budzik RF, Liebeskind DS, Smith WS. Mechanical Thrombectomy of Intracranial Internal Carotid Occlusion: Pooled Results of the MERCI and Multi MERCI Part I Trials. *Stroke* 2007;38:1274–1280. Available from:
<http://stroke.ahajournals.org/cgi/doi/10.1161/01.STR.0000260187.33864.a7>
- Gabriel DA, Muga K, Boothroyd EM. The Effect of Fibrin Structure on Fibrinolysis*. *J Biol Chem* 1992;267:24259–24263.
- Gao S, Zhang Y, Wu J, Shi WT, Lof J, Vignon F, Drvol L, Xie F, Muirhead D, Powers JE, High R, White ML, Porter TR. Improvements in Cerebral Blood Flow and Recanalization Rates With Transcranial Diagnostic Ultrasound and Intravenous Microbubbles After Acute Cerebral Emboli. *Invest Radiol* 2014;49:593–600.
- Gersh KC, Nagaswami C, Weisel JW. Fibrin network structure and clot mechanical properties are altered by incorporation of erythrocytes. *Thromb Haemost* 2009; Available from:
<http://www.schattauer.de/index.php?id=1214&doi=10.1160/TH09-03-0199>
- Graham SM, Mccullough LD, Murphy SJ. Animal Models of Ischemic Stroke : Balancing perimental Aims and Animal Care. *Comp Med* 2004;54:486–496.
- Gralla J, Schroth G, Remonda L, Fleischmann A, Fandino J, Slotboom J, Brekenfeld C. A dedicated animal model for mechanical thrombectomy in acute stroke. *AJNR Am J Neuroradiol* 2006 [cited 2013 Sep 29];27:1357–61. Available from:
<http://www.ajnr.org/content/27/6/1357.short>
- Gruber MJ, Bader KB, Holland CK. Cavitation thresholds of contrast agents in an in vitro human clot model exposed to 120-kHz ultrasound. *J Acoust Soc Am* 2014;135:646–653. Available from: <http://scitation.aip.org/content/asa/journal/jasa/135/2/10.1121/1.4843175>
- Gupta R, Jung E, Brunak S. Prediction of N-glycosylation sites in human proteins.
- Hacke W, Kaste M, Bluhmki E, Brozman M, Dávalos A, Guidetti D, Larrue V, Lees KR, Medeghri Z, Machnig T, Schneider D, von Kummer R, Wahlgren N, Toni D. Thrombolysis with Alteplase 3 to 4.5 Hours after Acute Ischemic Stroke. *N Engl J Med* 2008;359:1317–1329. Available from: <http://www.nejm.org/doi/abs/10.1056/NEJMoa0804656>
- Hashimoto T, Hayakawa M, Funatsu N, Yamagami H, Satow T, Takahashi JC, Nagatsuka K, Ishibashi-Ueda H, Kira J, Toyoda K. Histopathologic Analysis of Retrieved Thrombi Associated With Successful Reperfusion After Acute Stroke Thrombectomy. *Stroke* 2016;47:3035–3037. Available from:

<http://stroke.ahajournals.org/lookup/doi/10.1161/STROKEAHA.116.015228>

- He S, BLOMBÄCK M, YOO G, SINHA R, HENSCHEN -EDMAN AH. Modified Clotting Properties of Fibrinogen in the Presence of Acetylsalicylic Acid in a Purified System. *Ann N Y Acad Sci* Blackwell Publishing Ltd, 2006 [cited 2017 Aug 13];936:531–535. Available from: <http://doi.wiley.com/10.1111/j.1749-6632.2001.tb03540.x>
- Heck D V, Brown MD. Carotid stenting and intracranial thrombectomy for treatment of acute stroke due to tandem occlusions with aggressive antiplatelet therapy may be associated with a high incidence of intracranial hemorrhage. *J Neurointerv Surg* 2014;1–6. Available from: <http://www.ncbi.nlm.nih.gov/pubmed/25387730>
- Hedner U, Johansson L, Nilsson IM. Effects of porcine plasmin on the coagulation and fibrinolytic systems in humans. *Blood* 1978;51:157–64. Available from: <http://www.ncbi.nlm.nih.gov/pubmed/73391>
- Hellstern P, Haubelt H. Manufacture and composition of fresh frozen plasma and virus-inactivated therapeutic plasma preparations: Correlation between composition and therapeutic efficacy. *Thromb Res* 2002;107:3–8.
- Higashida RT, Furlan AJ, Roberts H, Tomsick T, Connors B, Barr J, Dillon W, Warach S, Broderick J, Tilley B, Sacks D. Trial design and reporting standards for intra-arterial cerebral thrombolysis for acute ischemic stroke. *Stroke* 2003 [cited 2013 Oct 4];34:e109-37. Available from: <http://www.ncbi.nlm.nih.gov/pubmed/12869717>
- Hitchcock KE, Holland CK. Ultrasound-assisted thrombolysis for stroke therapy: better thrombus break-up with bubbles. *Stroke* 2010 [cited 2012 Aug 1];41:S50-3. Available from: <http://www.pubmedcentral.nih.gov/articlerender.fcgi?artid=2955362&tool=pmcentrez&rendertype=abstract>
- Hitchcock KE, Ivancevich NM, Haworth KJ, Caudell Stamper DN, Vela DC, Sutton JT, Pyne-Geithman GJ, Holland CK. Ultrasound-enhanced rt-PA thrombolysis in an ex vivo porcine carotid artery model. *Ultrasound Med Biol* 2011 [cited 2013 May 7];37:1240–51. Available from: <http://www.ncbi.nlm.nih.gov/pubmed/21723448>
- Holland CK, Vaidya SS, Datta S, Coussios C-C, Shaw GJ. Ultrasound-enhanced tissue plasminogen activator thrombolysis in an in vitro porcine clot model. *Thromb Res* 2008 [cited 2013 Sep 29];121:663–73. Available from: <http://www.pubmedcentral.nih.gov/articlerender.fcgi?artid=2268623&tool=pmcentrez&rendertype=abstract>
- Huang S, Shekhar H, Holland CK. Comparative lytic efficacy of rt-PA and ultrasound in porcine versus human clots. *PLoS One* 2017;12:e0177786. Available from: <http://dx.plos.org/10.1371/journal.pone.0177786>
- Indik J, Alpert J. Detection of Pulmonary Embolism by D-Dimer Assay, Spiral Computed Tomography, and Magnetic Resonance Imaging. *Prog Cardiovasc Dis* 2000;42:261–272.
- Jadhav S, Eggleton C, Konstantopoulos K. Mathematical Modeling of Cell Adhesion in Shear

Flow: Application to Targeted Drug Delivery in Inflammation and Cancer Metastasis. *Curr Pharm Des* 2007;13:1511–1526. Available from: <http://www.eurekaselect.com/openurl/content.php?genre=article&issn=1381-6128&volume=13&issue=15&spage=1511>

- Jahan R. Solitaire flow-restoration device for treatment of acute ischemic stroke: safety and recanalization efficacy study in a swine vessel occlusion model. *AJNR Am J Neuroradiol* 2010 [cited 2013 Sep 23];31:1938–43. Available from: <http://www.ncbi.nlm.nih.gov/pubmed/20634306>
- Jauch EC, Saver JL, Adams HP, Bruno A, Connors JJB, Demaerschalk BM, Khatri P, McMullan PW, Qureshi AI, Rosenfield K, Scott PA, Summers DR, Wang DZ, Wintermark M, Yonas H. Guidelines for the early management of patients with acute ischemic stroke: A guideline for healthcare professionals from the American Heart Association/American Stroke Association. *Stroke* 2013;44:870–947.
- Jovin TG, Chamorro A, Cobo E, de Miquel MA, Molina CA, Rovira A, Román LS, Serena J, Abilleira S, Ribó M, Millán M, Urra X, Cardona P, López-Cancio E, Tomasello A, Castaño C, Blasco J, Aja L, Dorado L, Quesada H, Rubiera M, Hernandez-Pérez M, Goyal M, Demchuk AM, von Kummer R, Gallofré M, Dávalos A. Thrombectomy within 8 Hours after Symptom Onset in Ischemic Stroke. *N Engl J Med* 2015;372:1504-1703. Available from: <http://www.ncbi.nlm.nih.gov/pubmed/25882510>
- Kan I, Yuki I, Murayama Y, Viñuela F a., Kim RH, Vinters H V., Viñuela F. A novel method of thrombus preparation for use in a swine model for evaluation of thrombectomy devices. *Am J Neuroradiol* 2010;31:1741–1743.
- Kandadai MA, Meunier JM, Hart K, Holland CK, Shaw GJ. Plasmin-Loaded Echogenic Liposomes for Ultrasound-Mediated Thrombolysis. *Transl Stroke Res* 2014;6:78–87.
- Kapralov A, Vlasova II, Feng W, Maeda A, Walson K, Tyurin VA, Huang Z, Aneja RK, Carcillo J, Bayir H, Kagan VE. Peroxidase activity of hemoglobin·haptoglobin complexes. Covalent aggregation and oxidative stress in plasma and macrophages. *J Biol Chem* 2009;284:30395–30407.
- Kim EY, Heo JH, Lee SK, Kim DJ, Suh SH, Kim J, Kim DI. Prediction of thrombolytic efficacy in acute ischemic stroke using thin-section noncontrast CT. *Neurology* 2006;67:1846–1848.
- Kimura M, Iijima S, Kobayashi K, Furuhashi H. Evaluation of the thrombolytic effect of tissue-type plasminogen activator with ultrasonic irradiation: in vitro experiment involving assay of the fibrin degradation products from the clot. *Biol Pharm Bull* 1994 [cited 2014 Sep 8];17:126–30. Available from: <http://www.ncbi.nlm.nih.gov/pubmed/8148800>
- Kjærgaard B, Rasmussen BS, de Neergaard S, Rasmussen LH, Kristensen SR. Extracorporeal cardiopulmonary support may be an efficient rescue of patients after massive pulmonary embolism. An experimental porcine study. *Thromb Res* 2012 [cited 2014 Oct 13];129:e147-51. Available from: <http://www.ncbi.nlm.nih.gov/pubmed/22316657>
- Kumar A, Aakriti, Gupta V. A Review on Animal Models of Stroke: an Update. *Brain Res Bull*

- Elsevier Inc., 2016;122:35–44. Available from:
<http://linkinghub.elsevier.com/retrieve/pii/S0361923016300296>
- Kunitada S, FitzGerald G a, Fitzgerald DJ. Inhibition of clot lysis and decreased binding of tissue-type plasminogen activator as a consequence of clot retraction. *Blood* 1992;79:1420–7. Available from: <http://www.ncbi.nlm.nih.gov/pubmed/1547340>
- Kurola J, Leppikangas H, Magga J, Lindgren L, Kiviniemi V, Rutanen J, Ruokonen E. Effect of levosimendan in experimental verapamil-induced myocardial depression. *Scand J Trauma Resusc Emerg Med* 2010;18:12.
- Kwon JH, Kim JS, Kang DW, Bae KS, Kwon SU. The thickness and texture of temporal bone in brain CT predict acoustic window failure of transcranial doppler. *J Neuroimaging* 2006;16:347–352.
- Laing ST, Moody MR, Kim H, Smulevitz B, Huang S-L, Holland CK, McPherson DD, Klegerman ME. Thrombolytic efficacy of tissue plasminogen activator-loaded echogenic liposomes in a rabbit thrombus model. *Thromb Res Elsevier Ltd*, 2012 [cited 2012 Nov 12];130:629–35. Available from: <http://www.ncbi.nlm.nih.gov/pubmed/22133272>
- Landskroner K, Olson N, Jesmok G. Cross-Species Pharmacologic Evaluation of Plasmin as a Direct-Acting Thrombolytic Agent: Ex Vivo Evaluation for Large Animal Model Development. *J Vasc Interv Radiol* 2005;16:369–377.
- Leonards JR. The influence of solubility on the rate of gastrointestinal absorption of aspirin. *Clin Pharmacol Ther* 1963 [cited 2017 Aug 13];4:476–479. Available from: <http://doi.wiley.com/10.1002/cpt196344476>
- Levy G. Clinical pharmacokinetics of aspirin. *Pediatrics* 1978;62:867–72. Available from: <http://linkinghub.elsevier.com/retrieve/pii/B9780123854711000027>
- Lewandowski CA, Frankel M, Tomsick T a., Broderick J, Frey J, Clark W, Starkman S, Grotta J, Spilker J, Khoury J, Brott T. Combined Intravenous and Intra-Arterial r-TPA Versus Intra-Arterial Therapy of Acute Ischemic Stroke : Emergency Management of Stroke (EMS) Bridging Trial. *Stroke* 1999 [cited 2013 Mar 18];30:2598–2605. Available from: http://stroke.ahajournals.org/content/30/12/2598?ijkey=3e808d05146e3f12f31f38d2886dfd e575256361&keytype2=tf_ipsecsha
- Lewis JH. *Comparative Hemostasis in Vertebrates*. Plenum Press, 1996.
- Lewis MR, Callas PW, Jenny NS, Tracy RP. Longitudinal Stability of Coagulation, Fibrinolysis, and Inflammation Factors in Stored Plasma Samples. *Thromb Haemost Schattauer Publishers*, 2001;86:1495–1500. Available from: <http://www.schattauer.de/t3page/1214.html?manuscript=2993&L=1>
- Liebeskind DS, Sanossian N, Yong WH, Starkman S, Tsang MP, Moya AL, Zheng DD, Abolian AM, Kim D, Ali LK, Shah SH, Towfighi A, Ovbiagele B, Kidwell CS, Tateshima S, Jahan R, Duckwiler GR, Vinuela F, Salamon N, Villablanca JP, Vinters H V., Marder VJ, Saver JL. CT and MRI early vessel signs reflect clot composition in acute stroke. *Stroke*

2011;42:1237–1243.

- Lincoff AM, Bittl JA, Kleiman NS, Sarembock IJ, Jackman JD, Mehta S, Tannenbaum MA, Niederman AL, Bachinsky WB, Tift-Mann J, Parker HG, Kereiakes DJ, Harrington RA, Feit F, Maierson ES, Chew DP, Topol EJ. Comparison of bivalirudin versus heparin during percutaneous coronary intervention (the Randomized Evaluation of PCI Linking Angiomax to Reduced Clinical Events [REPLACE]-1 trial). *Am J Cardiol* 2004 [cited 2017 Aug 11];93:1092–1096. Available from: <http://linkinghub.elsevier.com/retrieve/pii/S0002914904001237>
- Linfante I, Llinas RH, Selim M, Chaves C, Kumar S, Parker RA, Caplan LR, Schlaug G. Clinical and vascular outcome in internal carotid artery versus middle cerebral artery occlusions after intravenous tissue plasminogen activator. *Stroke* 2002;33:2066–2071.
- Mangel WF, Lin BH, Ramakrishnan V. Characterization of an extremely large, ligand-induced conformational change in plasminogen. *Science* 1990;248:69–73. Available from: <http://www.ncbi.nlm.nih.gov/pubmed/2108500>
- Marder VJ, Chute DJ, Starkman S, Abolian AM, Kidwell C, Liebeskind D, Ovbiagele B, Vinuela F, Duckwiler G, Jahan R, Vespa PM, Selco S, Rajajee V, Kim D, Sanossian N, Saver JL. Analysis of Thrombi Retrieved From Cerebral Arteries of Patients With Acute Ischemic Stroke. *Stroke* 2006;37:2086–2093.
- Martini J, Maisch S, Pilshofer L, Streif W, Martini W, Fries D. Fibrinogen concentrate in dilutional coagulopathy: a dose study in pigs. *Transfusion* 2014 [cited 2014 Oct 13];54:149–57. Available from: <http://www.ncbi.nlm.nih.gov/pubmed/23672536>
- Masci PP, Whitaker a. N, Winzor DJ. A simple chromatographic procedure for the purification of the D dimer fragment from crosslinked fibrin. *Anal Biochem* 1985;147:128–135. Available from: <http://linkinghub.elsevier.com/retrieve/pii/0003269785900181>
- Meunier JM, Holland CK, Lindsell CJ, Shaw GJ. Duty cycle dependence of ultrasound enhanced thrombolysis in a human clot model. *Ultrasound Med Biol* 2007 [cited 2013 Oct 4];33:576–83. Available from: <http://linkinghub.elsevier.com/retrieve/pii/S0301562906018928>
- Meunier JM, Holland CK, Pancioli AM, Lindsell CJ, Shaw GJ. Effect of low frequency ultrasound on combined rt-PA and eptifibatide thrombolysis in human clots. *Thromb Res Elsevier Ltd*, 2009;123:528–36. Available from: <http://www.pubmedcentral.nih.gov/articlerender.fcgi?artid=2633628&tool=pmcentrez&rendertype=abstract>
- Moftakhar P, English JD, Cooke DL, Kim WT, Stout C, Smith WS, Dowd CF, Higashida RT, Halbach V V., Hetsch SW. Density of thrombus on admission CT predicts revascularization efficacy in large vessel occlusion acute ischemic stroke. *Stroke* 2013;44:243–245.
- Moore HB, Moore EE, Gonzalez E, Wiener G, Chapman MP, Dzieciatkowska M, Sauaia A, Banerjee A, Hansen KC, Silliman C. Plasma is the physiologic buffer of tissue plasminogen activator-mediated fibrinolysis: Rationale for plasma-first resuscitation after life-threatening hemorrhage. *J Am Coll Surg American College of Surgeons*, 2015;220:872–879. Available

from: <http://dx.doi.org/10.1016/j.jamcollsurg.2015.01.026>

- Morgan T, Zuccarello M, Narayan R, Keyl P, Lane K, Hanley D. Preliminary findings of the minimally-invasive surgery plus rtPA for intracerebral hemorrhage evacuation (MISTIE) clinical trial. *Cereb Hemorrhage* Springer, 2008;147–151.
- Mozaffarian D, Benjamin EJ, Go AS, Arnett DK, Blaha MJ, Cushman M, Das SR, de Ferranti S, Després J-P, Fullerton HJ, Howard VJ, Huffman MD, Isasi CR, Jiménez MC, Judd SE, Kissela BM, Lichtman JH, Lisabeth LD, Liu S, Mackey RH, Magid DJ, McGuire DK, Mohler ER, Moy CS, Muntner P, Mussolino ME, Nasir K, Neumar RW, Nichol G, Palaniappan L, Pandey DK, Reeves MJ, Rodriguez CJ, Rosamond W, Sorlie PD, Stein J, Towfighi A, Turan TN, Virani SS, Woo D, Yeh RW, Turner MB. Heart Disease and Stroke Statistics—2016 Update. *Circulation* 2016;133:e38–e360. Available from: <http://circ.ahajournals.org/lookup/doi/10.1161/CIR.0000000000000350>
- Münster A-MB, Olsen AK, Bladbjerg E. Usefulness of human coagulation and fibrinolysis assays in domestic pigs. *Comp Med* 2002 [cited 2014 Oct 13];52:39–43. Available from: <http://www.ncbi.nlm.nih.gov/pubmed/11900411>
- Mutch NJ, Koikkalainen JS, Fraser SR, Duthie KM, Griffin M, Mitchell J, Watson HG, Booth NA. Model thrombi formed under flow reveal the role of factor XIII-mediated cross-linking in resistance to fibrinolysis. *J Thromb Haemost* 2010;8:2017–2024.
- Nederhoed JH, Slikkerveer J, Meyer KW, Wisselink W, Musters RJP, Yeung KK. Contrast-enhanced sonothrombolysis in a porcine model of acute peripheral arterial thrombosis and prevention of anaphylactic shock. *Lab Anim (NY)* Nature Publishing Group, 2014;43:91–94. Available from: <http://www.labanimal.com/labandoi/10.1038/labandoi.438>
- Niessen F, Hilger T, Hoehn M, Hossmann KA. Differences in clot preparation determine outcome of recombinant tissue plasminogen activator treatment in experimental thromboembolic stroke. *Stroke* 2003;34:2019–2024.
- Nogueira RG, Gupta R, Nogueira RG, Lutsep HL, Gupta R, Jovin TG, Albers GW. Trevo versus Merci retrievers for thrombectomy revascularisation of large vessel occlusions in acute ischaemic stroke (TREVO 2): a randomised trial. *Lancet* 2012;380:1231–1240. Available from: <http://dx.doi.org/10.1016/>
- Notredame C, Higgins D, Heringa J. T-Coffee: A novel method for fast and accurate multiple sequence alignment. *J Mol Biol* 2000;302:205–217. Available from: <http://dx.doi.org/10.1006/jmbi.2000.4042>
- Olman MA, Williams WF, Strickland JH, Hagood JS, Simmons WL, Rivera KE. Facile Purification of Fibrinogen Fragments Using a Computer-Based Model with General Applicability to the Generation of Salt Gradients. *Protein Expr Purif* 1998;14:71–78. Available from: <http://linkinghub.elsevier.com/retrieve/pii/S1046592898909111>
- Park K, Mao FW, Park H. Morphological characterization of surface-induced platelet activation. *Biomaterials* 1990;11:24–31. Available from: <http://linkinghub.elsevier.com/retrieve/pii/014296129090047T>

- Petit B, Gaud E, Colevret D, Arditi M, Yan F, Tranquart F, Allémann E. In vitro sonothrombolysis of human blood clots with BR38 microbubbles. *Ultrasound Med Biol* 2012 [cited 2012 Aug 20];38:1222–33. Available from: <http://www.ncbi.nlm.nih.gov/pubmed/22542261>
- Petit B, Yan F, Bussat P, Bohren Y, Gaud E, Fontana P, Tranquart F, Allémann E. Fibrin degradation during sonothrombolysis – Effect of ultrasound, microbubbles and tissue plasminogen activator. *J Drug Deliv Sci Technol* 2015;25:29–35. Available from: <http://www.sciencedirect.com/science/article/pii/S1773224714000045>
- Pfaffenberger S, Devcic-Kuhar B, El-Rabadi K, Gröschl M, Speidl WS, Weiss TW, Huber K, Benes E, Maurer G, Wojta J, Gottsauner-Wolf M. 2MHz ultrasound enhances t-PA-mediated thrombolysis: comparison of continuous versus pulsed ultrasound and standing versus travelling acoustic waves. *Thromb Haemost* 2003 [cited 2014 Sep 8];89:583–9. Available from: <http://www.schattauer.de/de/magazine/uebersicht/zeitschriften-a-z/thrombosis-and-haemostasis/contents/archive/manuscript/3394.html>
- Pieters M, Hekkenberg RT, Barrett-Bergshoeff M, Rijken DC. The effect of 40 kHz ultrasound on tissue plasminogen activator-induced clot lysis in three in vitro models. *Ultrasound Med Biol* 2004 [cited 2014 Oct 22];30:1545–52. Available from: <http://www.ncbi.nlm.nih.gov/pubmed/15588966>
- Poncyłjusz W, Falkowski A, Kojder I, Cebula E, Sagan L, Czechowski J, Walecka A. Treatment of Acute Ischemic Brain Infarction with the Assistance of Local Intraarterial Thrombolysis with Recombinant Tissue-Type Plasminogen Activator. *Acta radiol* 2007 [cited 2017 Aug 11];48:774–780. Available from: <http://acr.sagepub.com/lookup/doi/10.1080/02841850701408228>
- Postert T, Federlein J, Przuntek H, Büttner T. Insufficient and absent acoustic temporal bone window: Potential and limitations of transcranial contrast-enhanced color-coded sonography and contrast-enhanced power-based sonography. *Ultrasound Med Biol* 1997;23:857–862.
- Prokop AF, Soltani A, Roy RA. Cavitation Mechanisms in Ultrasound-Accelerated Fibrinolysis. *Ultrasound Med Biol* 2007;33:924–933.
- Ringer AJ, Guterman LR, Hopkins LN. Site-specific thromboembolism: a novel animal model for stroke. *AJNR Am J Neuroradiol* 2004;25:329–32. Available from: <http://www.ncbi.nlm.nih.gov/pubmed/14970041>
- Roth GJ, Majerus PW. The mechanism of the effect of aspirin on human platelets. I. Acetylation of a particulate fraction protein. *J Clin Invest* 1975;56:624–632.
- Ryan EA, Mockros LF, Weisel JW, Lorand L. Structural origins of fibrin clot rheology. *Biophys J Elsevier*, 1999;77:2813–2826. Available from: [http://dx.doi.org/10.1016/S0006-3495\(99\)77113-4](http://dx.doi.org/10.1016/S0006-3495(99)77113-4)
- Sakharov D V., Nagelkerkel JF, Rijken DC. Rearrangements of the fibrin network and spatial distribution of fibrinolytic components during plasma clot lysis: Study with confocal microscopy. *J Biol Chem* 1996;271:2133–2138.

- Saqqur M, Uchino K, Demchuk AM, Molina CA, Garami Z, Calleja S, Akhtar N, Orouk FO, Salam A, Shuaib A, Alexandrov A V. Site of arterial occlusion identified by transcranial Doppler predicts the response to intravenous thrombolysis for stroke. *Stroke* 2007;38:948–954.
- Saver JL, Goyal M, Bonafe A, Diener H-C, Levy EI, Pereira VM, Albers GW, Cognard C, Cohen DJ, Hacke W, Jansen O, Jovin TG, Mattle HP, Nogueira RG, Siddiqui AH, Yavagal DR, Baxter BW, Devlin TG, Lopes DK, Reddy VK, du Mesnil de Rochemont R, Singer OC, Jahan R, de Rochemont R du M, Singer OC, Jahan R. Stent-Retriever Thrombectomy after Intravenous t-PA vs. t-PA Alone in Stroke. *N Engl J Med* 2015;372:2285–2295. Available from: <http://www.ncbi.nlm.nih.gov/pubmed/25882376><http://www.nejm.org/doi/abs/10.1056/NEJMoa1415061>
- Shafir E, de Vries A. STUDIES ON THE CLOT-PROMOTING ACTIVITY OF GLASS. *J Clin Invest* 1956;35:1183–1190. Available from: <http://www.jci.org/articles/view/103372>
- Shaw GJ, Bavani N, Dhamija A, Lindsell CJ. Effect of mild hypothermia on the thrombolytic efficacy of 120 kHz ultrasound enhanced thrombolysis in an in-vitro human clot model. *Thromb Res* 2006 [cited 2013 Oct 6];117:603–8. Available from: <http://www.ncbi.nlm.nih.gov/pubmed/15951005>
- Shaw GJ, Dhamija A, Bavani N, Wagner KR, Holland CK. Arrhenius temperature dependence of in vitro tissue plasminogen activator thrombolysis. *Phys Med Biol* 2007;52:2953–2967. Available from: <http://stacks.iop.org/0031-9155/52/i=11/a=002?key=crossref.f154e044fd0a48b9ae59c89ce2eabc74>
- Shaw GJ, Meunier JM, Huang S-L, Lindsell CJ, McPherson DD, Holland CK. Ultrasound-enhanced thrombolysis with tPA-loaded echogenic liposomes. *Thromb Res Elsevier Ltd*, 2009a [cited 2012 Jul 31];124:306–10. Available from: <http://www.pubmedcentral.nih.gov/articlerender.fcgi?artid=2731559&tool=pmcentrez&rendertype=abstract>
- Shaw GJ, Meunier JM, Lindsell CJ, Holland CK. Tissue plasminogen activator concentration dependence of 120 kHz ultrasound-enhanced thrombolysis. *Ultrasound Med Biol* 2008 [cited 2013 Oct 4];34:1783–92. Available from: <http://www.pubmedcentral.nih.gov/articlerender.fcgi?artid=2614894&tool=pmcentrez&rendertype=abstract>
- Shaw GJ, Sperling M, Meunier JM. Long-term stability of recombinant tissue plasminogen activator at -80 C. *BMC Res Notes* 2009b;2:117. Available from: <http://www.biomedcentral.com/1756-0500/2/117>
- Shimizu J, Fukuda T, Abe T, Ogihara M, Kubota J, Sasaki A, Azuma T, Sasaki K, Shimizu K, Oishi T, Umemura S, Furuhashi H. Ultrasound Safety with Midfrequency Transcranial Sonothrombolysis: Preliminary Study on Normal Macaca Monkey Brain. *Ultrasound Med Biol* 2012;38:1040–1050. Available from: <http://linkinghub.elsevier.com/retrieve/pii/S0301562912000877>

- Singh P, Doostkam S, Reinhard M, Ivanovas V, Christian A. Immunohistochemical analysis of thrombi retrieved during treatment of acute ischemic stroke: does stent-retriever cause intimal damage? *Stroke* 2013 [cited 2013 Oct 6];44:1720–2. Available from: <http://www.ncbi.nlm.nih.gov/pubmed/23674526>
- Smith WS, Sung G, Starkman S, Saver JL, Kidwell CS, Gobin YP, Lutsep HL, Nesbit GM, Grobelny T, Rymer MM, Silverman IE, Higashida RT, Budzik RF, Marks MP. Safety and Efficacy of Mechanical Embolectomy in Acute Ischemic Stroke: Results of the MERCI Trial. *Stroke* 2005;36:1432–1438. Available from: <http://stroke.ahajournals.org/cgi/doi/10.1161/01.STR.0000171066.25248.1d>
- Spraggon G, Everse SJ, Doolittle RF. Crystal structures of fragment D from human fibrinogen and its crosslinked counterpart from fibrin. *Nature* 1997;389:455–462.
- Suarez JI, Sunshine JL, Tarr R, Zaidat O, Selman WR, Kernich C, Landis DMD. Predictors of Clinical Improvement, Angiographic Recanalization, and Intracranial Hemorrhage After Intra-Arterial Thrombolysis for Acute Ischemic Stroke. *Stroke* 1999;30:2094–2100. Available from: <http://stroke.ahajournals.org/cgi/doi/10.1161/01.STR.30.10.2094>
- Suchkova VN, Baggs RB, Francis CW. Effect of 40-kHz Ultrasound on Acute Thrombotic Ischemia in a Rabbit Femoral Artery Thrombosis Model : Enhancement of Thrombolysis and Improvement in Capillary Muscle Perfusion. *Circulation* 2000;101:2296–2301. Available from: <http://circ.ahajournals.org/cgi/doi/10.1161/01.CIR.101.19.2296>
- Sutton JT, Haworth KJ, Pyne-Geithman G, Holland CK. Ultrasound-mediated drug delivery for cardiovascular disease. *Expert Opin Drug Deliv* 2013a;10:573–92. Available from: <http://www.ncbi.nlm.nih.gov/pubmed/23448121>
- Sutton JT, Ivancevich NM, Perrin SR, Vela DC, Holland CK. Clot Retraction Affects the Extent of Ultrasound-Enhanced Thrombolysis in an Ex Vivo Porcine Thrombosis Model. *Ultrasound Med Biol* 2013b [cited 2013 Mar 12];39:813–824. Available from: <http://www.ncbi.nlm.nih.gov/pubmed/23453629>
- Swindle MM. Surgery, anesthesia, and experimental techniques in swine. Iowa State University Press, 1998.
- Tanen DA, Ruha A-M, Curry SC, Graeme KA, Reagan CG. Hypertonic sodium bicarbonate is effective in the acute management of verapamil toxicity in a swine model. *Ann Emerg Med* 2000 [cited 2017 Aug 12];36:547–553. Available from: <http://linkinghub.elsevier.com/retrieve/pii/S0196064400500985>
- Tangen O, Wik KO, Almqvist IAM, Arfors K-E, Hint HC. Effects of dextran on the structure and plasmin-induced lysis of human fibrin. *Thromb Res* 1972;1:487–492. Available from: <http://linkinghub.elsevier.com/retrieve/pii/0049384872900552>
- Tanswell P, Seifried E, Stang E, Krause J. Pharmacokinetics and hepatic catabolism of tissue-type plasminogen activator. *Arzneimittelforschung* 1991 [cited 2013 Oct 4];41:1310–9. Available from: <http://www.ncbi.nlm.nih.gov/pubmed/1815534>

- The NINDS rt-PA Stroke Study Group. Tissue plasminogen activator for acute ischemic stroke. The National Institute of Neurological Disorders and Stroke rt-PA Stroke Study Group. *N Engl J Med* 1995 [cited 2013 Nov 10];333:1581–7. Available from: <http://www.ncbi.nlm.nih.gov/pubmed/7477192>
- Tsivgoulis G, Eggers J, Ribo M, Perren F, Saqqur M, Rubiera M, Sargentanis TN, Vadikolias K, Larrue V, Molina C a, Alexandrov A V. Safety and efficacy of ultrasound-enhanced thrombolysis: a comprehensive review and meta-analysis of randomized and nonrandomized studies. *Stroke* 2010 [cited 2013 Oct 4];41:280–7. Available from: <http://www.ncbi.nlm.nih.gov/pubmed/20044531>
- Undas A, Ariens RAS. Fibrin Clot Structure and Function: A Role in the Pathophysiology of Arterial and Venous Thromboembolic Diseases. *Arterioscler Thromb Vasc Biol* 2011;31:e88–e99. Available from: <http://atvb.ahajournals.org/cgi/doi/10.1161/ATVBAHA.111.230631>
- Undas A, Brummel-Ziedins KE, Mann KG. Antithrombotic properties of aspirin and resistance to aspirin: Beyond strictly antiplatelet actions. *Blood* 2007;109:2285–2292.
- Veklich Y, Francis CW, White J, Weisel JW. Structural Studies of Fibrinolysis by Electron Microscopy. *Blood* 1998 [cited 2017 Aug 22];92. Available from: <http://www.bloodjournal.org/content/92/12/4721.short?sso-checked=true>
- Velik-Salchner C, Schnürer C, Fries D, Müssigang PR, Moser PL, Streif W, Kolbitsch C, Lorenz IH. Normal values for thrombelastography (ROTEM) and selected coagulation parameters in porcine blood. *Thromb Res* 2006 [cited 2014 Oct 13];117:597–602. Available from: <http://www.ncbi.nlm.nih.gov/pubmed/15985284>
- Vieilledent C, Amiral J, Astaniou K. Assays for measurements of fibrin degradation products in plasma: Performances and applications. *Fibrinogen 2 Biochem Physiol Clin Relev Elsevier Science Publishers BV, Amsterdam*, 1987. pp. 213–217.
- Wagner KR. Modeling Intracerebral Hemorrhage: Glutamate, Nuclear Factor- B Signaling and Cytokines. *Stroke* 2007;38:753–758. Available from: <http://stroke.ahajournals.org/cgi/doi/10.1161/01.STR.0000255033.02904.db>
- Wagner KR, Xi G, Hua Y, Kleinholz M, de Courten-Myers GM, Myers RE, Broderick JP, Brott TG. Lobar Intracerebral Hemorrhage Model in Pigs : Rapid Edema Development in Perihematoma White Matter. *Stroke* 1996 [cited 2013 Oct 4];27:490–497. Available from: <http://stroke.ahajournals.org/cgi/doi/10.1161/01.STR.27.3.490>
- Wagner KR, Xi G, Hua Y, Zuccarello M, de Courten-Myers GM, Broderick JP, Brott TG. Ultra-early clot aspiration after lysis with tissue plasminogen activator in a porcine model of intracerebral hemorrhage: edema reduction and blood-brain barrier protection. *J Neurosurg* 1999;90:491–498.
- Wijnhoud AD, Franckena M, van der Lugt A, Koudstaal PJ, Dippel e. DWJ. Inadequate Acoustical Temporal Bone Window in Patients with a Transient Ischemic Attack or Minor Stroke: Role of Skull Thickness and Bone Density. *Ultrasound Med Biol* 2008;34:923–929.

- Williams S, Fatah K, Hjemdahl P, Blombäck M. Better increase in fibrin gel porosity by low dose than intermediate dose acetylsalicylic acid. *Eur Heart J* 1998;19:1666–1672.
- Wolberg AS. Thrombin generation and fibrin clot structure. *Blood Rev* 2007;21:131–142. Available from: <http://linkinghub.elsevier.com/retrieve/pii/S0268960X0600066X>
- Wolberg AS, Campbell RA. Thrombin generation, fibrin clot formation and hemostasis. *Transfus Apher Sci* 2008;38:15–23. Available from: <http://linkinghub.elsevier.com/retrieve/pii/S1473050207001826>
- Yuki I, Kan I, Vinters H V., Kim RH, Golshan a., Vinuela F a., Sayre JW, Murayama Y, Vinuela F. The impact of thromboemboli histology on the performance of a mechanical thrombectomy device. *Am J Neuroradiol* 2012;33:643–648.
- Zaidat OO, Lazzaro MA, McGinley E, Edgell RC, Nguyen T, Linfante I, Janjua N. Demand-supply of neurointerventionalists for endovascular ischemic stroke therapy. *Neurology* 2013a;81:305–306. Available from: <http://www.neurology.org/cgi/doi/10.1212/WNL.0b013e31829ce1f2>
- Zaidat OO, Yoo AJ, Khatri P, Tomsick TA, Von Kummer R, Saver JL, Marks MP, Prabhakaran S, Kallmes DF, Fitzsimmons BFM, Mocco J, Wardlaw JM, Barnwell SL, Jovin TG, Linfante I, Siddiqui AH, Alexander MJ, Hirsch JA, Wintermark M, Albers G, Woo HH, Heck D V., Lev M, Aviv R, Hacke W, Warach S, Broderick J, Derdeyn CP, Furlan A, Nogueira RG, Yavagal DR, Goyal M, Demchuk AM, Bendszus M, Liebeskind DS. Recommendations on angiographic revascularization grading standards for acute ischemic stroke: A consensus statement. *Stroke* 2013b;44:2650–2663.
- Zivin JA, Fisher M, DeGirolami U, Hemenway CC, Stashak JA. Tissue plasminogen activator reduces neurological damage after cerebral embolism. *Science* 1985;230:1289–1292.
- Zucker MB, Owen J. Non-decalcified barium sulfate-adsorbed plasma. A potentially useful reagent for studying blood clotting, platelets or complement. *Thromb Haemost* 1982;47:182–4. Available from: <http://www.ncbi.nlm.nih.gov/pubmed/6808695>